IRON-CATALYZED CROSS-COUPLING REACTIONS

XIN QIAN

Iron-catalyzed cross-coupling reactions

By

Xin Qian

B.Sc. Nankai University (2008)

Tian Jin, China

A dissertation submitted to the School of Graduate Studies in partial fulfillment of the requirements for the degree of Master of Science (M.Sc.)

Department of Chemistry

Memorial University of Newfoundland

St. John's, Newfoundland, Canada

2010

Abstract

This thesis concerns the synthesis and study of iron(III) halide complexes supported by amine-bis(phenolate) ligands. These paramagnetic molecules were characterized by a variety of methods including MALDI-TOF mass spectrometry and UV-vis spectroscopy. Two dimeric iron complexes, $\{FeCl[O_2N]^{BuMe\mathit{n}Pr}\}_2$ (**1**), $\{FeCl[O_2N]^{BuMeBn}\}_2$ (**5**) and one monomeric $FeBr_2[O_2NH]^{BuMe\mathit{n}Pr}$ (**8**), where $[O_2N]^{BuMe\mathit{n}Pr}$ = *n*-propylamine-N,N-bis(2-methylene-4-methyl-6-*tert*-butylphenolate) and $[O_2N]^{BuMeBn}$ = benzylamine-N,N-bis(2-methylene-4-methyl-6-*tert*-butylphenolate), were characterized in the solid state by single crystal X-ray diffraction. The abbreviated nomenclature for these ligands can be generalized by the form $[O_2N]^{RR'R''}$, where $[O_2N]$ describes the three donor atoms (two oxygens are phenolic and one nitrogen is aminic) of the ligand, R and R' define the substituents at the 2- and 4- positions, respectively, on the phenol group, and R" represents the alkyl group on the central amine donor (such as *n*Pr for *n*-propyl or Bn for benzyl). Variable temperature magnetic susceptibility data for $\{FeCl[O_2N]^{BuMe\mathit{n}Pr}\}_2$ (**1**) was also obtained using a SQUID magnetometer.

The easily synthesized, inexpensive, and relatively air-stable novel iron complex $\{FeCl[O_2N]^{BuMe\mathit{n}Pr}\}_2$ can be used as a mild and efficient catalyst for C-C cross-coupling of aryl Grignards with alkyl halides. Compared to other iron-catalyzed sp^3-sp^2 C-C cross-coupling reactions, it displays several advantages: i) the complex is easy to handle and has the potential for large-scale applications, ii) by employing microwave conditions, hindered Grignard reagents can react with primary alkyl halides bearing β-H atoms and gives excellent yields, iii) secondary alkyl chlorides and benzyl halides can be effectively

used as electrophilic substrates, iv) a number of functional groups are tolerated. Cross-coupling products are obtained in good to excellent yield as shown by GC-MS and ^{1}H NMR analysis. Screening of cross-coupling reactions for over thirty substrate combinations and the effect of microwave heating on reaction yields are described. Mechanistic studies suggest a radical-mediated route to cross-coupling as shown by "radical clock" experiments.

We also present the ability of $FeCl_3$ to cleave both C-Cl bonds in CH_2Cl_2 and two C-Cl bonds in $CDCl_3$ in the presence of Grignard reagents. Different conditions for the catalytic system are explored, and the products are obtained from low to excellent yields. The results are monitored by GC-MS and ^{1}H NMR. To our knowledge, this is the first time that such transformations have been observed using an iron pre-catalyst, leading to the first efficient double aryl-alkyl coupling of CH_2Cl_2. Hypotheses regarding the mechanism of cross-coupling are presented.

Keywords: Iron; Homogeneous catalyst; Green chemistry; C-C formation, Grignard reagent.

Acknowledgements

I would first like to thank my supervisor, Dr. Christopher Kozak, for his patience and support. His solid foundation in the science, a wealth of experience in teaching, and high degree of professionalism affected me deeply. I also wish to thank Dr. Francesca Kerton, whose recommendations and suggestions have been invaluable for my project. Without their guidance and direction, I would not have focused on organometallic chemistry as the objective of my study and a great cause for which I will struggle and work hard for further research.

I would like to thank my group members Rebecca, Hassan, Zhenzhong, Nduka, Kamrul, Samantha, Khaled and Uttam. They brought me into the wonderful world of research, and not only gave me valuable advice in academics, but also helped my transition into a different culture.

I would also like to thank all C-CART members: to Louise for all my crystal structure work; to Linda and Lidan for MALDI-TOF training and analysis; to Celine for NMR training and help.

Foremost, I would like to express my gratitude to my parents, family and boyfriend for their support and encouragement during my study. Your love enlightened my life.

Table of Contents

List of Schemes

Chapter 1

List of Figures

Chapter

Chapter 2

List of Tables

Chapter 2

Chapter 3

List of Abbreviations

Et_2O – diethylether

GC-MS – gas chromatography mass spectrometry

h – hour

MALDI-TOF MS – matrix-assisted laser desorption/ionization time of flight mass spectrometry

MeCN – acetonitrile

mL – millilitre

min – minute

mol – mole

MS – mass spectrometry

MW– microwave heat

m/z – mass-to-charge ratio

NMR – Nuclear magnetic resonance

RT – room temperature

SIPr•HCl – 1,3-Bis(2,6-diisopropylphenyl)imidazolinium Chloride

THF – tetrahydrofuran

UV – ultraviolet

Vis – visible

Chapter 1. Iron-Catalyzed Cross-coupling Reactions

1.1 Organometallic Background

The metal elements of groups 3-11 in the periodic table, which have partially filled d-orbitals, are named the transition metals (Group 12 elements have filled d-orbitals). They can form coordinate covalent bonds to carbon or heteroatom-containing ligands. The formed complexes exhibit a variety of structural and magnetic properties, and are useful candidate compounds for catalytic transformations used in academic research and industrial processes.

Many transition metals have several posssible oxidation states and may form complex ions, which can gain or lose electrons in redox reactions. This results in close contact among the metal ion, ligand and substrates, and is a reason why transition metals can be used in catalysis.[1] For example, transition-metal catalyzed cross-coupling reactions, such as C-C and C-heteroatom bond formation are extremely powerful processes in organic synthesis, as they help to construct more complex molecules from simpler precursors.

The need to address problems of environmental impact and energy efficiency has led to the development of green chemistry. This field seeks to develop cost-effective, environmentally responsible and efficient processes that minimize the energy used and reduce the generation of hazardous waste. Catalysis, therefore, is an important contributor to the development of "clean technology". However, the catalysts themselves must fulfill

the requirements of green chemistry. For this reason, iron-based catalysts are experiencing a renaissance.

1.2 Introduction to Catalytic Cross-Coupling Reactions Promoted by Iron

Over the past two decades, some of the most important and powerful methods for the construction of carbon-carbon bonds involve the use of transition-metal-catalyzed reactions and have served as indispensable tool in organic synthesis.[1] For the past 30 years, C-C cross-coupling reactions were overshadowed by Pd and Ni-catalyzed reactions, which have taken centre stage because of their generality and functional-group tolerance.[2-3] Modern efficiency requirements have promoted the search for greener catalysts. The cost of Pd and toxicity of Ni limit their application for pharmaceutical and healthcare products. Moreover, the need for structurally complex, costly and sensitive ligands cannot be ignored.[4]

During the rapid development of transition-metal catalyzed homo/cross-coupling reactions, iron has showed unique reactivity and attracted more and more chemists to join the quest for new catalysts. Iron-promoted C-C cross-coupling between alkyl, alkenyl, alkynyl, aryl and acyl moieties have been realized.[5-6] Iron-catalyzed reactions not only have the advantage of being cheap and environmentally friendly, but also show versatile reactivity and high functional-group tolerance. Thus, iron-catalyzed C-C bond formation reactions are potentially competitive with Pd and Ni-catalyzed reactions. Until now, iron-catalyzed C-C coupling reactions have been realized with organomagnesium,[22] zinc,[17-20] copper,[48, 49] or even organoboronic-acid derivatives[10]. While there are numerous

processes that have found use in modern synthetic chemistry, only three examples of cross-coupling reactions will be presented here to introduce the reader to the field.

1.2.1 Suzuki Coupling

The Suzuki reaction couples organo (aryl- or vinyl-) boronic acids/esters with organo halides (aryl, vinyl, or alkyl). It is one of the most versatile and widely used cross-coupling reactions because of the commercial availability and low toxicity of the starting materials, easy handling and high functional-group tolerance. Originally, Pd acted as an efficient catalyst and dominated in this field for a long time.[7, 8] Recently, Fu *et al.* have extended this field by showing alkyl bromides and chlorides can be used as substrates efficiently by using a Ni catalyst.[9]

Nakamura *et al.* have reported novel and well-defined iron catalyst precursors (**1.1**, **1.2** in scheme 1.1) for Suzuki couplings that can couple iodo-, bromo-, or even chloro-alkyl derivatives and arylboronic acids (Scheme 1.1. Bold bond indicates newly-formed bond).[10] Compared to analogous Pd-catalyzed Suzuki reactions, this catalytic system possesses simplicity, environmental acceptability and low cost and because of these, it has the potential for large scale application.

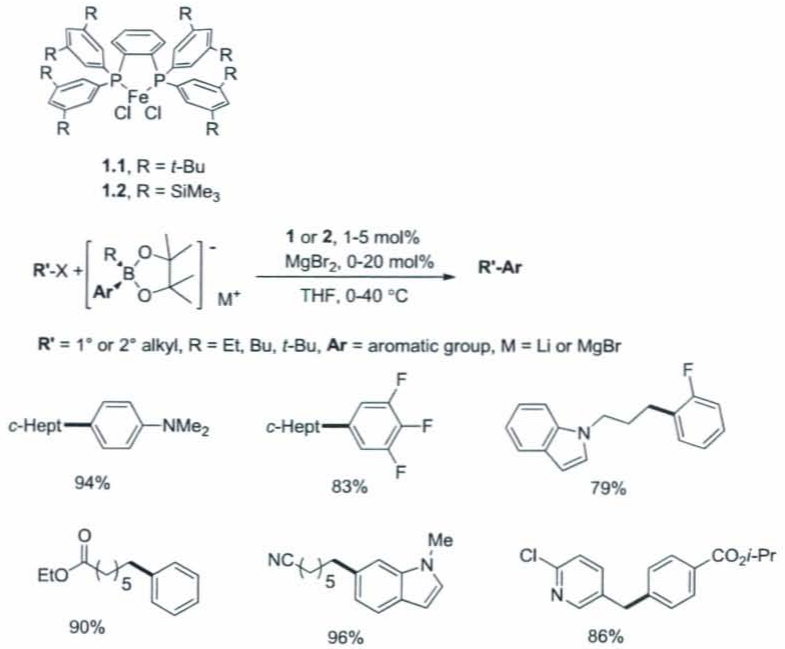

Scheme 1.1 Suzuki-type biaryl coupling by Nakamura *et al.*

Prior to this, Young and co-workers demonstrated that high pressure may have a positive effect in the liquid phase on iron-catalyzed Suzuki cross-coupling reactions. In the presence of $FeCl_3$ and dppy (2-(diphenylphosphino)pyridine), aryl halides and arylbronic acids can be coupled and give good yields of biaryls under high pressure (Scheme 1.2).[11]

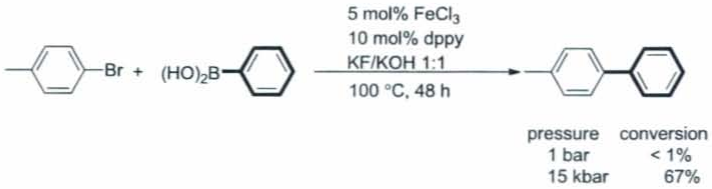

Scheme 1.2 Suzuki-type biaryl coupling under high pressure

1.2.2 Negishi Coupling

The Negishi reaction results in the formation of a new C-C bond between an organozinc compound and an organohalide. It is also an organic reaction that traditionally used Pd[12] and Ni[13-16] as catalysts. Recently, chemists found that iron salts can work very well to achieve this task. Compared to Grignard reagents, organozinc compounds are softer nucleophiles. Therefore, more functional groups are compatible and reactions are conducted under milder conditions with shorter reaction times. The corresponding products are obtained in good to excellent yields in a stereospecific manner.

Nakamura and co-workers developed two efficient iron-TMEDA catalytic systems that work well to couple organozinc compounds and alkyl halides (Scheme 1.3).[17,18] The pronounced effect of a magnesium salt was found to be the key to the promotion of the iron-catalyzed cross-coupling reaction of arylzinc with alkyl tosylates (Scheme 1.4).

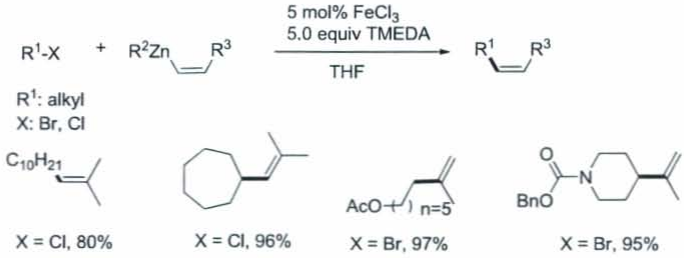

Scheme 1.3 Negishi type alkylations by Nakamura *et al.*

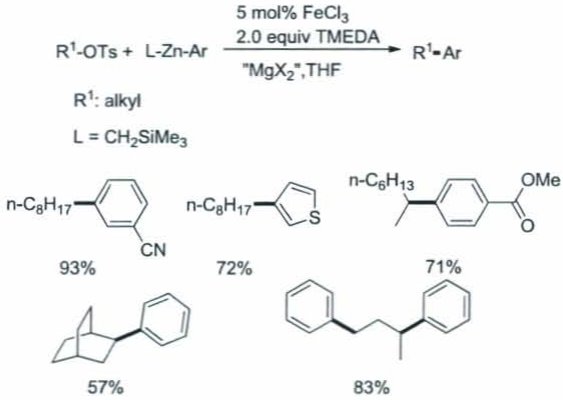

Scheme 1.4 Negishi type arylations by Nakamura *et al.*

Cahiez *et al.* reported the first iron-catalyzed oxidative cross-coupling reaction.[19] The coupling product was obtained by treating a mixture of aryl- and alkylzinc reagents with 1,2-dibromoethane in the presence of [Fe(acac)$_3$] (Scheme 1.5). Primary or secondary aliphatic diorganozinc reagents were both applicable in this reaction. Good yields were obtained under mild conditions (no extra ligand, room temperature, 3–6 h).

Scheme 1.5 Negishi type alkylations by Cahiez *et al.*

Bedford and co-workers built an efficient iron-based catalytic system, which gave excellent activity and good selectivity in the Negishi coupling of arylzinc reagents with a range of benzyl halides and phosphates (Scheme 1.6).[20] This is also a new and green route to synthesis of diarylmethane compounds.

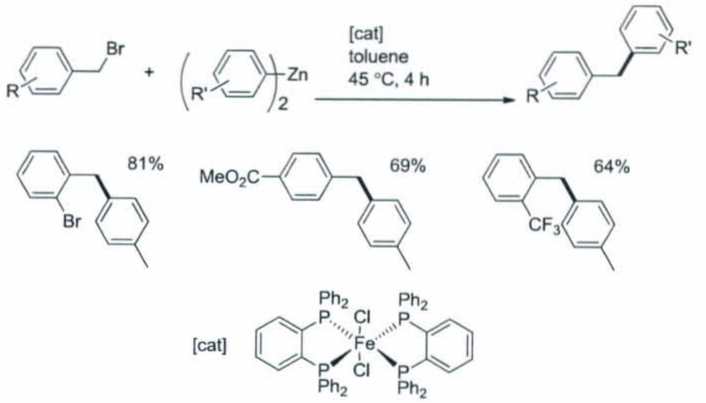

Scheme 1.6 Negishi type arylations by Bedford *et al.*

1.2.3 Heck Coupling

The Heck reaction is an important method of coupling of an unsaturated organohalide (aryl, benzyl, vinyl) and an alkene, which contains at least one proton and is

often electron-deficient, such as an acrylate ester or an acrylonitrile. In this reaction, a strong base is often necessary and a transition metal and ligand cooperate to act as the catalyst. Originally, palladium[4, 21] and nickel[23, 24] were the only choices of metal, with phosphines and diphosphines used as ligands.

Because the Heck cross-coupling reaction is one of the most important methods for the preparation of olefin compounds, more economical and environmentally friendly catalysts alternatives are needed. No doubt, iron salts are desirable candidates. Recently, Vogel and co-workers found that $FeCl_2$ catalyzed the arylation of alkenes using an aryl halide (I or Br), *t*-BuOK as the base and DMSO as the solvent.[25] Cheap and environmentally friendly proline and picolinic acid could be employed as effective ligands. The reactions proceeded in a short time, under mild conditions and gave good to excellent yields (Scheme 1.7).

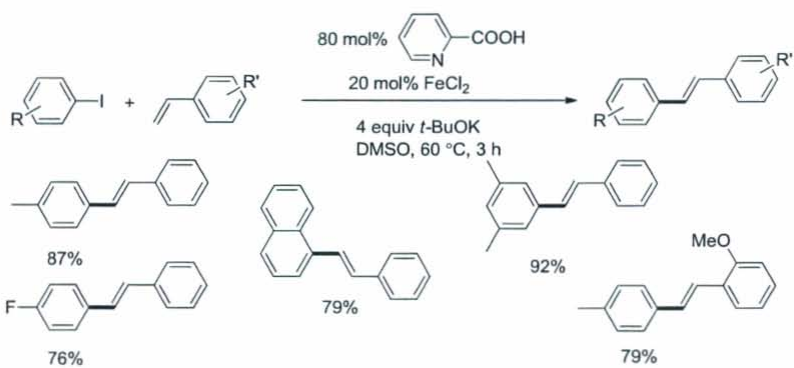

Scheme 1.7 Heck-type reactions by Vogel *et al.*

1.3 Kumada-type C-C Formation Reactions Promoted by Iron

During the past 100 years, Grignard reagents have been possibly the most widely used organometallic reagents because they are cheap, easy to synthesize and commercially available.[26] The reactions can be done in a short time under mild conditions (although atmospheric moisture and oxygen should be excluded). As early as 1972, Makoto Kumada reported the cross-coupling of organic groups by reacting Grignard reagents with alkenyl and aryl halides by using a nickel salt as the precatalyst. [27]

In the past 30 years, there has been rapid development in the use of iron catalysts in a variety of C-C bond formation reactions between molecules with differently-hybridized carbon atoms. Some reports have shown that Kumada type reactions can overcome the difficulties of functional group tolerance,[51,52] thus making such couplings more widely applicable. Thus, examples of Kumada type C-C cross-coupling reactions promoted by iron will now be introduced.

1.3.1 Cross-coupling with Acyl Electrophiles

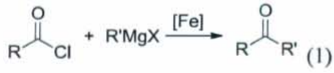

(1)

Functionalized ketones are very important in various natural products, pharmaceuticals and materials science target molecules. Reaction of Grignard reagents with activated acid derivatives posed a significant challenge to chemists (Equation 1). Although this reaction can be achieved without any transition metal catalyst, it is limited for wider exploration because the high reaction temperature needed and unpreventable

by-product formation. In an early report by Cook and co-workers, who explored different catalysts and conditions, they found that $FeCl_3$ was very efficient for the alkylation of acetyl chloride, affording 2-hexanone (70% yield compared with 31% for the uncatalyzed process).[28]

This study opened the door that allowed iron-catalyzed cross-coupling of acid chlorides, cyanides and thioesters with alkyl or aryl Grignard reagents. Fürstner *et al.* demonstrated that by using a small catalytic amount of $Fe(acac)_3$ without any other ligand, acyl chlorides can react with alkyl Grignard reagents at -78 °C efficiently (Scheme 1.8).[22] This method showed unique compatibility with a variety of functional groups in both reaction partners.

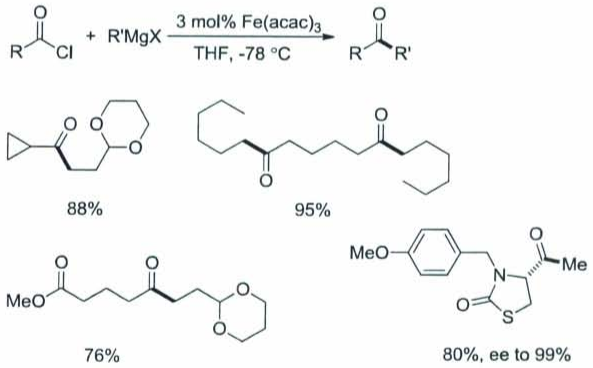

Scheme 1.8 Iron-catalyzed acylations reported by Fürstner *et al.*

Knochel and co-workers found by using $Fe(acac)_3$ in catalytic amounts without any other ligand, aryl and heteroaryl acyl cyanides can react with functionalized aryl and

heteroaryl Grignard reagents efficiently (Scheme 1.9).[29] This method is a very effective catalytic route to the synthesis of new polyfunctional diaryl ketones.

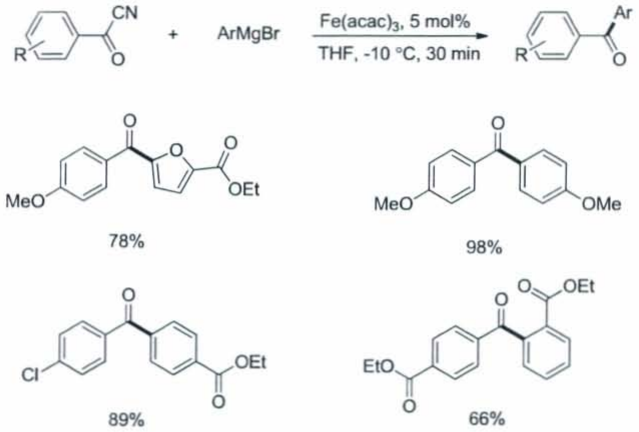

Scheme 1.9 Iron-catalyzed acylations according to Knochel *et al.*

1.3.2 Cross-coupling with Alkenyl Electrophiles

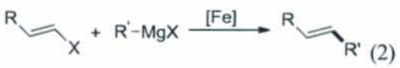

(2)

In 1971, Kochi and Tamura described an iron catalyzed vinylation reaction (Equation 2) of alkyl Grignard reagents with vinyl halides (Equation 2 and Scheme 1.10)[30] and, one year later, the Kumada-Corriu cross-coupling reaction was reported for the first time.[27] The reaction proceeds under very mild conditions, but its environmentally friendly and economic advantages were not identified at the time. More importantly, the procedure has high stereospecificity (Scheme 1.11). However, one obvious drawback of their work is the necessary use of excess alkenyl halide ($\geq$ 3 equiv).

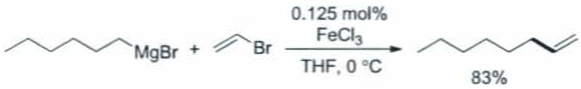

Scheme 1.10 First iron-catalyzed coupling of vinyl bromide with primary Grignard reagents by Kochi *et al.*

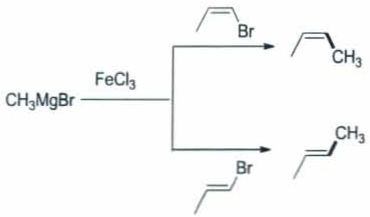

Scheme 1.11 Stereospecificity in the Kumada-Corriu Cross-coupling.

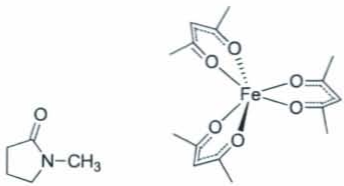

N-methylpyrrolidinone (NMP) Fe(acac)$_3$

Figure 1.1: Structures of NMP and Fe(acac)$_3$

The rather limited synthetic scope of the iron-catalyzed cross-coupling reactions between alkenyl electrophiles and alkyl-Grignard reagents was significantly improved by Cahiez and co-workers by introducing NMP as a co-solvent (Scheme 1.12, Figure 1.1).[31] The use of NMP resulted in shorter reaction times, higher yields, and improved stereoselectivity. More importantly, this method can tolerate various functional groups, such as esters, nitriles, halides, and ketones. As this method is easy to perform and highly

efficient, it was soon modified and developed by many other groups. It was found that it could be used to couple a variety of alkenyl halides and alkyl or aryl Grignard reagents efficiently. Some examples are shown below.

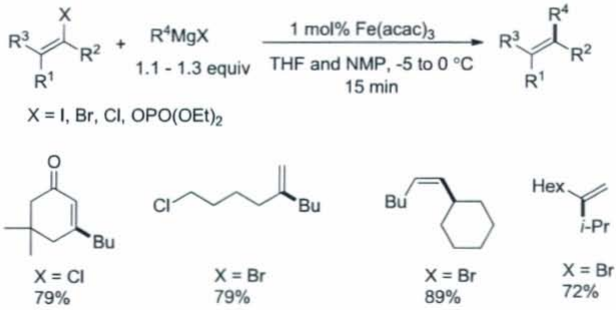

Scheme 1.12 Iron-catalyzed alkenylation of Grignard reagent by Cahiez *et al.*

Fürstner *et al.* developed general conditions for a variety of alkenyl triflates derived from ketones, β-ketoesters, or cyclic 1,3-diketones that can be efficiently cross-coupled with Grignard reagents in the presence of $Fe(acac)_3$ as the precatalyst of choice, affording the desired products in good to excellent yields in most cases (Scheme 1.13).[9] This procedure was also applied to the synthesis of Latrunculin B, (−)-α-cubebene,[32] and (−)-α-cubebol.[33]

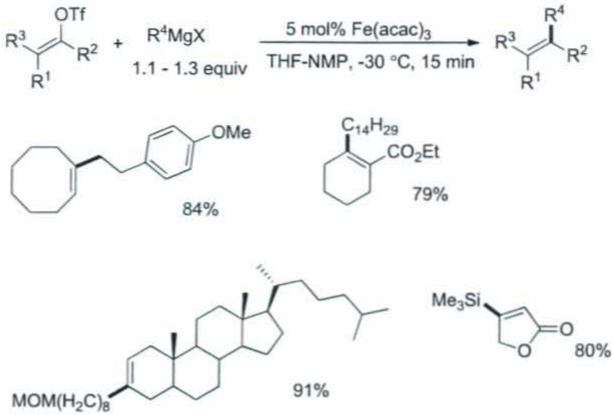

Scheme 1.13 Iron-catalyzed alkenylation of Grignard reagent by Fürstner *et al.*

Olsson and co-workers develop a general, high yielding and rapid iron-catalyzed cross-coupling reaction between Grignard reagents and imidoyl chlorides (Scheme 1.14).[34] The results showed that Grignard reagents bearing β-H tend to give higher yields while Grignard reagents without β-H typically give low to 0% yields. Under the mild conditions of the reaction, functional groups such as esters are unaffected.

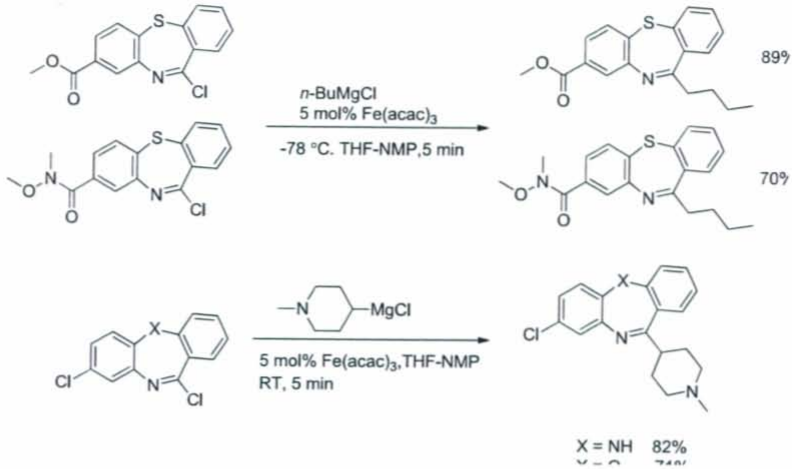

Scheme 1.14 Synthesis of Clozapine analogues by Olsson *et al.*

Alami and co-workers described a very efficient iron-catalyzed coupling of chloroenynes and alkyl Grignard reagents (Scheme 1.15).[35] This reaction is very general, stereospecific, and proceeds under very mild conditions (0 °C in a few minutes). Several functional groups are tolerated (*e.g.*, propargyl acetate, ethyl benzoate, aryl bromide, and hydroxyl groups).

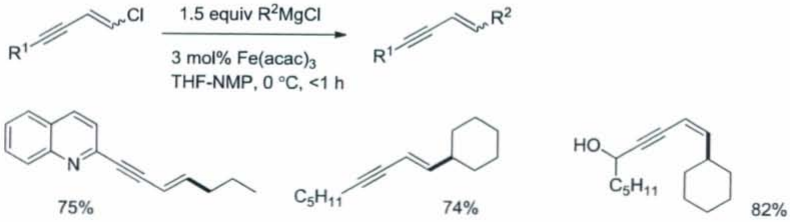

Scheme 1.15 Cross-coupling with chloroenynes by Alami *et al.*

1.3.3 Cross-coupling with Aryl Electrophiles

$$\text{Aryl-X}' + \text{R}'\text{-MgX} \xrightarrow{[\text{Fe}]} \text{Aryl-R}' \quad (3)$$

Fürstner *et al.* developed general conditions for the reactions of alkyl Grignard reagents with aryl halides and pseudohalides (Cl, OTf, OTs) (Scheme 1.16).[36] It is worth noting that aryl chlorides and triflates provide *a priori* better results than the corresponding bromides or iodides, which are the preferred substrates for Pd and Ni-catalyzed processes. Both [Fe(salen)Cl] and $Fe(acac)_3$ proved equally active with a wide substrate scope involving functionalized aromatic compounds.

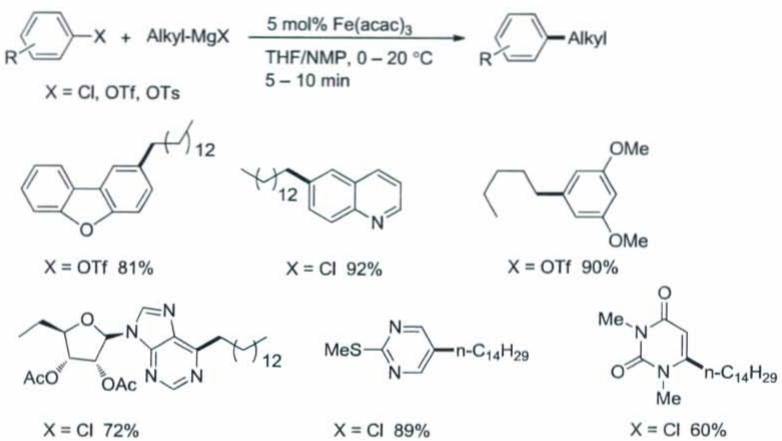

Scheme 1.16 Iron-catalyzed arylation of Grignard reagents by Fürstner *et al.*

Fürstner proposed a mechanistic rationale for iron-catalyzed cross-coupling reactions between aryl halides and alkylmagnesium halides.[37] According to the previous reports by Bogdanović, a formal $Fe(MgX)_2$ species was postulated to be the active low-

valent catalyst (Scheme 1.17).[38] Fürstner also observed that MeMgBr and EtMgBr exhibit strikingly different behavior in attempted cross-coupling reactions with aryl chlorides (Figure 1.2, Scheme 1.18).

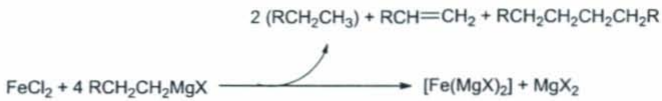

Scheme 1.17 Formation of an inorganic Grignard reagent described by Bogdanovic's group

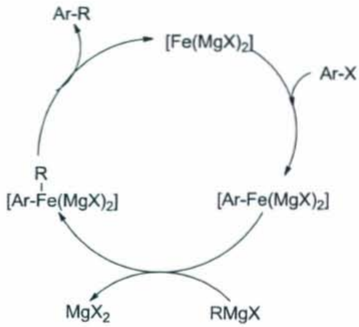

Figure 1.2: Fürstner and Leitner's proposal for the iron-catalyzed cross-coupling reaction of aryl halides

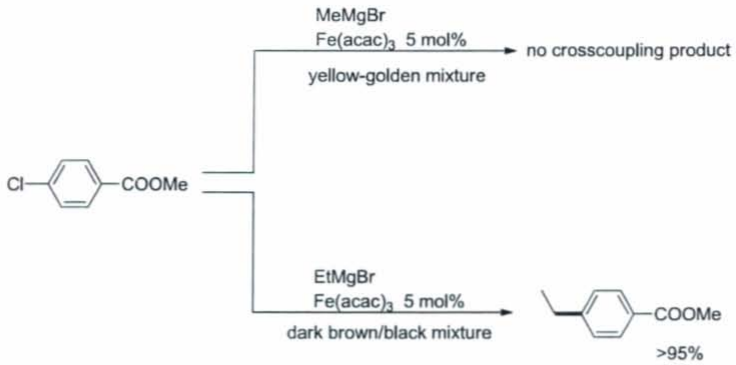

Scheme 1.18 Illustration of the strikingly different behavior of MeMgBr and EtMgBr in iron-catalyzed cross-coupling reactions

Another unique property shown by iron is its selective monoalkylation of dichloro-substituted arenes and heteroarenes in good yields as reported by Hocek and Fürstner (Scheme 1.19, 1.20).[39,40] The behavior of 1,4-dichlorobenzene was first investigated. Nickel-catalyzed reactions of this particular substrate tend to give a mixture favoring the dialkylation products, while palladium catalysts are unreactive. Iron-catalyzed Kumada-type reactions can give high product selectivity. The reactions with *ortho*-substituted substrates showed significantly lower reactivity, which may be because of steric effects.

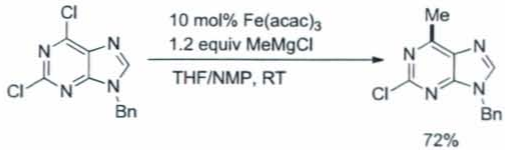

Scheme 1.19 Monoalkylation of dichloro-substituted heteroarenes by Fürstner *et al.*

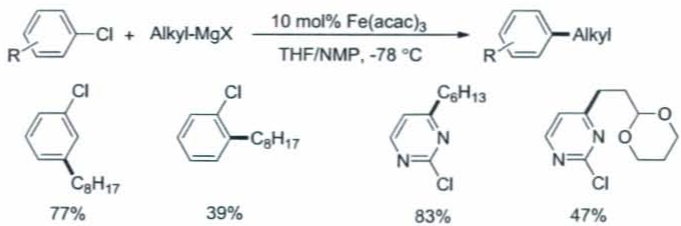

Scheme 1.20 Monoalkylation of dichloro-substituted arenes Fürstner *et al.*

Nagano and Hayashi first reported a system for oxidative homo-coupling of aryl Grignard reagents using $FeCl_3$ as the catalyst and 1,2- dichloroethane (1.2 equiv) as an oxidant in Et_2O at reflux.[41] Good to excellent yields were obtained with a variety of aryl Grignard reagents. Cahiez *et al.* modified this catalytic system.[42] They replaced the diethyl ether with THF for more convenience in large scale applications. Moreover, they lowered the quantity of the oxidant (dihaloethane) from 1.2 equiv to 0.6 equiv, but still observed high and reliable yields for a variety of biaryl products (Scheme 1.21).

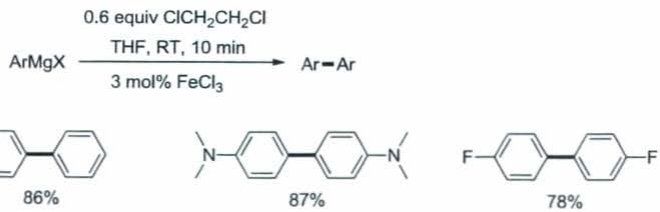

Scheme 1.21 Homo-coupling of aryl Grignard reagents by Cahiez *et al.*

Another exciting report from Cahiez and co-workers demonstrated that by using atmospheric air as the oxidant and $FeCl_3$ as the pre-catalyst, aryl or alkenyl Grignard reagents could be coupled efficiently and to give biaryl/alkenyl products in good to excellent yields with high chemo- and stereoselectivity (Scheme 1.22).[43] Sustainable development is now a real challenge for the chemical industry, and these economical and environmentally friendly procedures constitute an interesting contribution to this field.

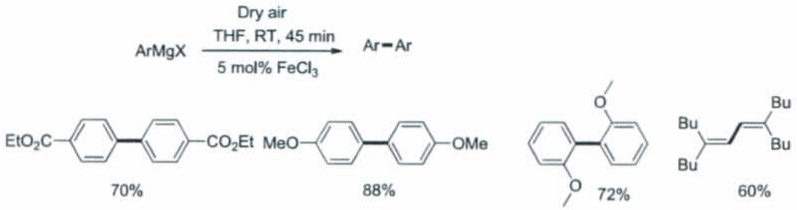

Scheme 1.22 Homo-coupling of aryl Grignard reagents by Cahiez *et al.*

Homo-coupling of organobromide compounds was reported by Pei and co-workers (Scheme 1.23).[44] Using a catalytic amount of iron salts and 2 equiv. of metallic magnesium, aryl bromides could be coupled successfully without the addition of an organodihalide as an oxidant (DBM: dibenzoylmethane). The Grignard nucleophile was formed *in situ.* Yields of biaryl or bibenzyl products were very good, but yields of bialkyl products were lower. This catalytic system has the potential for large scale application.

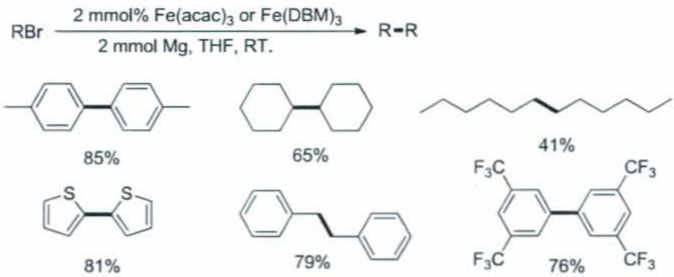

Scheme 1.23 Homo-coupling of Grignard reagents by Pei *et al.*

Aryl-aryl cross-coupling reactions are extremely important reactions, which can be seen in the context of the rapidly growing interest in azine and diazine natural products, pharmaceuticals, and building blocks for supramolecular chemistry or materials science. Traditionally, such kinds of reactions are usually catalyzed by Pd or Ni complexes. Iron-catalyzed aryl-aryl cross-coupling has remained a challenge because of competition from the homocoupling reaction caused by oxidation with organic halides or iron-catalyzed halogen-metal exchange.

Fegadere and co-workers first reported the aryl-aryl cross-coupling reaction between phenyl Grignard reagent and heteroaryl halides in the presence of $Fe(acac)_3$ with moderate to good results (Scheme 1.24).[45] Soon after, Fürstner *et al.* reported a similar catalytic system, which could couple chlorides of various π-electron deficient heteroaromatics in good yields.[36] Plé and co-workers also demonstrated the synthesis of various unsymmetrical polyaryl or polyheteroaryl compounds with π-electron deficient rings.[46]

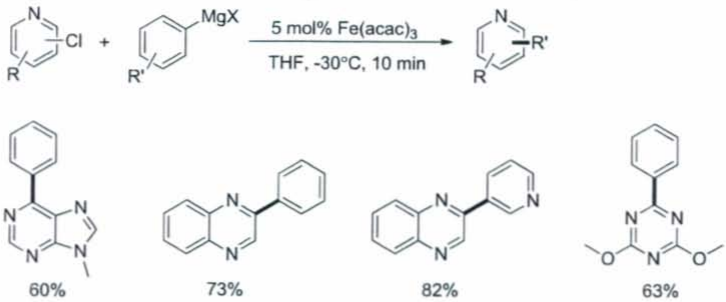

Scheme 1.24 Cross-coupling reaction between phenyl Grignard reagent and heteroaryl halides

A remarkable result in this field was reported by Knochel and co-workers (Scheme 1.25).[47] They showed that iron powder also efficiently catalyzes this transformation. This result supports the consideration that a reduced species might be the active catalyst.

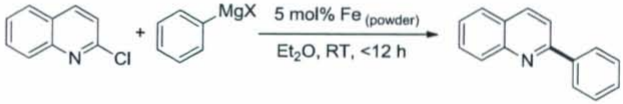

Scheme 1.25 Cross-coupling reaction between phenyl Grignard reagent and heteroaryl halides by Knochel *et al.*

Knochel also reported a process, which utilizes aryl copper reagents and reactive aryl iodides to suppress the homocoupling reaction and selectively yield the heterobiaryl products (Scheme 1.26).[48, 49] Some general trends in the reactivity were also reported. Furthermore, functional groups such as ketones, ethers, acetals, alkylsilanes, nitriles, and amides could be tolerated.

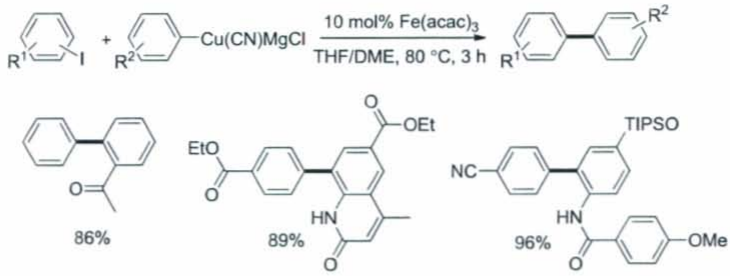

Scheme 1.26 Cross-coupling reaction between phenyl Grignard reagent and aryl halides by Knochel *et al.*

In 2007, Nakamura and co-workers demonstrated an iron-catalyzed selective cross-coupling reaction of aryl chlorides with aryl Grignard reagents (Scheme 1.27).[50] The addition of NHC ligand, SIPr•HCl, and iron fluoride salt, $FeF_3 \cdot 3H_2O$ proved critical to achieving high yield and selectivity. This method is practically simple and yields minimal by-products. A vast array of aromatic and heteroaromatic halides were also investigated, following the general trend Cl > OTf > Br ≈ I.

Scheme 1.27 Cross-coupling reaction between phenyl Grignard reagent and aryl halides by Nakamura *et al.*

1.3.4 Cross-coupling with Alkyl Electrophiles

$$\text{Alkyl-X}' + \text{R}'\text{-MgX} \xrightarrow{[\text{Fe}]} \text{Aryl-R}' \quad (4)$$

Cross-coupling of Grignard reagents with alkyl electrophiles (Equation 4) has many important contributors. Therefore, the most significant results will be presented grouped according to principal investigator.

1.3.4.1 Fürstner

For these reaction, Fürstner and co-workers postulated that the active catalysts were Fe/Mg clusters of formal composition $[Fe(MgX)_2]_n$ formed *in situ* (Scheme 1.28).[51] They then probed this theory by testing the known, well-defined iron(−II) complex $[Li(tmeda)]_2[Fe(C_2H_4)_4]$, which exhibits a d^{10} configuration, as the cross-coupling catalyst. Primary and secondary alkyl bromides or iodides were used successfully with aryl Grignard reagents. The coupling reaction showed remarkable functional-group compatibity, which implied that the iron-catalyzed activation of alkyl halides is significantly faster than the uncatalyzed attack of a Grignard reagent.

Scheme 1.28 Cross-coupling of alkyl halides with aryl Grignard reagents by Fürstner *et al.*

1.3.4.2 Nakamura and Cossy

Nakamura and co-workers reported an effective catalytic iron-amine system, which could couple primary or secondary alkyl halides with aryl Grignard reagent and gave excellent yields (Scheme 1.29).[52] An excess of TMEDA was needed to suppress the formation of olefinic products through a formal loss of HX. Certain trends in the reactivity of alkyl halides were observed (I >Br >Cl, electron-rich > electron-poor Grignard reagent). This is a rare report of acyclic secondary alkyl chlorides used as substrates in the field of sp^3-sp^2 Kumada cross-coupling reactions promoted by iron. Furthermore, the system tolerated functionalized substrates and was highly stereo- and chemoselective.

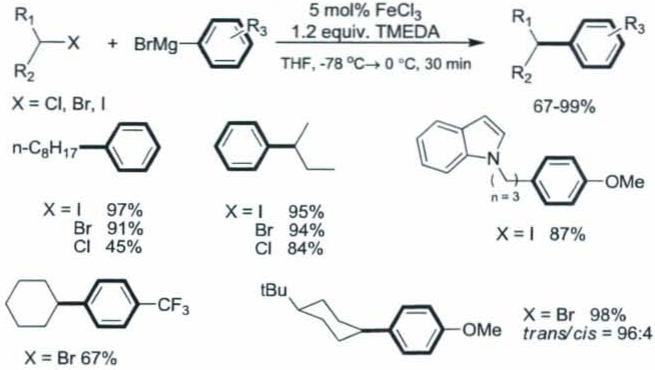

Scheme 1.29 Cross-coupling of alkyl halides with aryl Grignard reagents by Nakamura *et al.*

Cossy *et al.* developed a similar catalytic system that, in the presence of excess TMEDA, showed $FeCl_3$ can be used as an effective catalyst to couple alkyl halides and

alkenyl Grignard reagents (Scheme 1.30).[53] Furthermore, the system was capable of employing functionalized substrates, and the reactions were highly stereo- and chemoselective.

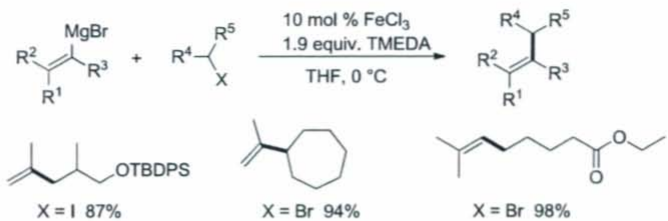

Scheme 1.30 Cross-coupling of alkyl halides with alkenyl Grignard reagents by Cossy *et al.*

1.3.4.3 Bedford

Inspired by Fürstner, who had shown previously that the Fe(III) salen complex **1.3** in Figure 1.3 could be used to couple alkyl Grignards with aryl halides (Scheme 1.31),[36] Bedford demonstrated that related Fe^{III} salen complexes could catalyze the cross-coupling of aryl Grignard reagents with alkyl halides bearing β-Hydrogens.[54] A series of transition-metal salen complexes were examined (M = V, Cr, Mn, Fe, Co, Ni, Cu, Zn). The highest conversion was obtained with [FeCl(salen)] **1.4**. The effect of structural modification of the Schiff base ligand was investigated. Increasing the size of the diamino linker lowered the catalytic ability of the Fe complex **1.5-1.7**, as did possessing an aromatic backbone (complex **1.8-1.10**). Increasing the steric bulk on the aryloxide groups (**1.11**) led to reactivity similar to that of **1.3** but gave less dicyclohexane by-product. The more

hindered naphthyl analogue **1.12** displayed lower activity than **1.4** but still outperformed **1.5**.

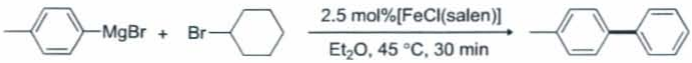

Scheme 1.31 Cross-coupling of alkyl halides with aryl Grignard reagents catalyzed by Fe(III) salen complex

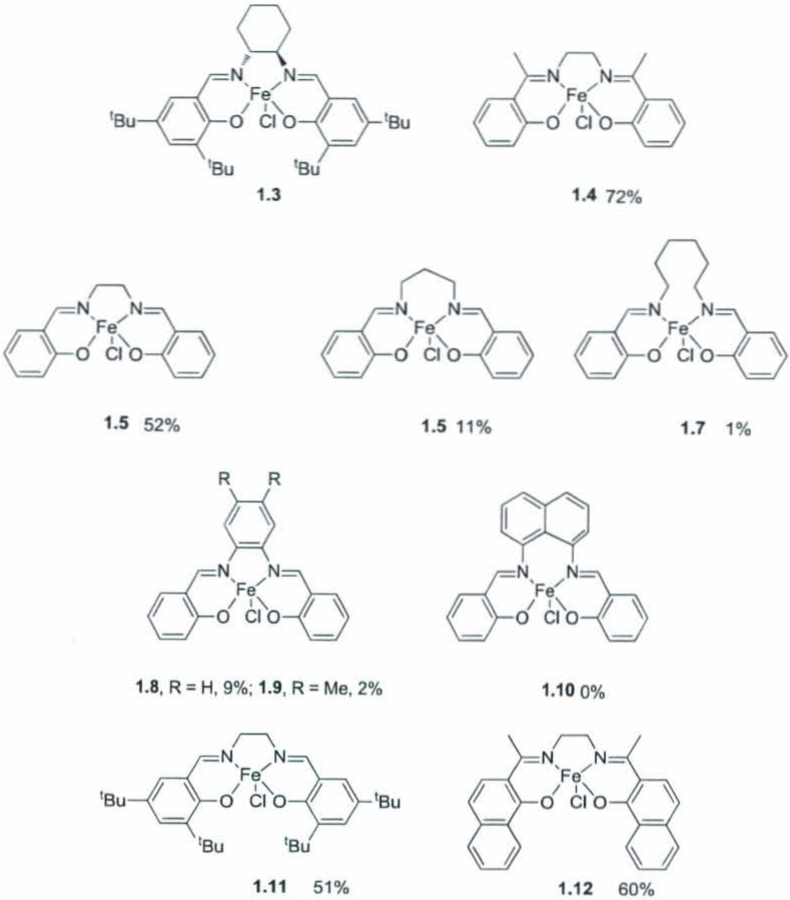

Figure 1.3: The effect of structural modification of the Schiff base ligand

A range of amine-Fe catalysts was later investigated (Scheme 1.32).[55] The three best ligands, triethylamine, DABCO and TMEDA, were then screened. Good to excellent

cross-coupling conversions were obtained from aryl Grignard reagents with primary and secondary alkyl halides.

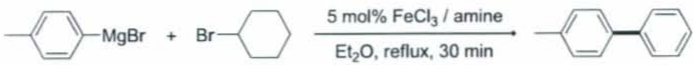

catalyst system	$FeCl_3$ / 2 equiv NEt_3	$FeCl_3$ / TMEDA	$FeCl_3$ / DABCO
conversion (%)	85%	75%	93%

Scheme 1.32 Cross-coupling of alkyl halides with aryl Grignard reagents catalyzed by iron-amine catalyst

They continued by trying some alternative catalyst systems employing phosphine, phosphite, arsine, or NHC ligands (Scheme 1.33).[56] They all turned out to be active catalysts able to couple aryl Grignard reagents with primary and secondary alkyl halide substrates bearing β-Hydrogens.

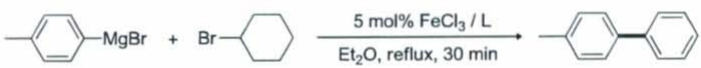

L:		Conversion:
10 mol%	$Ph_2P(CH_2)_6PPh_2$	91%
10 mol%	$Ph_2AsCH_2AsPPh_2$	89%
20 mol%	PCy_3	87%
20 mol%	$P(OMe)_3$	83%
20 mol%	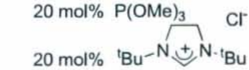	97%

Scheme 1.33 Cross-coupling of alkyl halides with aryl Grignard reagents employing different ligands

Furthermore, according to their observations in their previous reports, the reaction mixtures always turned black. They hypothesised that the black coloration suggested that

this may be nanoparticulate iron (Scheme 1.34).[57] Then they successfully identified that iron nanoparticles, either formed *in situ* and stabilized by 1,6-bis(diphenylphosphino)hexane or polyethylene glycol (PEG), or preformed and stabilized by PEG, were excellent catalysts for the cross-coupling of aryl Grignard reagents with primary and secondary alkyl halides bearing β-Hydrogens. They also proved effective in a tandem cyclization/cross-coupling reaction.

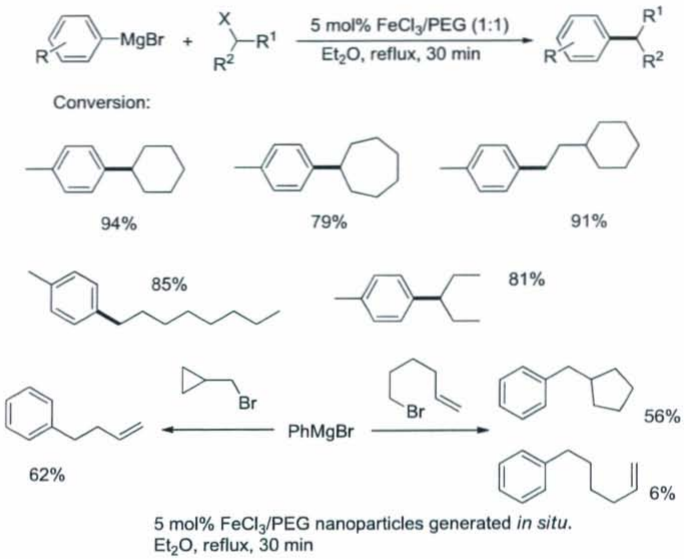

Scheme 1.34 Cross-coupling of alkyl halides with aryl Grignard reagents and tandem cyclization/cross-coupling reaction catalyzed by iron-nanoparticles

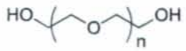

polyethylene glycol (PEG)

Figure 1.4: Structure of PEG

1.3.4.4 Cahiez

Cahiez *et al.* reportedtwo efficient and practical iron-catalyst systems: $Fe(acac)_3$/HMTA/TMEDA (1:1:2) and the complex $[(FeCl_3)_2(TMEDA)_3]$ (Scheme 1.35).[58,59] The quantities of amine ligands were reduced to catalytic amounts compared to Namamura's report.[52] Secondary and primary alkyl bromides were used successfully with aryl or alkenyl Grignard reagents in cross-coupling reactions, and gave good to excellent yields. Furthermore, the system was capable of using functionalized substrates, such as ester or nitrile groups. For the alkylation of alkenyl Grignard reagents, the coupling reaction was highly stereo- and chemoselective.

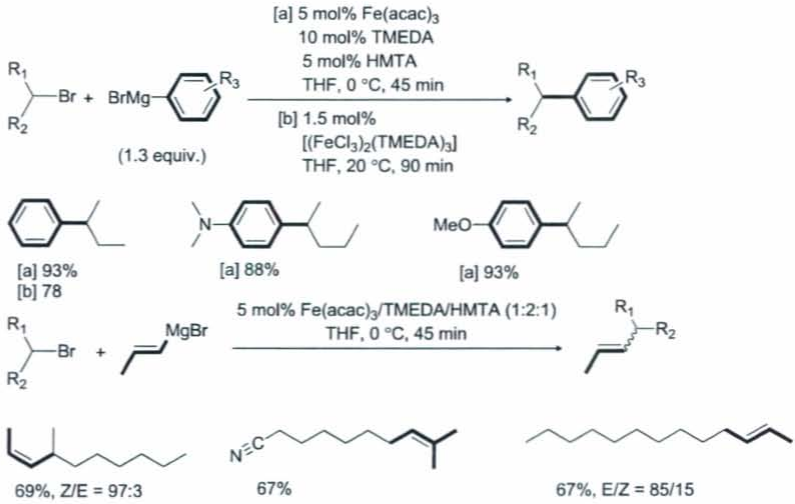

Scheme 1.35 Cross-coupling of alkyl halides with aryl/alkenyl Grignard reagents by Cahiez *et al.*

1.3.4.5 Others

Gaertner and Bica reported that the ionic liquid *n*-butylmethylimidazolium tetrachloroferrate (bmim-$FeCl_4$) could act as an effective and air-stable catalyst to couple primary and secondary alkyl Grignard reagents (Scheme 1.36).[60] Another selling point of this catalytic system was that it could be recycled and reused multiple times.

Scheme 1.36 Cross-coupling of alkyl halides with aryl Grignard reagents catalyzed by iron-ionic liquids

Nagano and Hayashi discovered that in the presence of catalytic amounts of $Fe(acac)_3$ in refluxing diethyl ether without another ligand, primary and secondary alkyl bromides could react with aryl Grignard reagents efficiently (Scheme 1.37).[61]

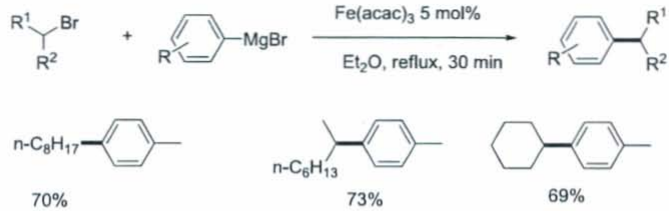

Scheme 1.37 Cross-coupling of alkyl halides with aryl Grignard reagents by Hayashi *et al.*

In 2009, Jacobi von Wangelin and co-workers reported on the first direct cross-coupling reaction between aryl halides and alkyl halides (Scheme 1.38).[62] In the presence of $FeCl_3$/amine, a mixture of an aryl halide (Br or Cl) and alkyl halide (Br or Cl) (1.2 equiv.) with a suspension of Mg in THF at 0 °C to ambient temperature, the corresponding cross-coupling product could be obtained in moderate to good yields. This catalytic system broke the limitation associated with unreactive aryl/alkyl chlorides in some conditions and has the potential for large scale application.

Scheme 1.38 Cross-coupling of alkyl halides with aryl Grignard reagents by Jacobi von Wangelin *et al.*

Successful reports for iron-catalyzed Kumada type $C(sp^3)$-$C(sp^3)$ bond formation reactions are few. Tanabe *et al.* optimized the cross-coupling reactions of *gem*-dichlorocyclopropanes with methyl Grignard reagent using $Fe(DMB)_3$ (DMB: dibenzoylmethane) as a pre-catalyst. The addition of 4-methoxytoluene significantly accelerated the reaction (Scheme 1.39).[63]

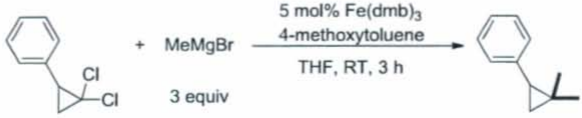

Scheme 1.39 Cross-coupling reactions of gem-dichlorocyclopropanes with methyl Grignard reagent

Another successful report was from Chai and co-workers, who found that $Fe(OAc)_2$ in combination with Xantphos in DME proved to be effective in coupling alkyl halides with alkyl Grignard reagents and gave good to high yields.[64] This was also the first exploitation of an sp^3-sp^3 cross-coupling reaction between primary alkylmagnesium bromides and unactivated primary alkyl bromides (Scheme 1.40).

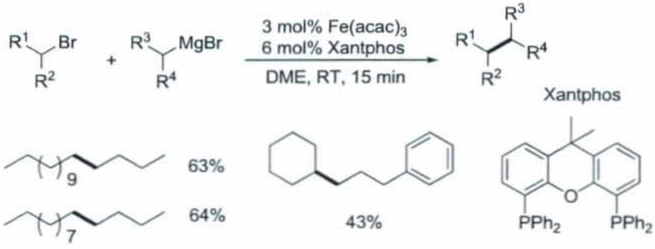

Scheme 1.40 Cross-coupling reactions of alkyl halides with alkyl Grignard reagents

1.4 Summary of Cross-coupling Reactions

A brief account of the current advances in the C-C bond formation reactions promoted by iron has been presented along with important applications. Iron catalysts have catalytic properties complementary to Pd and Ni. For example, Pd/Ni-catalyzed reactions may suffer from unproductive β-H elimination reactions when coupling unactivated alkyl halides and aryl Grignard reagents, but this problem is seldom present in iron-catalyzed sp^3-sp^2 Kumada cross-coupling reactions.

Obviously, aryl group compounds are ubiquitous in natural products. From previous reviews, it is known that many exciting results have been obtained in sp^3-sp^2 Kumada cross-coupling reactions promoted by iron. However, it is still a young field with much room for improvement.

Some key shortcomings include: i) besides Nakamura's report,[52] there are few successful reports of secondary alkyl chlorides as substrates, but they are desirable because they are a more abundant and cheaper feedstocks, ii) there are no reports of success with hindered Grignard reagents, such as 2,6-dimethylphenyl Grignard reagent, iii) there are few successful reports for iron-catalyzed Kumada type reaction using benzyl halides as substrates to give diarylmethane compounds, iv) an easy-to-handle, low catalyst/ligand loading system which has broad functional-group tolerance and is suitable for large scale application is desirable. Thus, the objectives of this thesis are to try to overcome these difficulties and make some breakthrough in these fields.

1.5 Introduction to Microwave Chemistry

Microwave-accelerated metal-catalyzed organic synthesis has attracted great attention since the beginning of this century.[65-68] Commercially available equipment can facilitate reactions through easy programming and documentation of information during the reaction, while at the same time commercial microwave reactors provide high reaction control and straightforward operation. Many reports have shown that microwave assisted organic synthesis catalyzed by transition-metals can bring many advantages that cannot be achieved by conventional heating. In this section, some background information will be provided for the reader. [69]

Under the electromagnetic field, dipolar molecules may give oriented oscillation, which will produce heating because of friction among the molecules. There are two main mechanisms in microwave heating: dipolar polarization and ionic conduction. Dipolar polarization causes the movement of molecules while ionic conduction causes the movement of ions.

Thus, for a substance to be able to generate heat under microwaves it must possess a dipole moment. The heating characteristic of a particular material under microwave irradiation conditions are dependent on the dielectric properties of the material. Highly dielectric materials, like polar organic solvents, lead to a strong absorption of microwaves and consequently to a rapid heating of the medium.

Conventional heating is driven into the substance from outside the vessel and moves through to the inside, including the solvent and the reactants. This is a slow and inefficient method for transferring energy into the reaction system. The reaction cannot

achieve a uniform and stable heat. Furthermore, traditionally used vessels for conventional heating cannot tolerate high pressure. That means it will limit the choice of temperature, solvents and reagents. Modern research microwave reactors allow rapid heating of sealed vessels under monitored pressure. Therefore, reactions can be safely performed at temperatures above the normal boiling point of the solvent, allowing an increased reaction rate in accordance with the Arrhenius equation.

1.6 References

(1) Cornils, B.; Herrmann, W. A. *Applied Homogeneous Catalysis with Organometallic Compounds: A Comprehensive Handbook in Three Volumes,* 2nd Ed.; Wiley-VCH: Weinheim, **2002**.

(2) Nicolaou, K. C.; Bulger, P. G.; Sarlah, D. *Angew. Chem. Int. Ed.* **2005**, *44*, 4442.

(3) Terao, J.; Kambe, N. *Acc. Chem. Res.* **2008**, *41*, 1545.

(4) Fu, G. C. *Acc. Chem. Res.* **2008**, *41*, 1555.

(5) Czaplik, W. M.; Mayer, M.; Cvengroš, J.; Jacobi von Wangelin, A. *ChemSusChem* **2009**, *2*, 396.

(6) Fürstner, A.; Martin, R. *Chem. Lett.* **2005**, *34*, 624.

(7) Martin, R.; Buchwald, S. L. *Acc. Chem. Res.* **2008**, *41*, 1461.

(8) Torborg, C.; Beller, M. *Adv. Synth. Catal.* **2009**, *351*, 3027.

(9) Saito, B.; Fu, G. C. *J. Am. Chem. Soc.* **2007**, *129*, 9602.

(10) Hatakeyama, T.; Hashimoto, T.; Kondo, Y.; Fujiwara, Y.; Seike, H.; Takaya, H.; Tamada, Y.; Ono, T.; Nakamura. M.; *J. Am. Chem. Soc.*, **2010**, *132*, 10674.

(11) Guo, Y.; Young, D. J.; Hor, T. S. A. *Tetrahedron Lett.* **2008**, *49*, 5620.

(12) Negishi, E.; Huang, Z.; Wang, G.; Mohan, S.; Wang, C.; Hattori, H. *Acc. Chem. Res.* **2008**, *41*, 1474.

(13) Zhou, J.; Fu, G. C. *J. Am. Chem. Soc.* **2003**, *125*, 14726.

(14) Smith, S. W.; Fu, G. C. *Angew. Chem. Int. Ed.* **2008**, *47*, 9334.

(15) Son, S.; Fu, G. C. *J. Am. Chem. Soc.* **2008**, *130*, 2756.

(16) Phapale, V. B.; Guisán-Ceinos, M.; Buñuel, E.; Cárdenas, D. J. *Chem. Eur. J.* **2009**, *15*, 1268.

(17) Hatakeyama, T.; Nakagawa, N.; Nakamura, M. *Org. Lett.* **2009**, *11*, 4496.

(18) Ito, S.; Fujiwara, Y.; Nakamura, E.; Nakamura, M. *Org. Lett.* **2009**, *11*, 4306.

(19) Cahiez, G.; Foulgoc, L.; Moyeux, A. *Angew. Chem. Int. Ed.* **2009**, *48*, 2969.

(20) Bedford, R. B.; Huwe, M.; Wilkinson, M. C. *Chem. Commun.* **2009**, 600.

(21) Trzeciak, A. M.; Ziółkowski, J. J. *Coord. Chem. Rev.* **2005**, *249*, 2308.

(22) Sherry, B.D.; Fürstner, A., *Acc. Chem. Res.* **2008**, *41*, 1500.

(23) Inamoto, K.; Kuroda, J.; Danjo, T.; Sakamoto, T. *Synlett* **2005**, 1624.

(24) Ma, S.; Wang, H.; Gao, K.; Zhao, F. *J. Mol. Catal. A: Chem.* **2006**, *248*, 17.

(25) Loska, R.; Rao Volla, C.; Vogel, P. *Adv. Synth. Catal.* **2008**, *350*, 2859.

(26) Seyferth, D. *Organometallics* **2009**, *28*, 1598.

(27) Tamao, K.; Kiso, Y.; Sumitani, K.; Kumada, M. *J. Am. Chem. Soc.* **1972**, *94*, 9268.

(28) Percival, W. C.; Wagner, R. B.; Cook, N. C. *J. Am. Chem. Soc.* **1953**, *75*, 3731.

(29) Duplais, C.; Bures, F.; Sapountzis, I.; Korn, T. J.; Cahiez, G.; Knochel, P. *Angew. Chem. Int. Ed.* **2004**, *43*, 2968.

(30) Kumada, M.; Kochi, J. K. *J. Am. Chem. Soc.* **1971**, *93*, 1487.

(31) Cahiez, G.; Avedissian, H. *Synthesis* **1998**, 1199.

(32) Fürstner, A.; De Souza, D.; Parra-Rapado, L.; Jensen, J. T. *Angew. Chem. Int. Ed.* **2003**, *42*, 5358.

(33) Fürstner, A.; Hannen, P. *Chem. Eur. J.* **2006**, *12*, 3006.

(34) Ottesen, L. K.; Ek, F.; Olsson, R. *Org. Lett.* **2006**, *8*, 1771.

(35) Seck, M.; Franck, X.; Hocquemiller, R.; Figadère, B.; Peyrat, J.; Provot, O.; Brion, J.; Alami, M. *Tetrahedron Lett.* **2004**, *45*, 1881.

(36) Fürstner, A.; Leitner, A.; Méndez, M.; Krause, H. *J. Am. Chem. Soc.* **2002**, *124*, 13856.

(37) Fürstner, A.; Martin, R.; Krause, H.; Seidel, G.; Goddard, R.; Lehmann, C. W. *J. Am. Chem. Soc.* **2008**, *130*, 8773.

(38) Bogdanović, B.; Schwickardi, M. *Angew. Chem. Int. Ed.* **2000**, *39*, 4610.

(39) Hocek, M.; Dvořáková, H. *J. Org. Chem.* **2003**, *68*, 5773.

(40) Scheiper, B.; Bonnekessel, M.; Krause, H.; Fürstner, A. *J. Org. Chem.* **2004**, *69*, 3943.

(41) Nagano, T.; Hayashi, T. *Org. Lett.* **2005**, *7*, 491.

(42) Cahiez, G.; Chaboche, C.; Mahuteau-Betzer, F.; Ahr, M. *Org. Lett.* **2005**, *7*, 1943.

(43) Cahiez, G.; Moyeux, A.; Buendia, J.; Duplais, C. *J. Am. Chem. Soc.* **2007**, *129*, 13788.

(44) Xu, X.; Cheng, D.; Pei, W. *J. Org. Chem.* **2006**, *71*, 6637.

(45) Quintin, J.; Franck, X.; Hocquemiller, R.; Figadère, B. *Tetrahedron Lett.* **2002**, *43*, 3547.

(46) Boully, L.; Darabantu, M.; Turck, A.; Plé, N. *J. Heterocycl. Chem.* **2005**, *42*, 1423.

(47) Korn, T. J.; Cahiez, G.; Knochel, P. *Synlett* **2003**, 1892.

(48) Sapountzis, I.; Lin, W.; Kofink, C. C.; Despotopoulou, C.; Knochel, P. *Angew. Chem. Int. Ed.* **2005**, *44*, 1654.

(49) Kofink, C. C.; Blank, B.; Pagano, S.; Götz, N.; Knochel, P. *Chem. Commun.* **2007**, 1954.

(50) Hatakeyama, T.; Nakamura, M. *J. Am. Chem. Soc.* **2007**, *129*, 9844.

(51) Martin, R.; Fürstner, A. *Angew. Chem. Int. Ed.* **2004**, *43*, 3955.

(52) Nakamura, M.; Matsuo, K.; Ito, S.; Nakamura, E. *J. Am. Chem. Soc.* **2004**, *126*, 3686.

(53) Guérinot, A.; Reymond, S.; Cossy, J. *Angew. Chem. Int. Ed.* **2007**, *46*, 6521.

(54) Bedford, R. B.; Bruce, D. W.; Frost, R. M.; Goodby, J. W.; Hird, M. *Chem. Commun.* **2004**, 2822.

(55) Bedford, R. B.; Bruce, D. W.; Frost, R. M.; Hird, M. *Chem. Commun.* **2005**, 4161.

(56) Bedford, R. B.; Betham, M.; Bruce, D. W.; Danopoulos, A. A.; Frost, R. M.; Hird, M. *J. Org. Chem.* **2006**, *71*, 1104.

(57) Bedford, R. B.; Betham, M.; Bruce, D. W.; Davis, S. A.; Frost, R. M.; Hird, M. *Chem. Commun.* **2006**, 1398.

(58) Cahiez, G.; Habiak, V.; Duplais, C.; Moyeux, A. *Angew. Chem. Int. Ed.* **2007**, *119*, 4442.

(59) Cahiez, G.; Duplais, C.; Moyeux, A. *Org. Lett.* **2007**, *9*, 3253.

(60) Bica, K.; Gaertner, P. *Org. Lett.* **2006**, *8*, 733.

(61) Nagano, T.; Hayashi, T. *Org. Lett.* **2004**, *6*, 1297.

(62) Czaplik, W. M.; Mayer, M.; Jacobi von Wangelin, A. *Angew. Chem. Int. Ed.* **2009**, *48*, 607.

(63) Nishii, Y.; Wakasugi, K.; Tanabe, Y. *Synlett* **1998**, 67.

(64) Dongol, K. G.; Koh, H.; Sau, M.; Chai, C. L. L. *Adv. Synth. Catal.* **2007**, *349*, 1015.

(65) Caddick, S.; Fitzmaurice, R. *Tetrahedron* **2009**, *65*, 3325.

(66) Kappe, C. O.; Dallinger, D. *Mol. Divers.* **2009**, *13*, 7.

(67) Kirschning, A.; Solodenko, W.; Mennecke, K. *Chem. Eur. J.* **2006**, *12*, 5972.

(68) Nilsson, P.; Olofsson, K.; Larhed, M. *Top. Curr. Chem.* **2006**, *266*, 103.

(69) Kappe, C. O.; Dallinger, D.; Murphree, S.; *Practical Microwave Synthesis for Organic Chemists: Strategies, Instruments, and Protocols;* Wiley-VCH: Weinheim. **2008**.

Chapter 2. Synthesis and Characterization of Amine-bis(phenolate) Ligands and Iron (III) Complexes

2.1 Introduction and research objectives

The Kozak group has previously reported that tetradentate amine-bis(phenolate)-ether iron(III) complexes catalyze cross-coupling reactions with primary and secondary alkyl halides bearing β-hydrogens.[1] The ligands used were easily synthesized and gave five-coordinate Fe(III) halide complexes that were air- and moisture-stable. The use of a suitable ligand is expected to give controlled catalysis and decrease or eliminate the formation of undesirable by-products as described in Chapter 1. Equation 2.1 shows a representative cross-coupling reaction of an aryl Grignard with a cyclic alkyl bromide. In addition to the desired cross-coupled product, one may observe several by-products, including the aryl of quenched Grignard reagent, homo-coupling of the Grignard and alkyl halide, respectively, as well as β-hydride elimination and hydrodehalogenation. By using a low-coordinate environment, the transition metal centre may become a more reactive for catalysis. Therefore, it is anticipated that tridentate ligands would lead to exciting new chemistry.

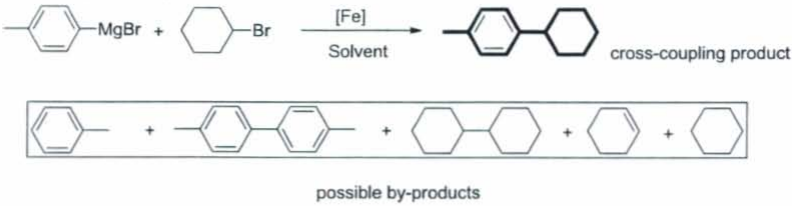

Equation 2.1 Iron-catalyzed C-C cross-coupling reactions.

2.2 Synthesis of the $[O_2N]$ – type ligands

Ligand precursors were synthesized via a modified Mannich condensation reactions in water.[3] There are single pot reactions using a phenol, an amine and formaldehyde (Scheme 2.1). The mixtures were refluxed for 12 h in water and the solids were separated using filtration. Some of the products were obtained as viscous yellow oils, which were collected by decanting the aqueous phase. Removal of residual solvent under vacuum and washing the residue with methanol allowed isolation of these products as white solids. The ligands were purified by recrystallization from hot ethanol. A ligand library of seven combinations was prepared. Disubstituted phenols possessing methyl, *t*-butyl and fluoro groups were employed while the amines possessed either *n*-propyl, isopropyl or benzyl groups (Figure 2.1).

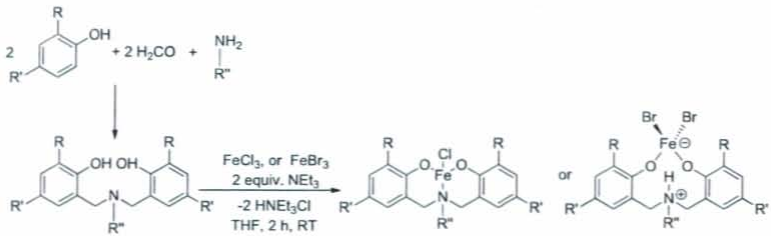

Scheme 2.1 General procedure for the ligands and complexes synthesis

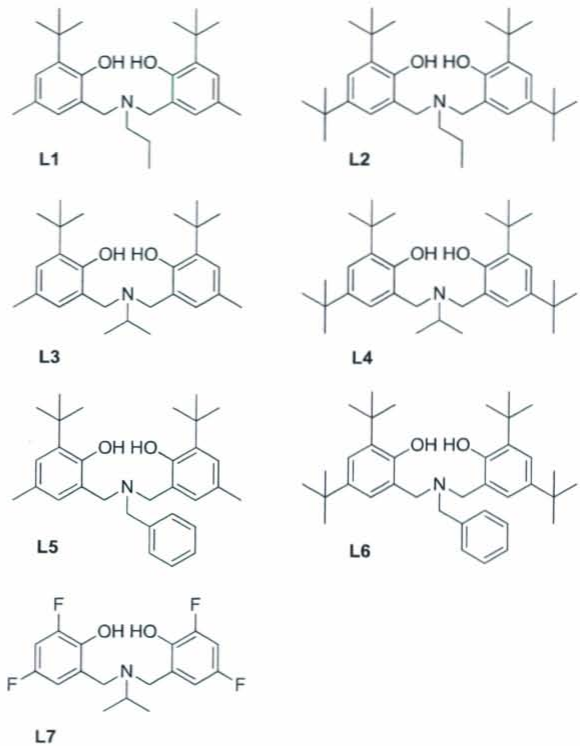

Figure 2.1: Library of ligands synthesized

2.3 Characterization of the ligands

The ^{1}H and ^{13}C NMR spectra confirmed the formation of the ligands. The signal of the phenolic OH cannot be identified clearly, this may be because the protons of the phenolic OH undergo exchange. A representative ^{1}H NMR spectrum of a pure ligand, **L1**, is shown in Figure 2.2, which will be discussed in detail below.

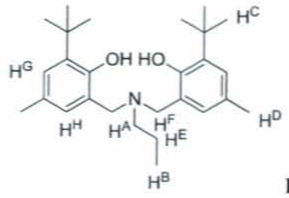

L1

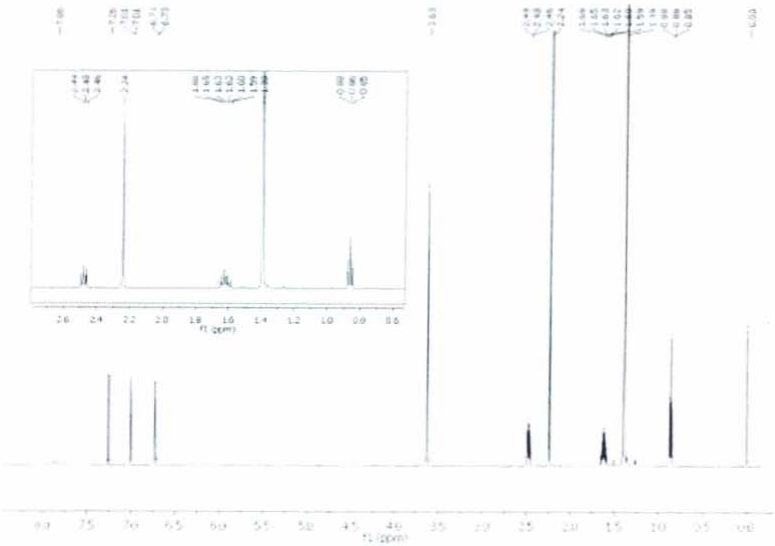

Figure 2.2: ^{1}H NMR spectrum of (**L1**) $H_2[O_2N]^{BuMenPr}$

The ^{1}H NMR spectrum for **L1** measured in $CDCl_3$ (Figure 2.2) exhibited two singlets at 7.03 ppm and 6.76 ppm. These singlets correspond to the aromatic H atoms of the benzene ring. The singlet at 3.66 ppm is ArCH_2. This means there is free rotation in solution resulting in equivalent proton environments. The triplet at 2.48 ppm is assigned to NCH_2CH_2, which is split due to coupling to the neighbouring methylene group, H^E. The expected singlet at 2.27 ppm corresponds to the H atoms of the methyl groups on the benzene ring. The multiplet at 1.65 ppm results from the methylene protons coupled to the adjacent methylene and methyl groups, H^A and H^B, respectively. The singlet at 1.42 ppm corresponds to the H atoms of the *t*-butyl groups on the benzene ring. Lastly, the triplet at 0.89 ppm results from the H^B protons is $CH_2CH_2CH_3$, which is split into a triplet by the protons H^E.Table 2.1 summarizes the ^{1}H NMR spectrum.

Table 2.1: Assignment of resonances in the ^{1}H NMR spectrum of **L1**

Protons	No. of equiv. protons	Chemical Shift (δ)	Peak	Proton types
H^H	2	7.03	s	Aromatic
H^G	2	6.76	s	Aromatic
H^F	4	3.66	s	ArCH_2
H^A	2	2.48	t	NCH_2CH_2
H^D	6	2.27	s	ArCH_3
H^E	2	1.65	m (tq)	$CH_2CH_2CH_3$
H^C	18	1.42	s	$C(CH_3)_3$
H^B	3	0.89	t	$CH_2CH_2CH_3$

2.4 Synthesis of Fe(III) complexes

As mentioned above, iron(III) complexes of tetradent amine-bis(phenolate) ligands catalyze cross-coupling reactions with primary and secondary alkyl halides bearing β-hydrogens. The hard aryloxide and amine donors of these ligands stabilize metals in higher oxidation states and it was anticipated tridentate ligands may give more reactive catalysts. The Fe-complexes can be prepared by a protonolysis reaction between the ligand precursor and the anhydrous Fe(III) salts.[4]

A THF solution of anhydrous $FeCl_3$ was added dropwise to a THF solution of the ligand at room temperature (Scheme 2.1). A dark red-purple solution was generated, to which NEt_3 was added to neutralize the HCl produced. However, addition of excess base may result in a yellow-brown precipitate. Stirring was continued for 2 h. The mixture was filtered through Celite and the solvents and other volatile components were removed in *vacuo*. A dark black-purple product was obtained and crystals were obtained from toluene. A similar procedure was followed while preparing $FeBr_2[O_2NH]^{BuMe\mathit{n}Pr}$ complex **8**, using $FeBr_3$ (Figure 2.3). The product obtained using $FeBr_3$ differed from that obtained from $FeCl_3$ when using this method. Only one bromide ligand was displaced but both phenolic –OH sites were deprotonated. In addition to forming one equiv. of HBr, the protonation of the central amine was observed, producing a quaternized ammonium fragment. The structure of **8** is discussed in the next section.

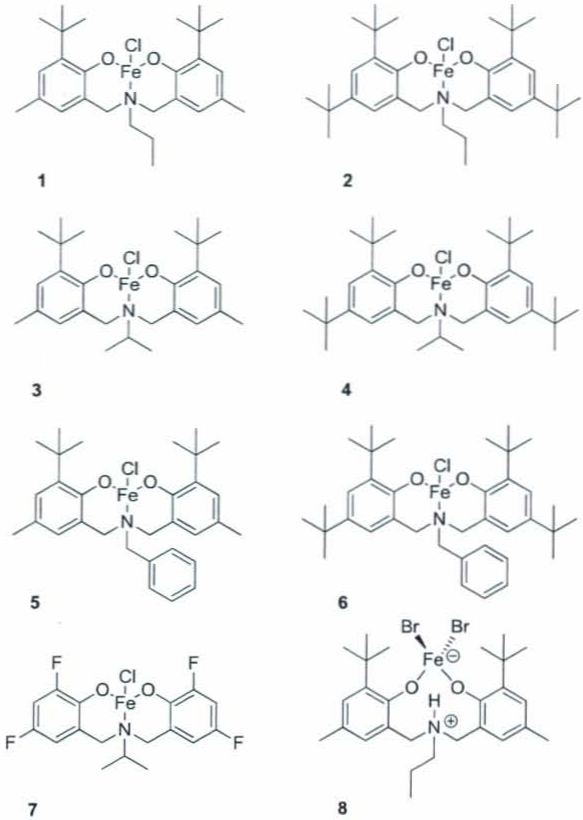

Figure 2.3: Library of iron(III) complexes synthesized

2.5 Characterization of Fe(III) complexes

2.5.1 MALDI-TOF MS

MALDI-TOF mass spectrometry was used to analyze the metal complexes. Anthracene was the chosen matrix. The mass spectrum exhibited peaks at masses higher than expected for the monometallic complexes shown in Figure 2.3. This suggested the formation of multimetallic species, such as dimers, in the gas phase. For complex **1**, a fragment possibly arising from the $\{FeCl[O_2N]^{BuMenPr}\}_2$ (2M) complex was observed $[2M\text{-}Cl]^+$, (965.4531) in addition to the molecular-ion and fragment peaks of the monometallic complexes, namely, $[M]^+$, (m/z = 499.1992); $[M\text{-}Cl]^+$, (m/z = 464.2276); $[M\text{-}FeCl]^+$, (m/z = 411.315) under mass-spectrometic conditions (Figure 2.4). Amine-bis(phenolate) complexes of iron(III) previously reported by the Kozak group typically show loss of the halide ligand and the $[M^+]$ ion peak is very weak. For tridentate ligands the iron halide complexes would be four-coordinate. Therefore, it is possible for the metal centre to achieve a more stable five- coordinate geometry through bridging ligands. Both the halide ligand and the phenolate-oxygen donors possess additional lone pairs capable of forming bridges between two iron centres. Thus, the mass spectrometric data may give some indication that dimeric structures of the iron(III) complexes may be expected in the solid state. Indeed, such structures were observed via single crystal X-ray diffraction, which will be discussed in the next section.

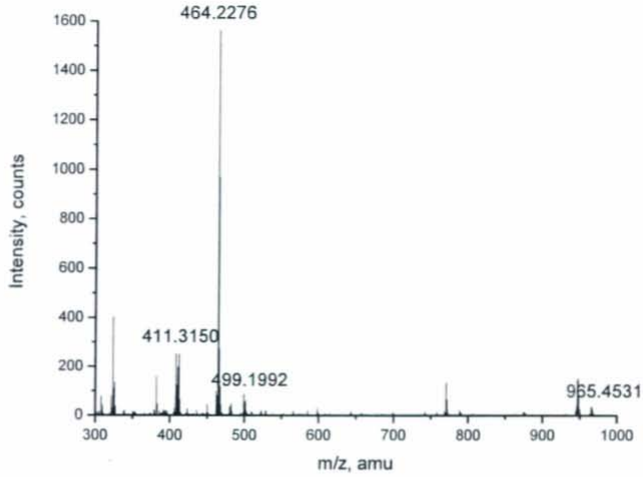

Figure 2.4: MALDI-TOF MS for $\{FeCl[O_2N]^{BuMenPr}\}_2$ (**1**)

The mass spectrum obtained for **5** differs slightly from that obtained for **1**. That is, unlike the spectrum of **1**, no peaks suggesting the existance of $\{FeCl[O_2N]^{BuMeBn}\}_2$ (2M) were observed. Instead, only lower mass fragments, namely $[M\text{-}Cl]^+$, (m/z = 512.2318) and $[M\text{-}FeCl]^+$, (m/z = 456.167) were observed under MALDI conditions (Figure 2.5). At this point, it is interesting to relate some pertinent structural parameters for complexes **1** and **5**. A comparison of the Fe-Cl and Fe-O distances shows that these bond lengths in **5** are longer than those in **1**, meaning the Fe-Cl and Fe-O bond energies in **5** are lower than those in **1**. Thus, it is likely that fragmentation of **5** under MALDI conditions is more extensive than in **1**, therefore ions such as $[2M\text{-}Cl]^+$ and $[M]^+$ are not observed for **5** under our conditions. Similar observations can be made in the mass spectrum of complex **2** (see

Appendix Figure A7), but a high mass peak (m/z = 896.4744, presently unassigned) was also observed.

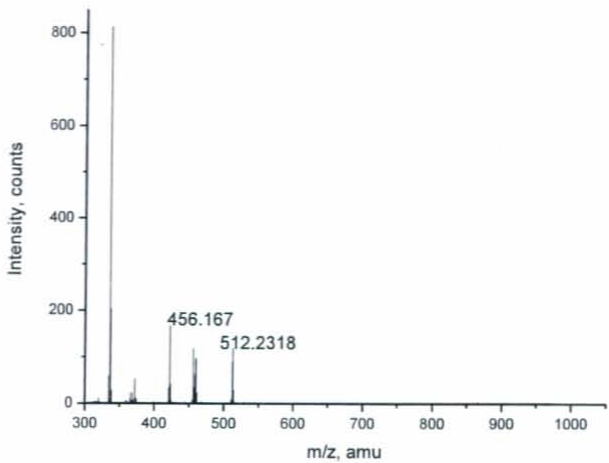

Figure 2.5: MALDI-TOF MS for $\{FeCl[O_2N]^{BuMeBn}\}_2$ (**5**)

The molecular ion for $FeBr_2[O_2NH]^{BuMe\mathit{n}Pr}$ (**8**) was observed as well as appropriate fragment ions: $[M]^+$, (m/z = 626.3681); $[M\text{-}Br]^+$, (m/z = 545.150); $[M\text{-}2Br]^+$, (m/z = 465.233); $[M\text{-}FeBr_2]^+$, (m/z = 408.2807) under MALDI conditions (Figure 2.6). These results are similar to iron(III) bromide complexes that the Kozak group previously reported.[4] The $[M^+]$ ion peak is very weak, while peaks arising from loss of one or both bromide ligands are higher in intensity. Unlike complex **1**, no dimeric fragment can be detected from the mass spectrum. However, the presence of a peak at 626.3681 supports the existence of a protonated central amine, which produces a quaternized ammonium

fragment, and two bromides on an iron ion. Alternatively, the phenolate oxygen may remain protonated leaving the nitrogen atom to act as a neutral donor. Clearly, molecular structure data obtained from single crystal X-ray diffraction is required to unequivocally confirm the nature of these complexes, at least in the solid state. These data will be discussed in the next section.

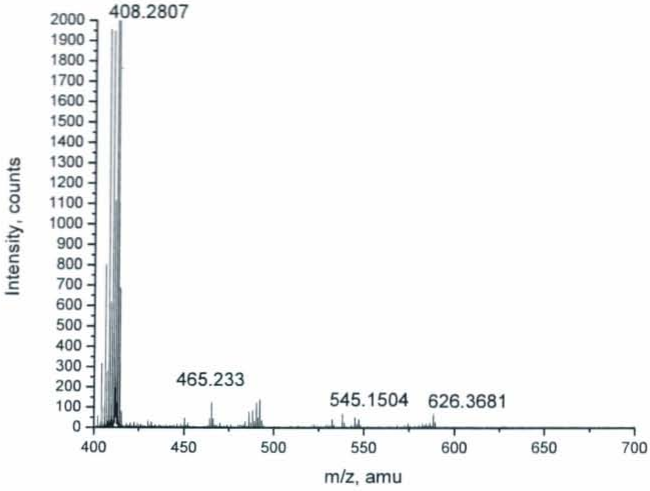

Figure 2.6: MALDI-TOF MS for $FeBr_2[O_2NH]^{BuMenPr}$ (**8**)

2.5.2 Molecular structure determinations

In the solid state, complex **1** exhibits a centrosymmetric dimeric structure resulting in trigonal bipyramidal Fe^{III} centres bridged by chloride ligands as shown in Figure 2.7.

Complete Tables of bond lengths, angles and torsion angles are given in the Apppendix. The Fe(1)···Fe(2) interatomic distance of 3.4658(7) Å precludes any bonding interaction between the metal centres. The two phenolate oxygen donor atoms and a bridging chloride occupy the equatorial plane around Fe, where the sum of bond angles is 359.88° indicating near perfect planarity. The amine nitrogen and another bridging chloride take up the axial positions, giving a Cl(2)-Fe(1)-N(1) bond angle of 178.32(9)°. The *cis*-orientated chloride ligands are nearly orthogonal with a Cl(1)-Fe(1)-Cl(2) bond angle of 87.36(4)°. The asymmetric nature of the bridging chlorides is demonstrated by the different Fe-Cl bond lengths of 2.298(2) for Fe(1)-Cl(1) and 2.4911(18) Å for Fe(1)-Cl(2). Since the Kozak group has previously reported mononuclear trigonal bipyramidal iron(III) complexes of related tetradentate diamine-bis(phenolate) ligands (abbreviated [O_2NN'], where N' represents a pendant dimethylaminoethyl or pyridyl arm),[4] an informative comparison of bond distances can be made. For example, the terminally bonded Fe-Cl bond lengths in FeCl[O_2NN'] of 2.3051(10) and 2.2894(5) Å are very similar to the shorter Fe-Cl interaction observed in **1**. The Fe-N distance of 2.183(3) Å is shorter than those observed in previously reported mononuclear iron(III) complexes from the Kozak group, which show Fe-N distances of 2.2706(15) and 2.248(2) Å between the five-coordinate iron atom and the central amine nitrogen donor. The phenolate oxygen atoms exhibit bond distances of 1.818(2) and 1.817(2) Å for Fe(1)-O(1) and Fe(1)-O(2), respectively. These interactions are shorter than those observed in Kozak's FeCl[O_2NN'] complexes, where average Fe-O distances of 1.86 Å are observed. Detailed crystallographic data and refinements for **1** are shown in Table 2.2.

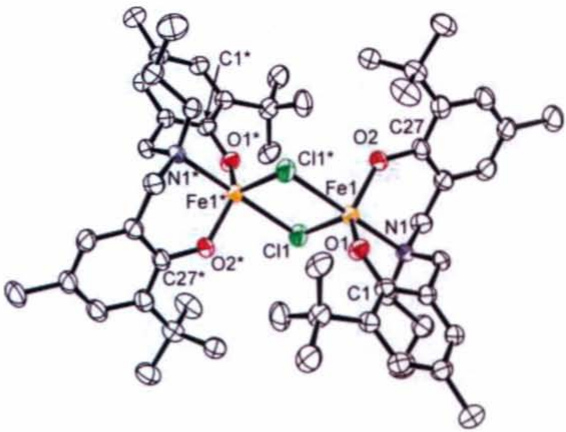

Figure 2.7: Molecular structure (ORTEP) and partial atom labelling of **1**.

Ellipsoids shown at 50% probability. Hydrogen atoms omitted for clarity.

Table 2.2: Crystallographic data and refinements for **1**

Chemical formula	$C_{54}H_{78}Cl_2Fe_2N_2O_4$	V/ Å^3	1331.9(16)
Formula weight	1001.82	Z	1
T/K	123	D_c/g cm^{-3}	1.249
Crystal color, Habit	black, chunk	μ(Mo-Kα)/cm^{-1}	6.88
Crystal dimensions/mm	0.31 × 0.23 × 0.21	F(000)	534
Crystal system	Triclinic	θ range for collection/°	2.5 to 31.1
Space group	P-1 (#2)	Reflections collected	10935
a/ Å	9.997(6)	Independent reflections	5309
b/ Å	11.386(8)	R(int)	0.0467
c/ Å	12.879(9)	R, wR^2 (all)	0.0961, 0.2516
α/°	80.65(5)	R, wR^2 [$I > 2\sigma(I)$]	0.0916, 0.5309
β/°	71.77(4)	GOF on F^2	1.104
γ/°	73.69(5)		

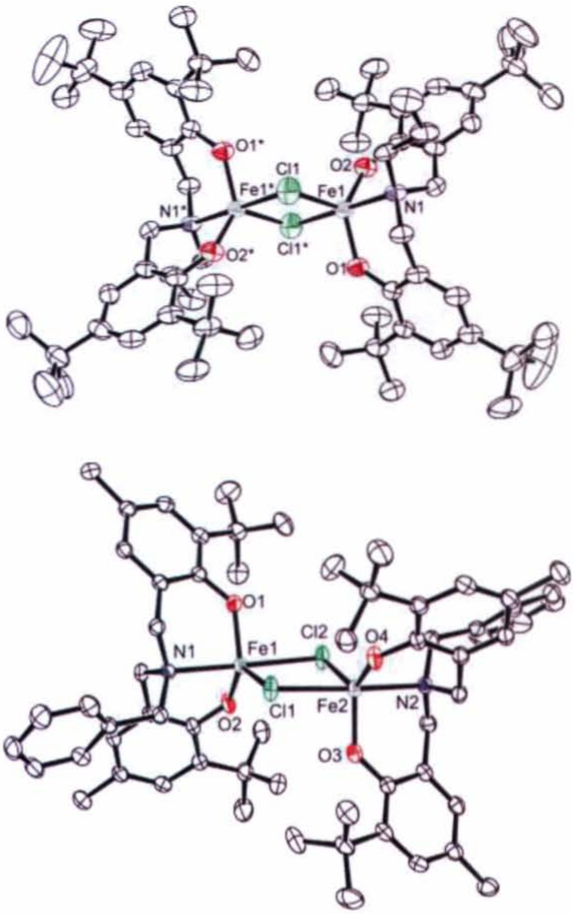

Figure 2.8: Molecular structures (ORTEP) and partial atom labelling of **2** (top) and **5** (bottom). Ellipsoids shown at 50% probability. Hydrogen atoms omitted for clarity.

Structures of two other iron(III) chloride complexes (**2** and **5**) were obtained and are shown in Figure 2.8. Detailed crystallographic data and refinements for **2** and **5** are shown in Tables 2.4 and 2.5, respectively. Complexes **2** and **5** exhibit similar dimeric

structures resulting in trigonal bipyramidal Fe^{III} centres bridged by chloride ligands, similar to that observed in complex **1**. Table 2.3 presents a comparison of the selected bond lengths and angles of these three complexes, which shows the effect of different substituents of the ligands (**L1**, **L2**, and **L5**). The Fe-O, Fe-N and Fe-Cl distances in **1**, **2** and **5** are experimentally identical to each other. The bond angles around each iron centre in these compounds, however, show moderate variation. Most notable is the difference in O-Fe-O bond angles, with benzylamine-containing complex **5** exhibiting the narrowest angle whereas the *n*-propylamine-containing **1** and **2** contain slightly wider O-Fe-O angles. The ligand **L2**, possessing 2,4-*tert*-butyl groups may be considered slightly more electron rich than **L1**, which possesses 2-*tert*-butyl,4-methyl groups. Therefore, the marginal differences in bond lengths around the iron centre may be attributed to subtle variations in electronic effects, as well as modest steric differences. Detailed crystallographic data and refinements for **2** and **5** are shown in Tables 2.4 and 2.5 respectively.

Table 2.3: Selected bond lengths (Å) and bond angles (°) of **1**, **2** and **5**. Symmetry operators used to generate equivalent atoms: (*) -x + 1, -y + 1, -z + 1.

	1	**2**	**5**
Fe(1)-O(1)	1.818(3)	1.825(4)	1.8276(13)
Fe(1)-O(2)	1.817(3)	1.834(4)	1.8222(12)
Fe(1)-N(1)	2.183(4)	2.184(4)	2.1819(10)
Fe(1)-Cl(1)	2.298(2)	2.315(3)	2.3290(4)
Fe(1)-Cl(1)*	2.4911(18)	2.495(3)	
Fe(1)-Cl(2)			2.5025(3)
O(1)-Fe(1)-O(2)	124.63(14)	128.99(17)	119.36(5)
N(1)-Fe(1)-Cl(1)	93.92(10)	91.86(12)	93.59(3)
N(1)-Fe(1)-Cl(1)*	178.32(9)	176.57(11)	
N(1)-Fe(1)-Cl(2)			177.28(3)
Cl(1)-Fe(1)-Cl(1)*	87.36(6)	91.27(9)	
Cl(1)-Fe(1)-Cl(2)			84.341(14)
Fe(1)-Cl(1)-Fe(1)*	92.64(6)	88.73(9)	
Fe(1)-Cl(1)-Fe(2)			95.384(14)
O(1)-Fe(1)-Cl(1)	113.18(11)	118.89(14)	114.96(4)
O(1)-Fe(1)-Cl(1)*	89.86(11)	89.23(13)	
O(1)-Fe(1)-Cl(2)			88.91(3)
O(2)-Fe(1)-Cl(1)	122.08(12)	112.12(13)	125.52(4)
O(2)-Fe(1)-Cl(1)*	89.41(11)	89.18(12)	
O(2)-Fe(1)-Cl(2)			92.60(3)

O(1)-Fe(1)-N(1)	88.99(13)	88.04(16)	90.38(4)
O(2)-Fe(1)-N(1)	90.62(13)	90.93(16)	90.03(4)

Table 2.4: Crystallographic data and refinements for **2**

Chemical formula	$C_{66}H_{102}Cl_2Fe_2N_2O_4$	V/ Å^3	1663(2)
Formula weight	1170.14	Z	1
T/K	123	D_c/g cm^{-3}	1.168
Crystal color, Habit	dark brown	μ(Mo-Kα)/cm^{-1}	0.560
Crystal dimensions/mm	0.22×0.19×0.15	F(000)	630
Crystal system	Triclinic	θ range for collection/°	2.7660 to 30.8904
Space group	P-1 (#2)	Reflections collected	11654
a/ Å	10.248(8)	Independent reflections	5702
b/ Å	11.616(9)	R(int)	0.1134
c/ Å	14.662(12)	R, wR^2 (all)	0.1381, 0.3987
α/°	99.827(14)	R, wR^2 [$I > 2\sigma(I)$]	0.1327, 0.3793
β/°	104.057(12)	GOF on F^2	1.627
γ/°	92.03(2)		

Table 2.5: Crystallographic data and refinements for **5**

Chemical formula	$C_{62}H_{78}Cl_2Fe_2N_2O_4$	V/ Å^3	2917.2(10)
Formula weight	1097.91	Z	2
T/K	153	D_c/g cm^{-3}	1.250
Crystal color, Habit	Dark purple, prism	μ(Mo-Kα)/cm^{-1}	6.35
Crystal dimensions/mm	0.46 × 0.41 × 0.30	F(000)	1164
Crystal system	Triclinic	θ range for collection/°	2.3254-30.5381
Space group	P-1 (#2)	Reflections collected	27483
a/ Å	13.052(3)	Independent reflections	11990
b/ Å	13.686(3)	R(int)	0.0215
c/ Å	18.072(3)	R, wR^2 (all)	0.0382, 0.0948
α/°	100.960(2)	R, wR^2 [$I > 2\sigma(I)$]	0.0361, 0.0928
β/°	101.664(3)	GOF on F^2	1.045
γ/°	106.866(2)		

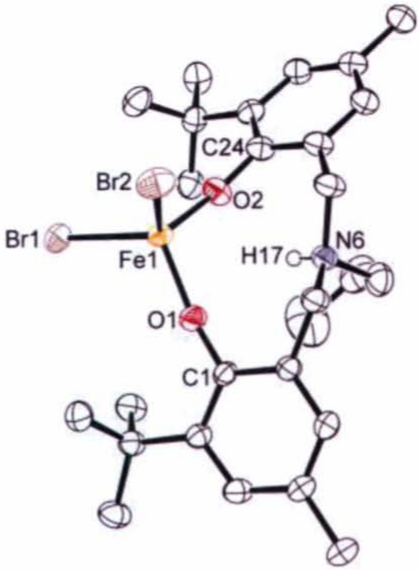

Figure 2.9: Molecular structure (ORTEP) and selective atom labelling of **8**. Ellipsoids shown at 50% probability. Hydrogen atoms, except for H17, are omitted for clarity.

In the solid state, complex **8** exhibits a monomeric structure resulting in tetrahedral Fe^{III} centres as shown in Figure 2.9. Tables of bond lengths, angles and dihedral angles are given in the Appendix (Tables A7, A8 and A9). Unlike complexes **1**, **2**, and **5**, and also unlike the previously reported iron(III) complexes of amine-bis(phenolate) ligands reported by the Kozak group, the bis(phenolate) ligand binds in a bidentate rather than a tridentate (or tetradentate fashion). As discussed above in Section 2.5.1, the mass spectrometry data suggested a complex possessing an iron atom, two bromines and a monoprotonated amine-bis(phenolate) ligand, i.e. [O_2NH]. The single crystal X-ray diffraction data confirm and clarify the connectivity and structure of

complex **8**. The central amine nitrogen atom is protonated resulting in a quaternized amonium group. The two phenolate groups remain anionic, thereby resulting in a net monoanionic amonium-bis(phenolate) ligand. The iron(III) centre is further bonded to two bromide ions, hence the four-coordinate iron(III) centre is formally anionic, resulting in an overall zwitterionic complex. The two phenolate oxygen donor atoms and two bromide ions compose the tetrahedral ligand sphere around Fe. The bond angles around the metal range from 105.23(15)° to 112.88(11)°, which are only moderately distorted from the ideal tetrahedral angle of 109.5°. The bond lengths of Fe-Br(1) and Fe-Br(2) are slightly asymmetrical at 2.3569(7) and 2.3723(7) Å, respectively. Since the Kozak group has previously reported mononuclear square pyramidal iron(III) bromide complexes of related linear tetradentate *N,N*-dimethyl-*N',N'*-bis(2-methylene-4-methyl-6-*tert*-butylphenolate)ethylenediamine ligand (abbreviated $[O_2N_2]$),[4] an informative comparison of bond distances can be made. For example, the terminally bonded Fe-Br bond length in $FeBr[O_2N_2]$ of 2.3683(11) Å appears to be intermediate of the two Fe-Br bond lengths observed in **8**. The phenolate oxygen atoms exhibit bond distances to iron of 1.828(3) and 1.836(3) Å for Fe(1)-O(1) and Fe(1)-O(2), respectively. These interactions are similar to those observed in $FeBr[O_2N_2]$ complexes, where average Fe-O distances of 1.837 Å are observed. Detailed crystallographic data and refinements for **8** are shown in Table 2.6.

Table 2.6: Crystallographic data and refinements for **8**

Chemical formula	$C_{30.50}H_{44}Br_2FeNO_2$	V/ Å^3	3213.3(9)
Formula weight	672.34	Z	4
T/K	123	D_c/g cm^{-3}	1.390
Crystal color, Habit	black, irregular	μ(Mo-Kα)/cm^{-1}	29.82
Crystal dimensions/mm	0.30 × 0.29 × 0.28	F(000)	1384.0
Crystal system	Monoclinic	θ range for collection/°	2.3498-30.8607
Space group	$P2_1/n$ (#14)	Reflections collected	40002
a/ Å	11.5336(18)	Independent reflections	6630
b/ Å	16.678(3)	R(int)	0.0494
c/ Å	16.891(3)	R, wR^2 (all)	0.0618, 0.1674
α/°	98.510(3)	R, wR^2 [$I > 2\sigma(I)$]	0.0573, 0.6630
β/°	90	GOF on F^2	1.075
γ/°	90		

Although a large number of systems containing the high-spin, tetrahedral $[FeX_4]^-$ anions are known,[5,6] there are few neutral, heteroleptic tetrahedral iron(III) complexes in the literature. [FeI([D_5]pyridine)(N-RAr$_f$)$_2$] (R = $C(CD_3)_2CH_3$, Ar$_f$ = 2,5-C_6H_3FMe)[7] and the thiourea iron(III) iodide complex $FeI_3[SC(NMe_2)_2]$[8] are two examples. Moreover, tetrahedral iron(III) complexes bonded to two halides atoms normally exhibit dimeric structures. The Leznoff group has reported two such examples, $\{FeBr[MesN(SiMe_2)]_2O\}_2$[9] and $\{FeBr_2Li[Me_3PhN(SiMe_2)]_2O\}_2$[10] (Figure 2.10). The iron(III) complex, $FeBr_2[O_2NH]^{BuMenPr}$ (**8**), therefore shows an unusual monomeric, neutral tetrahedral structure. A comparison of selected bond lengths for **8**, $\{FeBr[MesN(SiMe_2)]_2O\}_2$ and $\{FeBr_2Li[Me_3PhN(SiMe_2)]_2O\}_2$ is shown in the Table 2.7. As expected, the terminal Fe-Br distances of **8** are shorter than those in the bromide-

bridged dimeric complexes.

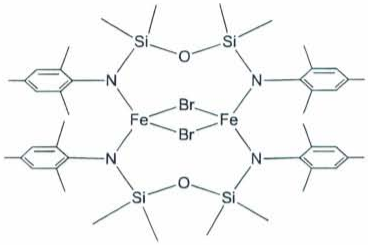

{FeBr[MesN(SiMe$_2$)]$_2$O}$_2$

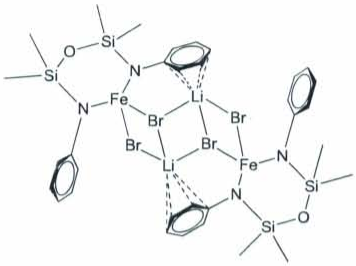

{FeBr$_2$Li[Me$_3$PhN(SiMe$_2$)]$_2$O}$_2$

Figure 2.10: The structures of {FeBr[MesN(SiMe$_2$)]$_2$O}$_2$ and {FeBr$_2$Li[Me$_3$PhN(SiMe$_2$)]$_2$O}$_2$ from references 20 and 21

Table 2.7: Comparison of selected bond lengths in **8** and related complexes

FeBr$_2$[O$_2$NH]^{BuMenPr}	**{FeBr[MesN(SiMe$_2$)]$_2$O}$_2$**	**{FeBr$_2$Li[Me$_3$PhN(SiMe$_2$)]$_2$O}$_2$**
Fe-Br(1): 2.3569(7)	Fe-Br(1): 2. 471(2)	Fe-Br(1): 2.4601(11)
Fe-Br(2): 2.3723(7)	Fe-Br(2): 2.503(2)	Fe-Br(2): 2.4313(11)
Fe-O(1): 1.828(3)	Fe-N(1): 1.864(8)	Fe-N(1): 1.905(4)
Fe-O(2): 1.836(3)	Fe-N(2): 1.880(7)	Fe-N(2): 1.877(5)
Fe···N(6): 3.435(3)		Fe···O(1): 3.330

2.5.3 UV-visible Spectroscopy

Electronic absorption spectra of all the synthesized iron(III) complexes show multiple intense bands in the UV and visible regions. The spectra of three complexes were obtained in a variety of solvents for examination of solvent polarity effects. Electronic absorption spectra of **1**, **5**, and **8** are shown in Figures 2.11, 2.12, and 2.13, respectively. In complexes **1**, **5** and **8**, the absorption maxima observed in the near-UV regions (below 300 nm) are caused by π-π^* transitions involving the phenolate units – absorptions in this region are also observed in the spectra of the unmetallated ligand precursors (shown in Figure 2.11). Intense, high energy bands are also observed in the region between 300 and 450 nm, which are assigned to charge transfer transitions from the out-of-plane p_π orbital (HOMO) of the phenolate oxygen to the half-filled d_{σ^*} orbitals of high spin Fe(III). The lowest energy bands (between 480 and 600 nm) are proposed to arise from charge-transfer transitions from the in-plane p_π orbital of the phenolate to the half-filled d_{π^*} orbitals of Fe(III). A shift of these LMCT bands is observed on changing the solvent used. Table 2.8 summarizes the wavelengths and the molar absorptivity values of the chloride and bromide compounds.

In complex **1**, the absorption spectrum in MeOH shows the visible band at lowest wavelength (596 nm) compared to other solvents examined. The absorption spectra in MeCN, THF and pentane display similar LMCT bands around 490 nm (Figure 2.11).

In complex **8**, the absorption spectrum in MeOH shows the wavelength of the lowest energy visible band at a wavelength of 600 nm. The absorption spectra in THF displays an obvious shift of this band to higher energy toward the near-UV region (Figure 2.13).

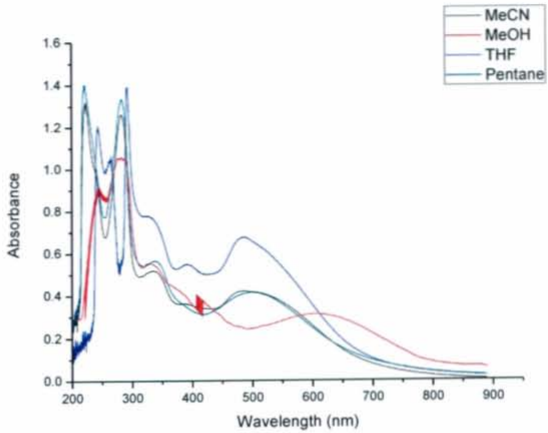

Figure 2.13: UV-vis spectra for $FeBr_2[O_2NH]^{BuMe\mathit{n}Pr}$ (**8**)

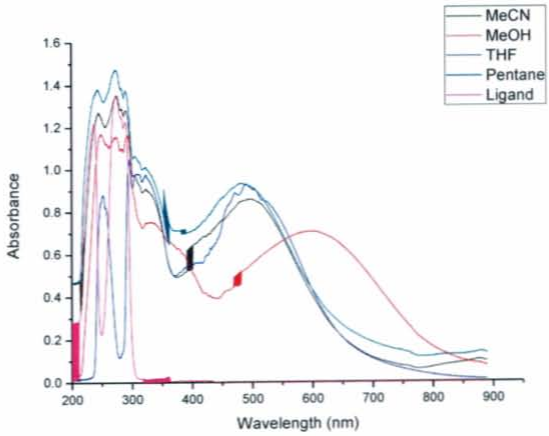

Figure 2.11: UV-vis spectra for $\{FeCl[O_2N]^{BuMe\mathit{n}Pr}\}_2$ (**1**)

In complex **5**, the absorption spectrum in MeOH shows the visible band at a wavelength of 519 nm. The absorption spectra in MeCN, THF and pentane display similar this LMCT band around 490 nm (Figure 2.12).

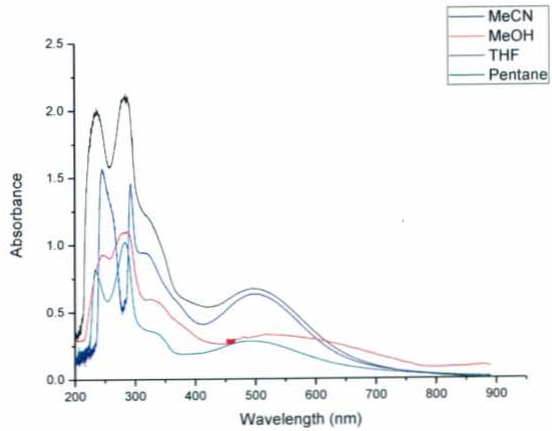

Figure 2.12: UV-vis spectra for $\{FeCl[O_2N]^{BuMeBn}\}_2$ (**5**)

Table 2.8: Comparison of the molar absorptivity values of the chloride and bromide compounds

Complex / Solvent	$FeCl[O_2N]^{BuMe\mathit{n}Pr}$ λ(nm), ε(L mol^{-1}cm^{-1})	$FeBr_2[O_2NH]^{BuMe\mathit{n}Pr}$ λ(nm), ε(L mol^{-1}cm^{-1})	$FeCl[O_2N]^{BuMeBn}$ λ(nm), ε(L mol^{-1}cm^{-1})
MeCN	λ(499) = 2583 λ(323) = 2736	λ(486) = 1266 λ(335) = 1563	λ(499) = 2010 -
MeOH	λ(596) = 2121 λ(334) = 2262	λ(600) = 936 λ(328) = 1668	λ(519) = 999 λ(323) = 1797
THF	λ(491) = 2796 λ(323) = 2934	λ(486) = 2028 λ(325) = 2334	λ(499) = 1890 λ(321) = 2796
Pentane	λ(480) = 2805 λ(323) = 3039	λ(497) = 1252 λ(339) = 1698	λ(490) = 1124 λ(320) = 1296

2.5.4 Magnetic studies

Variable temperature magnetic susceptibility studies were performed on representative complex **1**. The μ_{eff} vs T plot for **1** is shown in Figure 2.14. The temperature dependant magnetic behavior of **1** was examined in the range of 2 to 300 K. Variable temperature magnetic studies show a very weak decrease in the magnetic moment from 7.67 μ_B at 300 K to 7.26 μ_B at 40 K per mole of dimer complex (5.42 μ_B per mole of iron). Below this temperature, the moment drops rapidly. The room temperature moment is slightly lower than expected for two magnetically dilute high spin d^5 ions and is likely a result of zero-field splitting. A plot of $1/\chi$ vs. T gives a straight line indicating **1**

obeys the Curie-Weiss law [$\chi_m = C/(T - \theta)$] (Figure 2.15) with $C = 7.5$ cm^3 K mol^{-1} and θ = -5.4 K (C is Curie constant and θ is Weiss Constant, a negative θ value indicates antiferromagnetic intermolecular interactions between iron(III) centres). These results confirm the presence of high-spin d^5 Fe^{III} centres ($S = 5/2$) and minimal coupling between the iron atoms of the dimer.

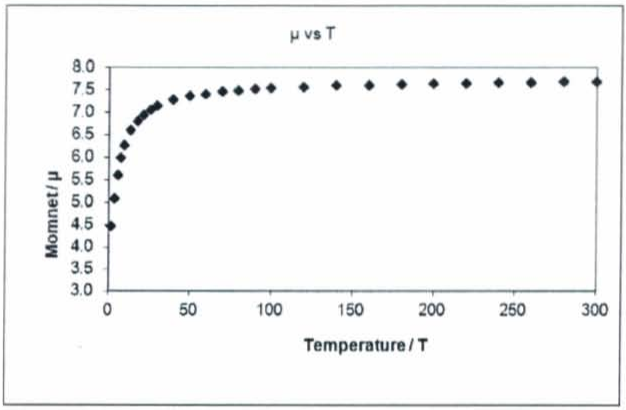

Figure 2.14: Magnetic moment vs. temperature plot

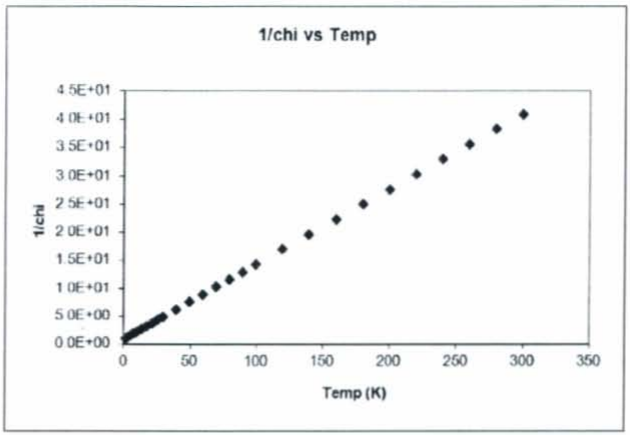

Figure 2.15: $1/\chi$ vs. temperature

The absence of intramolecular coupling between iron centres in **1** is perhaps surprising. The similar five-coordinate, iron(III) halide bridged dimers with distorted trigonal bipyramidal geometries, $\{FeX[^tBuN(SiMe_2)]_2O\}_2$ (X = Cl, Br) (Figure 2.16), have been shown to exhibit the rare form of magnetic behavior known as quantum mechanical spin-admixture.[11] This reported complex exhibits a μ_{eff} value of 4.5 μ_B at 300 K, which is much lower than the expected spin-only value for a pure S = 5/2 high spin state (μ_{eff} = 5.92 μ_B, five unpaired electrons) and significantly higher than the spin-only value for a pure S = 3/2 intermediate spin state (μ_{eff} = 3.87 μ_B for three unpaired electrons). However, the data are readily explained if the Fe(III) metal centres exist in a 3/2, 5/2 spin-admixed state. Moreover, the UV-vis spectra of these compounds also provide evidence of spin-admixture. Absorbances in the visible region were observed that could be assigned as d-d transitions, which are not allowed in a pure S = 5/2 spin state.

For comparative purposes, selected bond lengths in ($\{FeCl[O_2N]^{BuMenPr}\}_2$ (**1**) and $\{FeCl[^tBuN(SiMe_2)]_2O\}_2$) are shown in the Table 2.9. Most notably, the interatomic Fe-Fe distance in **1** is shorter than that observed in the reported $\{FeCl[^tBuN(SiMe_2)]_2O\}_2$ complex. However, the Fe-Cl bond lengths in the two complexes tell a different story. One of the Fe-Cl bond lengths in $\{FeCl[^tBuN(SiMe_2)]_2O\}_2$ is shorter than the corresponding distance in **1**. As a result, it is likely due to stronger overlap between the iron and chloride-centred orbitals in $\{FeCl[^tBuN(SiMe_2)]_2O\}_2$ which gives rise to the unique magnetic behaviour of this complex. The Fe-O and Fe-N interactions in are significantly different between the two complexes, but this is explained by the nature of the donors in each ligand. Whereas in complex **1** the *O*-donors are anionic, the *O*-donor in $\{FeX[^tBuN(SiMe_2)]_2O\}_2$ is neutral. On the other hand, the *N*-donor in **1** is neutral while the N-donors in $\{FeX[^tBuN(SiMe_2)]_2O\}_2$ are anionic. Coordinate covalent bonds between an ion and a Lewis base are typically longer than the corresponding bond between two ions.

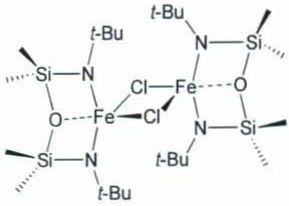

$\{FeCl[^tBuN(SiMe_2)]_2O\}_2$

Figure 2.16: Molecular structure of $\{FeCl[^tBuN(SiMe_2)]_2O\}_2$.

Table 2.9: Selected bond lengths of $\{FeCl[O_2N]^{BuMenPr}\}_2$ and $\{FeX[^tBuN(SiMe_2)]_2O\}_2$

$\{FeCl[O_2N]^{BuMenPr}\}_2$	Å	$\{FeCl[^tBuN(SiMe_2)]_2O\}_2$	Å
Fe(1)···Fe(2)	3.4658(7)	Fe(1)···Fe(2)	3.4784(20)
Fe(1)-Cl(1)	2.2976(12)	Fe(1)-Cl(1)	2.3181(19)
Fe(1)-Cl(2)	2.4912(14)	Fe(1)-Cl(2)	2.4652(17)
Fe(1)-O(1)	1.818(2)	Fe(1)-N(1)	1.887(5)
Fe(1)-O(2)	1.817(2)	Fe(1)-N(2)	1.894(4)
Fe(1)-N(1)	2.183(3)	Fe(1)-O(1)	2.597(4)

2.6 Experimental Section

2.6.1 Materials

Chemical reagents were purchased from Aldrich, Alfa Aesar or Strem. Commercially available reagents were used without further purification except for solvents, which were dried using either an MBraun solvent purification system or, in the case of THF, distilled under nitrogen using sodium benzophenone ketyl. The amines were handled carefully as they have strong smells.

2.6.2 Methods

All reactions for synthesizing the ligands and the iron complexes were carried out in a well ventilated fume hood. All of the complexes were synthesized under nitrogen using Schlenk techniques. The iron complexes were stored in a glove box and all recrystallization attempts were performed therein.

Suitable crystals of **1**, **2**, **5** and **8** were selected and mounted on a diffraction loop using Paratone-N oil and freezing to –150 °C. All measurements were made on a Rigaku Saturn CCD area detector with graphite monochromated Mo-Kα radiation. The data were processed[12] and corrected for Lorentz and polarization effects and absorption.[13] Neutral atom scattering factors for all non-hydrogen atoms were taken from the *International Tables for X-ray Crystallography.*[14] The structures were solved by direct methods[15] and expanded using Fourier techniques.[16] All non-hydrogen atoms were refined anisotropically. Hydrogen atoms were refined using the riding model. Anomalous dispersion effects were included in F_{calc};[17] the values for $\Delta f'$ and $\Delta f''$ were those of Creagh and McAuley.[18] The values for the mass attenuation coefficients are those of Creagh and Hubbell.[19] All calculations were performed using the CrystalStructure[20,21] crystallographic software package except for refinement, which was performed using SHELXL-97.[22]

2.6.3 Instruments

^{1}H-NMR and ^{13}C-NMR were recorded in $CDCl_3$ on Bruker Avance-500 or AvanceIII-300 Fourier Transform spectrometers with Me_4Si as an internal standard. Data are reported as follows: chemical shift, multiplicity (s = singlet, d = doublet, dd = doublet of doublets, t = triplets, b = broad, m = multiplet), coupling constant (J, Hz), assignment and integration. ^{1}H-NMR and ^{13}C-NMR spectra were processed using MestreNova software.

The MALDI-TOF MS spectra were recorded on an Applied Biosystems Voyager DE-PRO equipped with a reflectron, delayed ion extraction and high performance

nitrogen laser (337 nm). Samples were prepared at a concentration of 0.01 mg L^{-1}in methanol. Matrix (anthracene) was mixed at a concentration of 0.01 mg L^{-1} to promote desorption and ionization. UV-vis spectra were recorded on an Ocean Optics USB4000+ spectrophotometer. CHN analyses were carried out by Canadian Microanalytical Services, Delta, British Columbia, Canada.

The crystal structures were solved on a AFC8-Saturn 70 single crystal X-ray diffractometer from Rigaku/MSC, equipped with an X-stream 2000 low temperature system. The collimator capillary measures 0.3 mm and Crystalclear software was used for data collection and processing. The variable temperature magnetic measurements were run on a Quantum Designs MPMS5 SQUID magnetometer.

2.6.4 Synthesis

Unfortunately, the characterization of several compounds is incomplete due to lack of time. Complete characterization for the ligands should include ^{1}H and ^{13}C NMR, and for **L7** ^{19}F NMR. Also, either elemental analysis or high resolution mass spectrometry is still required for several iron complexes. The ligands **L1**, **L2**, **L5** and **L6** have been described previously. However, no characterization data was given, except for **L2**.

$H_2[O_2N]^{BuMe\mathit{n}Pr}$ (L1)[3]

A mixture of 2-*t*-butyl,4-methylphenol (20.24 g, 0.123 mol), *n*-propylamine (3.64 g, 0.0615 mol), and 37% aqueous formaldehyde (9.17 mL, 0.123 mol) in deionized

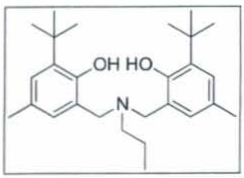

water (75 mL) was stirred and refluxed for 12 h. Upon cooling, a white precipitate formed and the liquid phase was a colorless solution. The upper phase was decanted and the remaining oily residue was triturated with cold methanol to give a pure, white powder (23.0 g, 91%). ^{1}H NMR (500 MHz, $CDCl_3$, δ): 7.03 (s, ArH, 2H); 6.76 (s, ArH, 2H); 3.66 (s, CH_2, 4H); 2.48 (t, ^3J = 5Hz, CH_2, 2H); 2.27 (s, CH_3, 6H); 1.65 (m, CH_2, 2H); 1.42 (s, CH_3, 18H); 0.89 (t, ^3J = 7.5Hz, CH_3, 3H). $^{13}C\{^1H\}$ NMR (500 MHz, 298 K, $CDCl_3$): δ 152.7 (Ar*C*OH); 137.0 (Ar); 129.1 (Ar); 128.3 (Ar); 127.5 (Ar); 122.7 (Ar); 57.3 (*C*H_2); 55.7 (*C*H_2); 34.8 (*C*(CH_3)$_3$); 29.9 (C(*C*H_3)$_3$); 21.0 (Ar*C*H_3); 19.7 (*C*H_2); 12.0 (*C*H_3).

$H_2[O_2N]^{BuBunPr}$ (L2)[23,24]

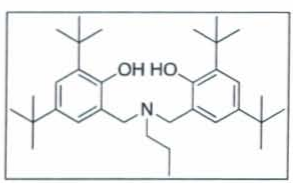

A mixture of 2,4-di-*t*-butylphenol (25.62 g, 0.123 mol), *n*-propylamine (3.64 g, 0.0615 mol), and 37% aqueous formaldehyde (9.17 mL, 0.123 mol) in deionized water (75 mL) was stirred and refluxed for 12 h. Upon cooling, a yellow-brown solid formed. The liquid phase was decanted and the remaining oily residue was triturated with cold methanol to give a pure, white powder (17.7 g, 58%). ^{1}H NMR (500 MHz, $CDCl_3$, δ): 7.25 (s, ArH, 2H); 6.95 (s, ArH, 2H); 3.70 (s, CH_2, 4H); 2.53 (t, ^3J = 7.5Hz, CH_2, 2H); 1.65 (m, CH_2, 2H); 1.42 (s, CH_3, 18H); 1.30 (s, CH_3, 18H); 0.90 (t, ^3J = 7.5 Hz, CH_3, 3H). $^{13}C\{^1H\}$ NMR (75 MHz, 298 K, $CDCl_3$): δ 152.40 (Ar); 141.5 (Ar) 136.04 (Ar); 128.93 (Ar); 128.08 (Ar); 125.06 (Ar); 123.48 (Ar); 121.76 (Ar); 57.24 (Ar*C*H_2); 55.53 (Ar*C*H_2); 34.88 (*C*(CH_3)$_3$); 34.22 (*C*(CH_3)$_3$); 31.68 (C(*C*H_3)$_3$); 29.73 (C(*C*H_3)$_3$); 19.40 (*C*H); 16.67 (CH(*C*H_3)$_2$).

$H_2[O_2N]^{BuMe/Pr}$ (L3)

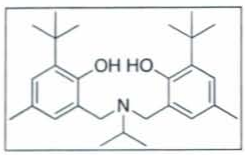

A mixture of 2-*t*-butyl-4-methylphenol (20.24 g, 0.123 mol), isopropylamine (3.64 g, 0.0615 mol), and 37% aqueous formaldehyde (9.17 mL, 0.123 mol) in deionized water (75 mL) was stirred and refluxed for 12 h. Upon cooling, a pale yellow precipitate formed. The liquid phase was decanted and the remaining oily residue was triturated with cold methanol to give a pure, white powder (15.3 g, 60%). ^{1}H NMR (500 MHz, $CDCl_3$, δ): 7.03 (s, ArH, 2H); 6.76 (s, ArH, 2H); 3.68 (s, CH_2, 4H); 3.17 (septet, CH, 1H); 2.26 (s, CH_3, 6H); 1.41 (s, CH_3, 18H); 1.19 (d, ^3J=5Hz, CH_3, 6H). $^{13}C\{^1H\}$ NMR (75 MHz, 298 K, $CDCl_3$): δ 152.70 (Ar); 136.85 (Ar); 128.93 (Ar); 128.08 (Ar); 127.26 (Ar); 122.41 (Ar); 51.69 (CH_2); 48.33 (*C*H); 34.63 ($C(CH_3)_3$); 29.69 ($C(CH_3)_3$); 20.85 ($ArCH_3$); 16.67 ($CH(CH_3)_2$).

$H_2[O_2N]^{BuBu/Pr}$ (L4)

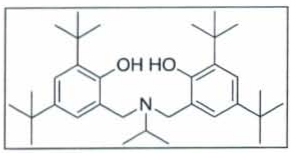

A mixture of 2,4-*t*-butylphenol (25.62 g, 0.123 mol), isopropylamine (3.64 g, 0.0615 mol), and 37% aqueous formaldehyde (9.17 mL, 0.123 mol) in deionized water (75 mL) was stirred and refluxed for 12 h. Upon cooling, a yellow-brown solid formed. The liquid phase was decanted and the remaining oily residue was triturated with cold methanol to give a pure, white powder (8.21 g, 27%). ^{1}H NMR (500 MHz, $CDCl_3$, δ): 7.25 (s, ArH, 2H); 6.95 (s, ArH, 2H); 3.74 (s, CH_2, 4H); 3.20 (m, CH, 1H); 1.42 (s, CH_3, 18H); 1.31 (s, CH_3, 18H); 1.21 (d, ^3J = 5 Hz, CH_3, 6H). $^{13}C\{^1H\}$ NMR (500 MHz, 298 K, $CDCl_3$): δ 153.4 (Ar*C*OH); 137.6 (Ar); 129.6 (Ar); 128.7 (Ar); 127.9 (Ar);

123.1 (Ar); 52.4 (CH_2); 49.0 (CH_2); 35.3 ($C(CH_3)_3$); 30.3 ($C(CH_3)_3$); 21.5 (CH); 17.4 (CH_3).

$H_2[O_2N]^{BuBuBn}$ (L5)[3,25]

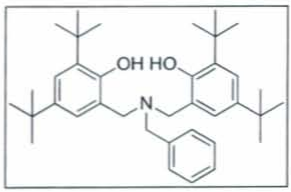

A mixture of 2,4-di-*t*-butylphenol (25.62 g, 0.123 mol), benzyl amine (6.62 g, 0.0615 mol), and 37% aqueous formaldehyde (9.17 mL, 0.123 mol) in deionized water (75 mL) was stirred and refluxed for 12 h. Upon cooling, a yellow-brown solid formed. The upper phase was decanted and the remaining oily residue was triturated with cold methanol to give a pure, white powder (19.40 g, 58%). ^{1}H NMR (500 MHz, $CDCl_3$, δ): 7.21 (s, ArH, 2H); 6.81 (s, ArH, 2H); 4.85 (s, CH_2, 2H); 4.04 (s, CH_2, 2H); 3.94 (s, CH_2, 2H); 1.44 (s, CH_3, 18H); 1.31 (s, CH_3, 18H). $^{13}C\{^1H\}$ NMR (75 MHz, 298 K, $CDCl_3$): δ 150.63 (Ar); 142.17 (Ar); 138.45 (Ar); 136.61 (Ar); 129.18 (Ar); 128.48 (Ar); 127.34 (Ar); 122.09 (Ar); 121.97 (Ar); 118.95 (Ar); 80.98, (ArCH_2); 55.68 (ArCH_2); 51.01 (ArCH_2); 34.88 ($C(CH_3)_3$); 34.22 ($C(CH_3)_3$); 31.64 ($C(CH_3)_3$); 29.73 ($C(CH_3)_3$).

$H_2[O_2N]^{BuMeBn}$ (L6)[3]

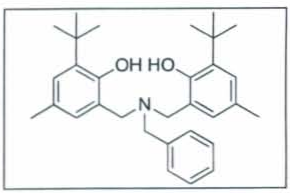

A mixture of 2-*t*-butyl,4-methylphenol (20.24 g, 0.123 mol), benzyl amine (6.62 g, 0.0615 mol), and 37% aqueous formaldehyde (9.17 mL, 0.123 mol) in deionized water (75 mL) was stirred and refluxed for 12 h. Upon cooling, a pale yellow precipitate formed. The upper phase was decanted and the remaining oily residue was triturated with cold methanol to give a pure, white powder

(18.0 g, 60%). ^{1}H NMR (300 MHz, $CDCl_3$, δ): 7.37 (s, Ar*H*, 1H); 7.35 (s, Ar*H*, 1H); 7.32 (s, Ar*H*, 1H); 7.29 (s, Ar*H*, 1H); 7.22 (s, Ar*H*, 1H); 6.99 (d, J = 1.6 Hz, Ar*H*, 2H); 6.74 (d, J = 1.6 Hz, Ar*H*, 2H); 3.58 (s, CH_2, 4H); 3.53 (s, CH_2, 2H); 2.22 (s, ArCH_3, 6H); 1.38 (s, CH_3, 18H). ^{13}C{^{1}H} NMR (75 MHz, 298 K, $CDCl_3$): δ 152.27 (Ar); 137.59 (Ar); 136.76 (Ar); 129.56 (Ar); 129.06 (Ar); 129.02 (Ar); 128.04 (Ar); 127.99 (Ar); 127.44 (Ar); 58.51 (*C*H$_2$); 56.59 (*C*H$_2$); 34.66 (*C*(CH$_3$)$_3$); 29.62 (C(*C*H$_3$)$_3$); 20.81 (Ar*C*H$_3$).

$H_2[O_2N]^{FF/iPr}$(L7)

A mixture of 2,4-difluorophenol (16.02g, 0.123 mol), *i*-propylamine (3.64 g, 0.0615 mol), and 37% aqueous formaldehyde (9.17 mL, 0.123 mol) in deionized water (75 mL) was stirred and refluxed for 12 h. Upon cooling, a white solid formed. The upper phase was decanted and the remaining oily residue was triturated with cold methanol to give a pure, white powder (5.70 g, 27%). ^{1}H NMR (500 MHz, $CDCl_3$, δ): 6.78 (m, Ar*H*, 2H); 6.42 (m, Ar*H*, 2H); 3.75 (s, CH_2, 4H); 3.11 (septet, C*H*, H); 1.20 (d, CH_3, 6H).

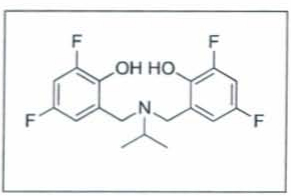

{FeCl[O_2N]$^{BuMe\mathit{n}Pr}$ }$_2$ (1)

To an ethanolic slurry of recrystallized **L1** (2.68 g, 6.52 mmol) was added a solution of anhydrous $FeCl_3$ (1.06 g, 6.52 mmol) in THF resulting in an intense purple solution. To this solution was added triethylamine (1.32 g, 13.0 mmol) and the resulting mixture was stirred for 2 h then filtered through Celite. Removal of the solvent under vacuum yielded a dark purple solid (2.87 g, 88%). Anal. calcd for **1**: C, 64.74; H, 8.11; N, 2.99. Found: C, 65.02; H, 7.85; N, 2.80. MS (MALDI-TOF) *m/z* (%, ion): 408.1 (26, [M-

FeCl]$^+$), 464.2 (100, [M-Cl]$^+$), 499.2 (20, [M]$^+$), 965.45 (10, [2M-Cl]$^+$). UV-vis λ_{max}, nm (ε): (Pentane) 480 (2805), 323 (3039); (MeCN) 499 (2583), 323 (2736); (MeOH) 596 (2121), 334 (2262); (THF) 491 (2796), 323 (2934). μ_{eff} (solid, 27 °C) 7.67 μ_B per mol of dimer.

{FeCl[O$_2$N]^{BuBunPr} }$_2$ (2)

To an ethanolic slurry of recrystallized **L2** (3.23 g, 6.52 mmol) was added a solution of anhydrous $FeCl_3$ (1.06 g, 6.52 mmol) in THF resulting in an intense purple solution. To this solution was added triethylamine (1.32 g, 13.0 mmol) and the resulting mixture was stirred for 2 h then filtered through Celite. Removal of solvent under vacuum yielded a dark purple product (3.50 g, 92%). MS (MALDI-TOF) *m/z* (%, ion): 495.4 (25, [M-FeCl]$^+$), 548.3 (100, [M-Cl]$^+$).

{FeCl[O$_2$N]^{BuMeiPr} }$_2$ (3)

To an ethanolic slurry of recrystallized **L3** (2.68 g, 6.52 mmol) was added a solution of anhydrous $FeCl_3$ (1.06 g, 6.52 mmol) in THF resulting in an intense purple solution. To this solution was added triethylamine (1.32 g, 13.0 mmol) and the resulting mixture was stirred for 2 h then filtered through Celite. Removal of solvent under vacuum yielded a dark purple product (2.97 g, 91%). MS (MALDI-TOF) *m/z* (%, ion): 408.1 (21, [M-FeCl]$^+$), 464.2 (100, [M-Cl]$^+$), 965.4 (10, [2M-Cl]$^+$).

{FeCl[O$_2$N]^{BuBuiPr} }$_2$ (4)

To an ethanolic slurry of recrystallized **L4** (3.23 g, 6.52 mmol) was added a solution of anhydrous $FeCl_3$ (1.06 g, 6.52 mmol) in THF resulting in an intense purple

solution. To this solution was added triethylamine (1.32 g, 13.0 mmol) and the resulting mixture was stirred for 2 h then filtered through Celite. Removal of solvent under vacuum yielded a dark purple product (3.31 g, 87%). MS (MALDI-TOF) *m/z* (%, ion): 495.4 (100, $[M\text{-}FeCl]^+$), 549.3 (65, $[M\text{-}Cl]^+$), 584.3 (5, $[M]^+$).

$\{FeCl[O_2N]^{BuMeBn}\}_2$ (5)

To an ethanolic slurry of recrystallized **L5** (2.99 g, 6.52 mmol) was added a solution of anhydrous $FeCl_3$ (1.06 g, 6.52 mmol) in THF resulting in an intense purple solution. To this solution was added triethylamine (1.32 g, 13.0 mmol) and the resulting mixture was stirred for 2 h then filtered through Celite. Removal of solvent under vacuum yielded a dark purple product (3.21 g, 90%). MS (MALDI-TOF) *m/z* (%, ion): 456.2 (20, $[M\text{-}FeCl]^+$), 512.2 (15, $[M\text{-}Cl]^+$). UV-vis λ_{max}, nm (ε): (Pentane) 490 (1124), 320 (1296); (MeCN) 499 (2010); (MeOH) 519 (999), 323 (1797); (THF) 499 (1890), 321 (2796).

$\{FeCl[O_2N]^{BuBuBn}\}_2$ (6)

To an ethanolic slurry of recrystallized **L6** (3.54 g, 6.52 mmol) was added a solution of anhydrous $FeCl_3$ (1.06 g, 6.52 mmol) in THF resulting in an intense purple solution. To this solution was added triethylamine (1.32 g, 13.0 mmol) and the resulting mixture was stirred for 2 h then filtered through Celite. Removal of solvent under vacuum yielded a dark purple product (3.51 g, 85%). MS (MALDI-TOF) *m/z* (%, ion): 540.4 (67, $[M\text{-}FeCl]^+$), 596.3 (58, $[M\text{-}Cl]^+$), 631.3 (10, $[M]^+$).

$\{FeCl[O_2N]^{FF/Pr}\}_2$ (7)

To an ethanolic slurry of recrystallized **L7** (2.24 g, 6.52 mmol) was added a solution of anhydrous $FeCl_3$ (1.06 g, 6.52 mmol) in THF resulting in an intense purple solution. To this solution was added triethylamine (1.32 g, 13.0 mmol) and the resulting mixture was stirred for 2 h then filtered through Celite. Removal of solvent under vacuum yielded a dark purple product (1.58 g, 37%). MS (MALDI-TOF) *m/z* (%, ion): 342.1 (90, $[M\text{-}FeCl]^+$), 397.0 (40, $[M\text{-}Cl]^+$).

$FeBr_2[O_2NH]^{BuMe\mathit{n}Pr}$ (8)

To an ethanolic slurry of recrystallized **L1** (2.68 g, 6.52 mmol) was added a solution of anhydrous $FeBr_3$ (1.92 g, 6.52 mmol) in THF resulting in an intense purple solution. To this solution was added triethylamine (1.32 g, 13.0 mmol) and the resulting mixture was stirred for 2 h then filtered through Celite. Removal of solvent under vacuum yielded a dark purple product (3.75 g, 92%). MS (MALDI-TOF) *m/z* (%, ion): 465.2 (100, $[M\text{-}2Br]^+$), 545.2 (48, $[M\text{-}Br]^+$), 626.4(10, $[M]^+$). UV-vis λ_{max}, nm (ε): (Pentane) 497 (1242), 339 (1698); (MeCN) 486 (1266), 335 (1563); (MeOH) 600 (936), 328 (1668); (THF) 486 (2028), 325 (2334). Anal. Calcd for **8**: C, 51.78; H, 6.44; N, 2.24. Found: C, 52.04; H, 6.76; N, 2.58.

2.7 Conclusions

A small library of ligands has been synthesized using modified Mannich condensation to produce diprotic tridentate ligands. The tridentate ligands were coordinated to Fe(III) ions. The yields of the complexes were good and they were quite simple to synthesize. The mass spectral data indicate that the metal complexes fragment

extensively under MALDI conditions. Interestingly, $\{FeCl[O_2N]^{BuMenPr}\}_2$ seems more stable to fragmentation than $\{FeCl[O_2N]^{BuMeBn}\}_2$. Of the eight complexes synthesized, complexes **1**, **2**, **5** and **8** have been structurally characterized by single crystal X-ray diffraction. The chloride complexes **1**, **2** and **5** are five-coordinate exhibiting mildly distorted trigonal bipyramidal geometries around Fe, whereas **8** is four-coordinate tetrahedral geometry. The UV-vis data show the complexes exhibit strong ligand to metal charge transfer (LMCT) bands. Magnetic studies show the representative dimeric chloride complex **1** is a magnetically dilute high-spin d^5 system.

2.8 References:

(1) Chowdhury, R. R.; Crane, A. K.; Fowler, C.; Kwong, P.; Kozak, C. M. *Chem. Commun.* **2008**, 94.

(2) Rothenberg, G. *Catalysis*, Wiley-VCH: Weinheim, **2008**.

(3) Kerton, F. M.; Holloway, S.; Power, A.; Soper, R. G.; Sheridan, K.; Lynam, J. M.; Whitwood, A. C.; Willans, C. E., *Can. J. Chem.* **2008,** *86*, 435.

(4) Hasan, K.; Fowler, C.; Kwong, P.; Crane, A. K.; Collins, J. L.; Kozak, C. M. *Dalton Trans.* **2008**, 2991.

(5) Pohl, S.; Saak, W. Z. *Anorg. Allg. Chem.* **1985**, *523*, 25; Saak, W. Z.; Pohl, S. *Anorg. Allg. Chem.* **1987**, *552*, 186; Nelson, S. M. in *Comprehensive Coordination Chemistry*, Vol. 4 (Eds.: Wilkinson, G.; Gillard, R. D.; McCleverty, J. A.) Pergamon Press, Oxford, **1987**, 217.

(6) Nishijo, J.; Miyazaki, A.; Enoki, T.; Watanabe, R.; Kuwatani, Y.; Iyada, M. *Inorg. Chem.* **2005**, *44*, 2493.

(7) Stokes, S. L.; Davis, W. M.; Odom, A. L.; Cummins, C. C.; *Organometallics*. **1996**, *15*, 4521.

(8) Pohl, S.; Bierbach, U.; Saak, W. *Angew. Chem. Int. Ed. Engl.* **1989**, *28*, 776.

(9) Das, A. K.; Moatazedi, Z.; Mund, G.; Bennet, A. J.; Batchelor, R. J.; Leznoff, D. B. *Inorg. Chem.* **2007**, *46*, 366.

(10) Mund, G.; Vidovic, D.; Batchelor, R. J.; Britten, J. F.; Sharma, R. D.; Jones, C. H. W.; Leznoff, D. B. *Chem. Eur. J.* **2003**, *9*, 4757.

(11) Mund, G.; Batchelor, R. J.; Sharma, R. D.; Jones, C. H. W.; Leznoff, D. B. *Chem. Soc., Dalton Trans.* **2002**, 136.

(12) Pflugrath, J. W. *Acta Cryst.* **1999**, *55*, 1718.

(13) Larson, A. C. *Crystallographic Computing,* ed. Ahmed, F. R.; Munksgaard, Copenhagen, **1970**, 291.

(14) Cromer, D. T.; Waber, J. T. *International Tables for X-ray Crystallography*, vol. IV, The Kynoch Press, Birmingham, England, Table 2.2 A, **1974**.

(15) Altomare, A.; Cascarano, G.; Giacovazzo, C.; Guagliardi, A.; Burla, M.; Polidori, G.; Camalli, M. *J. Appl. Cryst.* **1994**, *27*, 435.

(16) Beurskens, P. T.; Admiraal, G.; Beurskens, G.; Bosman, W. P.; de Gelder, R.; Israel, R.; Smits, J. M. M. *DIRDIF99, The DIRDIF-99 program system,* Technical

Report of the Crystallography Laboratory, University of Nijmegen, The Netherlands, **1999**.

(17) Ibers, J. A.; Hamilton, W. C. *Acta Crystallogr.* **1964**, *17*, 781.

(18) Creagh, D. C.; McAuley, W. J. *International Tables for Crystallography*, vol C, (Wilson, A. J. C. ed.), Kluwer Academic Publishers, Boston, Table 4.2.6.8, pages 219-222, **1992**.

(19) Creagh, D. C.; Hubbell, J. H. *International Tables for Crystallography*, vol C, (Wilson, A.J.C. ed.), Kluwer Academic Publishers, Boston, Table 4.2.4.3, pages 200-206, **1992**.

(20) *CrystalStructure 3.7.0: Crystal Structure Analysis Package,* Rigaku and Rigaku/MSC, **2000-2005**.

(21) Watkin, D. J.; Prout, C. K.; Carruthers, J. R.; Betteridge, P. W. *CRYSTALS Issue 10,* Chemical Crystallography Laboratory, Oxford, UK, **1996**.

(22) Sheldrick, G. M. *SHELX97*, **1997**.

(23) Tshuva, E. Y.; Goldberg, I.; Kol, M.; Goldshimidt, Z. *Inorg. Chem.* **2001**, *40*, 4263.

(24) Tshuva, E. Y.; Goldberg, I.; Kol, M.; Goldshimidt, Z. *Organometallics*. **2001**, *20*, 3017.

(25) Chmura, A. J.; Chuck, C. J.; Davidson, M. G.; Jones, M. D.; Lunn, M. D.; Mahon, M. F. *Dalton Trans.* **2006**, 887.

Chapter 3. Iron-Catalyzed sp^3-sp^2 Kumada C-C Cross-coupling Reactions

3.1 Introduction

Transition metal catalyzed Grignard cross-coupling is an important class of C-C bond forming reactions,[1] including nickel- and palladium-catalyzed Kumada-Corriu couplings of Grignard reagents with organohalides.[2-4] Recently, following early reports by Kochi,[5] and in the interest of sustainability (lower cost and toxicity), there has been a surge in the study of iron-based catalysts.[3-6-10] Iron catalysts are complementary to Ni and Pd in that they successfully couple alkyl halides with Grignard reagents, which is not easily achieved using Ni or Pd due to competing β-hydride elimination. However, unactivated alkyl halides,[3-4] particularly alkyl chlorides, continue to pose a challenge and only a few examples of C-C bond formation using alkyl chlorides have been reported.[11-14] Also, there have been few reports of the synthesis of diarylmethane compounds via iron-catalyzed coupling of aryl Grignards with benzyl halides,[15] and others have found these products required the use of aryl zinc nucleophiles because aryl Grignard reagents proved unsatisfactory.[16] A catalytic system that can address these shortcomings is required.

The breadth of iron-catalyzed methods used for Kumada-type cross-coupling is diverse. [11-17-28] Use of $FeCl_3$, whether on its own or to generate an active catalyst *in situ*, is often inconvenient on a large scale because it is highly hygroscopic and yields vary according to its purity and commercial origin.[27] Although $Fe(acac)_3$ is a more convenient, less hygroscopic starting material,[17] amine additives are often employed to achieve high

conversions and yields of cross-coupled products.[26,27] An easy to use, non-hygroscopic single component catalyst precursor is, therefore, highly desireable. Also, whereas many studies have been performed at low temperatures,[11,25,27,28] others require heating[17,18,23] and the most commonly used solvents for these reactions, diethyl ether and THF, have relatively low boiling points. However, use of microwave radiation to superheat solutions in these solvents has potential to significantly shorten reaction times as well as to achieve product formation previously hindered by high activation barriers, such as those caused by steric constraints in the cross-coupling partners.[29-34] Kappe has reported the use of microwaves to facilitate high yielding Pd-catalyzed Kumada cross-coupling between aryl Grignards and aryl chlorides,[35] but the use of microwave-assisted heating has, to our knowledge, not been investigated for iron-catalyzed cross-coupling.

The Kozak group has previously reported the synthesis of iron chloride complexes of tetradentate amine-bis(phenolate) ligands[36] and their use in catalytic cross-coupling of aryl Grignard reagents with primary and secondary alkyl halides.[15] In order to generate more reactive catalysts, yet still maintain the robust nature of the catalyst precursor, attention was turned to tridentate amine-bis(phenolate) ligands. This Chapter reports investigations of the catalytic activity of a structurally authenticated amine-bis(phenolate) iron(III) complex for C-C cross coupling of aryl Grignard reagents with alkyl halides, particularly primary and secondary alkyl chlorides, including benzyl chlorides. Furthermore, reactions for certain substrates that give poor conversions at room temperature were found to give vastly higher yields under microwave irradiation.

3.2 Results & Discussion

3.2.1 General Procedure

Reactions were first carried out using a tridentate amine-bis(phenolate) iron complex as catalyst. Different Grignard reagents and electrophile substrates were screened, and the reactions that gave poor results were optimized with respect to different reaction conditions, such as temperature. A catalyst loading of 5 mol% of Fe^{III} complex **1** (Figure 3.1) was added to flasks followed by the alkyl halides, solvent and the Grignard reagents. The ratio of Grignard reagent to the halide was 2:1. It has been proposed that iron-catalyzed cross-coupling of Grignard reagents with electrophiles proceeds by the formation of reduced Fe as the active species, which is generated by excess Grignard reagent.[19-21] The reaction mixture was stirred for 30 min at room temperature or for 10 min, at 100 °C by microwave-assisted heating, after which it was quenched by adding HCl (aq 2.0 M, 5.0 mL). The product yields were quantified by GC-MS (relative to standard curves) and in several cases by ^{1}H NMR.

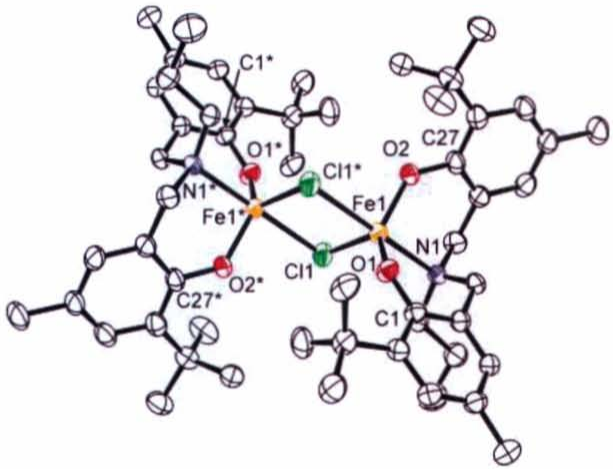

Figure 3.1 Structure of $\{FeCl[O_2N]^{BuMe\mathit{n}Pr}\}$ (**1**)

3.2.2 Cyclohexyl halides as substrates

Based on previous work in the Kozak group with Fe^{III} compounds supported by tetradentate amine-bis(phenolate)-ether ligands, complex **1** was employed under similar reaction conditions for our preliminary investigations. It was previously found that diethyl ether is superior to THF as a solvent for cross-coupling of Grignard reagents with alkyl halides using these complexes,[15] therefore it was the solvent of choice for the current study. Also, it was previously found that reactions performed at room temperature gave superior results to those conducted at lower temperatures. Under these conditions, 5.0 mol% of complex **1** was an effective catalyst for cross-coupling of typical substrates and excellent yields were obtained for secondary alkyl halides, specifically cyclohexyl bromide when combined with phenylmagnesium bromide on a scale of 1.0 gram of alkyl

halide (Table 3.1, entry 1). Excellent yields were also obtained with *m*-anisyl and *p*-fluorophenyl Grignards (Table 3.1, entries 2 and 3), indicating good nucleophilicity even at a deactivated *meta*-position, or with electronegative groups in the *para*-position. The more sterically demanding 2,6-dimethylphenylmagnesium bromide was attempted. Unfortunately, no cross-coupling product was obtained with cyclohexyl bromide, even after microwave heating to 100 °C (Table 3.1, entry 4), although this method was successful for other substrate combinations (see below). Bedford has reported a similar reluctance of 2,6-dimethylphenylmagnesium bromide to undergo cross-coupling with cyclohexyl bromide.[18,22-24] Reaction of 1-naphthylmagnesium bromide with cyclohexyl bromide, however, gave a moderate yield (Table 3.1, entry 5).

Cyclohexyl chloride was found to give modest to good yields, depending on the Grignard reagent. *p*-Tolylmagnesium bromide (Table 3.1, entry 6) gave poorer yield of cross-coupled product than *o*-tolylmagnesium bromide (Table 3.1, entry 7), which was in turn superior to the Kozak group's previously reported result.[15] Cyclohexyl chloride gave poor yields with *p*-anisylmagnesium bromide, even at 40 °C (Table 3.1, entry 8). Microwave heating to 100 °C for 10 minutes, however, improved the conversion markedly for cyclohexyl chloride, giving the cross-coupled product in 91% yield. Since this was such a significant improvement upon microwave heating, we questioned whether microwave heating alone could account for the rise in yield. Performing this reaction in the absence of **1**, however, gave no yield of cross-coupled product.

Table 3.1: Kumada type sp^3-sp^2 cross-coupling using cyclohexyl halides as substrates

Entry	ArMgBr	Alkyl Halide	Product	Yield (%)
1	Ph			>95[a]
2	*m*-Anisyl	"	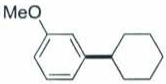	>95
3	*p*-FPh	"	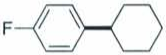	>95
4	2,6-Me_2Ph	"	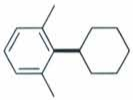	Trace[b]
5	1-Naphthyl	"	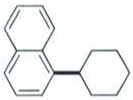	36
6	*p*-Tolyl		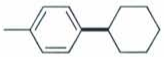	47
7	*o*-Tolyl	"	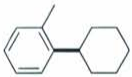	86
8	*p*-Anisyl	"	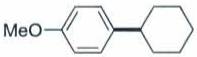	22 26[c] 91[b] 0[d]

[a] Reaction performed using 1.00 g of alkyl halide. [b] Microwave heating for 10 min at 100 °C. [c] Performed for 30 min at 40 °C. [d] Microwave heating for 10 min at 100 °C in the absence of compound **1**.

3.2.3 Benzyl halides as substrates

Formation of diarylmethane motifs by iron-catalyzed coupling of benzyl halides with aryl Grignard reagents has been reported to be unsatisfactory, giving low yields and poor selectivity resulting in the formation of homo-coupled by-products.[16] Excellent yields were obtained for coupling of *o*-tolylmagnesium bromide with benzyl chloride (Table 3.2, entry 1). The previous report from the Kozak group resulted in only 68% conversion when benzyl bromide was used.[15] Surprisingly, unlike cychohexyl bromide (Table 3.1, entry 4), benzyl bromide was found to couple with the sterically crowded 2,6-dimethylphenylmagnesium bromide in 78% yield, even at room temperature (Table 3.2, entry 2). Excitingly, double arylation of 1,3-bis(bromomethyl)benzene with *o*-tolylmagnesium bromide was achieved in high yield (Table 3.2, entry 3). 2.0 equiv. of Grignard reagent per halide functional group was required. Poor yields were obtained for the double arylation using 2,6-dimethylphenylmagnesium bromide (Table 3.2, entry 4). High quantities (72%) of the homo-coupled diaryl product were formed instead.

Table 3.2: Kumada type sp^3-sp^2 cross-coupling by using benzyl halides as substrates

Entry	ArMgBr	Alkyl Halide	Product	Yield (%)
1	*o*-Tolyl		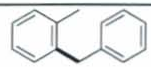	>95
2	2,6-Me_2Ph	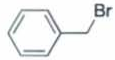	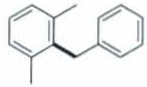	78
3	*o*-Tolyl	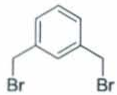	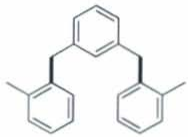	>95
4	2,6-Me_2Ph	"	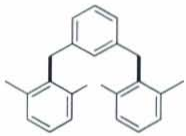	19

3.2.4 Primary alkyl halides as substrates

A competitive arylation reaction of 1-bromo-3-chloropropane resulted in selective attack at the bromide site, resulting in a moderate yield of 1-(3-chloropropyl)-2-methylbenzene (Table 3.3, entry 1). Arylation by *p*-fluorophenylmagnesium bromide was poor, even under microwave heating conditions (Table 3.3, entry 2). Interestingly, while double arylation of 1,4-dichlorobutane with *o*-tolylmagnesium bromide was not observed, an excellent yield of the singly arylated 1-(4-chlorobutyl)-2-methylbenzene was obtained (Table 3.3, entry 3). Again, 2.0 equiv. of Grignard reagent were required per halide functional group.

Other primary halides were also screened (Table 3.3, entries 4-8). The previous report from the Kozak group showed very good yields for cross-coupling of *o*-tolylmagnesium bromide with *n*-octylbromide,[15] hence we investigated whether this reaction could be performed on a larger scale. Reaction of 1.0 gram of *n*-octylbromide with 2.0 equiv. of Grignard reagent gave very good yield of cross-coupled product (Table 3.3, entry 4). Using the more sterically demanding 2,6-dimethylphenylmagnesium bromide gave trace quantities of product when the reaction was conducted at room temperature but, unlike the reaction with cyclohexyl bromide (Table 3.1, entry 4), microwave irradiation to 100 °C for 10 minutes increased the yield to 94% (Table 3.3, entry 5). In comparison, Hayashi reported the cross-coupling of 2,4,6-trimethylphenylmagnesium bromide with *n*-octylbromide in 60% yield using $Fe(acac)_3$ in refluxing diethyl ether.[17] Better results were obtained for 1-iodopropane, where cross-coupling to *o*-tolylmagnesium bromide and *p*-fluorophenylmagnesium bromide resulted in 76% and 67% yields, respectively (Table 3.3, entries 6 and 7). Again, 2,6-dimethylphenylmagnesium bromide gave trace quantities of product at room temperature but microwave irradiation gave the product in 88% yield (Table 3.3, entry 8). This contrasts with the selectivity for double arylation seen with benzyl halide substrates (Table 3.2, entry 3).

Table 3.3: Kumada type sp^3-sp^2 cross-coupling by using primary alkyl halides as substrates

Entry	ArMgBr	Alkyl Halide	Product	Yield (%)
1	*o*-Tolyl		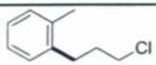	61
2	*p*-FPh	"	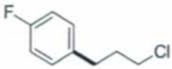	28[a]
3	*o*-Tolyl			90[b]
4	*o*-Tolyl	n-$C_8H_{17}Br$	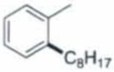	85[c]
5	2,6-Me_2Ph	n-$C_8H_{17}Br$	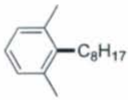	Trace 94[a]
6	*o*-Tolyl		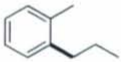	76
7	*p*-FPh	"	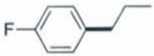	67
8	2,6-Me_2Ph	"	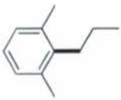	Trace 88[a]

[a] Microwave heating for 10 min at 100 °C. [b] Ratio between alkyl halides to aryl Grignard reagent is 12.5:1. [c] Reaction performed using 1.00 g of alkyl halide.

3.2.5 Acyclic secondary alkyl halides as substrates

Acyclic secondary halides were also investigated. Unfortunately, the hindered 2,6-dimethylphenylmagnesium bromide showed no cross-coupling product with 2-bromobutane, even under microwave heating (Table 3.4, entry 1). However, some promising results were observed for less hindered aryl Grignards with alkyl chlorides. Reaction of 2-chlorobutane with various Grignard reagents gave modest yields at room temperature and mild improvement under microwave heating (Table 3.4, entries 2 to 5). There are few reports of Kumada-type cross-coupling using secondary alkyl chlorides. The most remarkable report comes from the group of Nakamura, where $FeCl_3$/TMEDA catalyzed cross-coupling of phenylmagnesium bromide with cyclohexyl chloride proceeds nearly quantitatively, and in 84% yield with 2-chlorobutane. Slow addition of the Grignard reagent was required in both cases and heating to 40 °C was required in the latter.[25] Interestingly, when $Fe(acac)_3$/TMEDA was employed by Cahiez and co-workers, only traces of product were observed for the coupling of PhMgBr with 2-chlorobutane.[27]

Table 3.4: Kumada type sp^3-sp^2 cross-coupling by using acyclic secondary alkyl halides as substrates

Entry	ArMgBr	Alkyl Halide	Product	Yield (%)
1	2,6-Me_2Ph	Br		Trace[a]
2	*p*-Anisyl	Cl	MeO	35 37[a]
3	*o*-Tolyl	"		20 30[a] 30[b]
4	Ph	"		36 58[a]
5	*p*-Tolyl	"		64

[a] Microwave heating for 10 min at 100 °C. [b] Microwave heating for 10 min at 180 °C.

3.2.6 Functional-group alkyl halides as substrates

Functionalized alkyl bromides were generally well tolerated with *o*-tolylmagnesium bromide at room temperature. 2-(2-Bromoethyl)-1,3-dioxane, 6-bromo-1-hexanol and ethyl-6-bromohexanoate showed moderate to excellent yields (Table 3.5, entries 1 to 3). Clearly, the alcohol functionality in entry 2 was deprotonated by excess Grignard reagent and regenerated upon quenching with dilute acid. The position of the ester group relative to the halide was influential on the outcome of the cross-coupling, as

well as the nature of the nucleophile.[37] When the bromo group was present in the ε-position of the ester, an excellent yield of cross-coupled product was observed for *o*-tolylmagnesium bromide at room temperature (Table 3.5, entry 3), but cross-coupling of ethyl-6-bromohexanoate with *p*-fluorophenyl Grignard, however, was modest, even upon microwave heating (Table 3.5, entry 4). When 2-bromoethylbenzoate was employed with *o*-tolyl Grignard, no cross-coupling was observed (Table 3.5, entry 5). Reacting 1-bromo-2-methoxyethane with *o*-tolylmagnesium bromide gave only poor yields (Table 3.5, entry 6). Stereochemical investigations were performed by arylation of *exo*-2-bromonorbornene, where retention of stereochemistry was observed (Table 3.5, entry 7).

Table 3.5: Kumada type sp^3-sp^2 cross-coupling by using functional-group alkyl halides as substrates

Entry	ArMgBr	Alkyl Halide	Product	Yield (%)
1	*o*-Tolyl	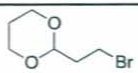	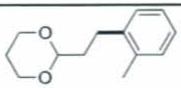	61
2	*o*-Tolyl	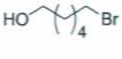	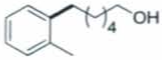	54
3	*o*-Tolyl	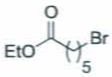	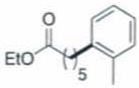	91
4	*p*-FPh	"	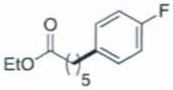	30 32[a]
5	*o*-Tolyl	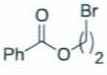	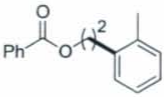	0 0[a]
6	*o*-Tolyl		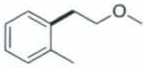	19
7	*o*-Tolyl		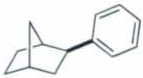	93 99[a]

[a] Microwave heating for 10 min at 100 °C.

3.3 Mechanistic Studies

Recently, iron-based catalytic systems have attracted increasing interest from many groups because of their unique catalytic properties and low environmental impact. Iron is able to cross-couple a wide variety of sp^3 and sp^2 nucleophiles and electrophiles.

Until very recently, however, little was known about the mechanisms of iron-catalyzed reactions because of the paramagnetic nature of Fe and the instability of the alkyliron intermediates.[38] Chemists can only propose some possible pathways according to their results and observations. This section will discuss the mechanistic study of sp^3-sp^2 Kumada C-C cross-coupling promoted by iron.

Fürstner[19-21] and co-workers demonstrated that well-defined iron-complexes of oxidation states Fe(+1)/Fe(+3), Fe(0)/Fe(+2), and Fe(-2)/Fe(0) can all be active catalytic species, according to the acquired data that C-C bond formations can occur, *a priori*, along different catalytic cycles shuttling between metal centres of the formal oxidation states (Figure 3.2).

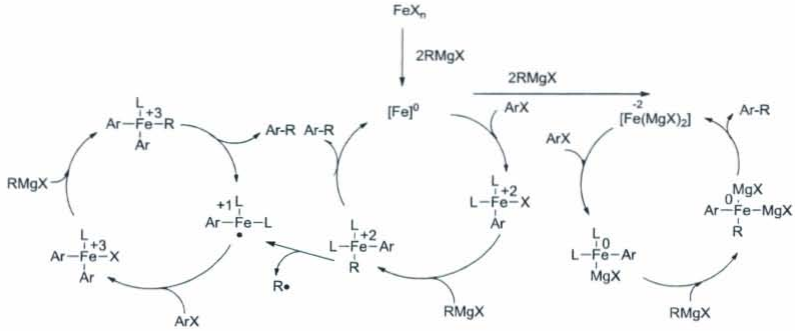

Figure 3.2 One of many conceivable scenarios of

interconnected catalytic redox cycles

Hayashi *et al.* illustrated a plausible mechanism according to the distribution of products in the reaction of aryl Grignard reagent and alkyl halide bearing a β-H (Figure 3.3). [17] This cross-coupling cycle explains the formation of alkene, alkane and biaryl by-

products. By screening the ratio of product/by-product distribution one can obtain details regarding stability of intermediates and qualitative rates of the different steps in the cycle.

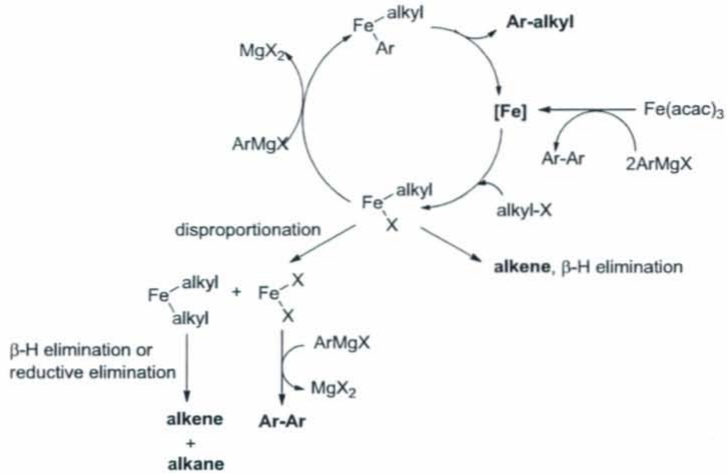

Figure 3.3: Plausible mechanism for the aryl-alkyl coupling from Hayashi *et al.*

In Nakamura's iron-catalyzed sp^3-sp^2 Kumada type C-C cross-coupling report,[25] they showed different reaction conditions lead to different results: when phenyl Grignard reagent combined with 1-bromo-5-hexene were added to a mixture of TMEDA and $FeCl_3$ at -78 °C and warmed to room temperature, the product of radical-initiated ring closing, benzyl cyclopentane, can be detected. No cyclic-product was observed when a mixture of PhMgBr and TMEDA was added dropwise to a solution of 1-bromo-5-hexene and $FeCl_3$. This suggested the existence of two processes, one involving a short-lived radical and the other a long lived-radical.[39,42] Further research for the effect of TMEDA was performed by using (TMEDA)Fe(Ar)Br on the basis of the isolation and reaction of these organoiron complexes.[39] When (TMEDA)$FeAr_2$ reacted with bromomethylcyclopropane, it gave a

mixture of cyclic- and alkenyl products. This implied single electron transfer was involved in the reaction. A proposed cycle is shown in Figure 3.4.

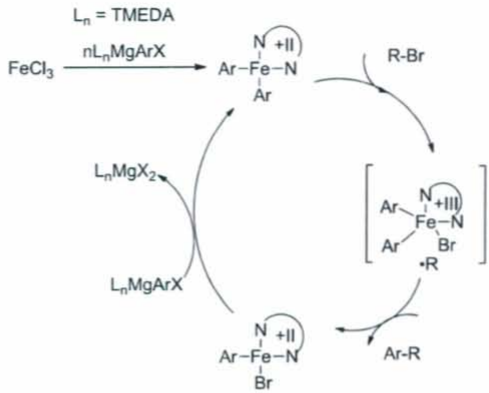

Figure 3.4: Plausible mechanism from Nakamura *et al.*

Bedford *et al.* suggested a possible radical-based coupling mechanism. [18, 22-24] When in the presence of their catalysts (Fe/amine, Fe/phosphine, Fe-based nanoparticles), phenyl Grignard reagent reacts with bromomethylcyclopropane or 6-bromohexene, to generate products formed by predominantly radical-based routes. As shown in Figure 3.5, the Grignard reagent first reacts with the iron pre-catalyst, then the active iron species in oxidation state n reacts with the alkyl halide by the transfer of a single electron to generate an alkyl radical (via the intermediate formation of a radical anion) and an $[Fe^{(n+1)}X]$ species. Transmetallation to give an organo-iron species is followed by reductive elimination to give the cross-coupled product.

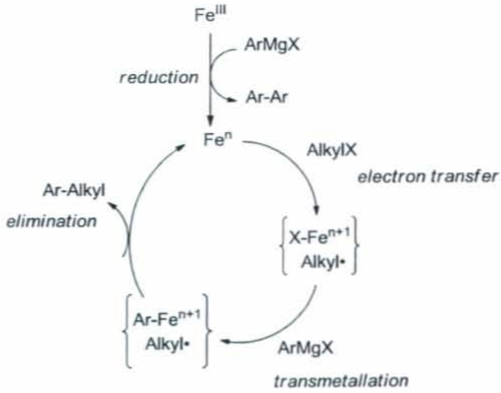

Figure 3.5: Plausible mechanism for the aryl-alkyl coupling from Bedford *et al.*

Cahiez and co-workers suggested a two-step single-electron transfer mechanism[26, 27] based on the reports of Fu *et al.*[40, 41] and their own observations. Fu and co-workers showed that the secondary alkyl halides do not react under palladium catalysis as the oxidative addition is too slow. They believe the main reason is steric effects. However, from the results of Cahiez involving iron catalysts, there is not much difference between primary and secondary alkyl halides as substrates. Both steric cyclic and acyclic secondary alkyl bromides can be used successfully. Therefore, Cahiez proposed a two-step single-electron transfer pathway in their catalytic cycle as shown in Figure 3.6.

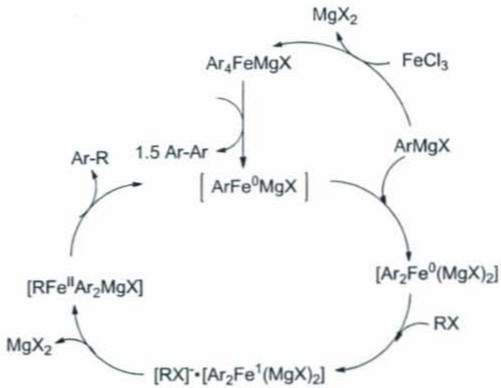

Figure 3.6: Plausible mechanism for the aryl-alkyl coupling from Cahiez *et al.*

In our conditions, reaction of *o*-tolyl Grignard with bromomethylcyclopropane in the presence of $\{FeCl[O_2N]^{BuMenPr}\}_2$ (**1**) yielded a mixture of the cyclopropyl and alkene products (34% to 52%, respectively) implying both oxidative addition and single electron transfer processes compete during the catalytic cycle (Scheme 3.1). However, reaction of Grignard with 6-bromo-1-hexene gave predominantly alkene product in 60% yield by GC. The estimated rate of ring opening of cyclopropylmethyl radical is 1.3×10^8 M^{-1} s^{-1} and of 5-hexenyl radical cyclization is 1.0×10^8 M^{-1} s^{-1}.[39,42] The above results suggest that the lifetime of the radical intermediate is too short for the cyclization of 5-hexenyl radical to occur, but long enough to allow the partial ring opening of the cyclopropylmethyl radical. Also, successful coupling with secondary alkyl halides as electrophile substrates also implied a radical is involved in the catalytic pathway.

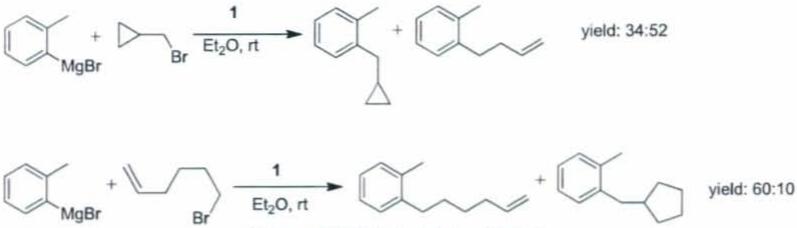

Scheme 3.1 "Radical Clock" Study

3.4 Experimental

3.4.1 Instrumentation

NMR spectra were recorded in $CDCl_3$ on a Bruker Avance-500 spectrometer. Gas chromatography mass spectrometry (GC-MS) analyses were performed using an Agilent Technologies 7890 GC system coupled to an Agilent Technologies 5975C mass selective detector (MSD). The chromatograph is equipped with electronic pressure control, split/splitless and on-column injectors, and an HP5-MS column. All catalytic reactions were performed on a Radleys Carousel Reactor™. Twelve 45 mL reaction tubes were fitted with threaded Teflon caps equipped with valves for connection to the inert gas or vacuum supply of Schlenk apparatus, and septa for the introduction of reagents. Microwave-heated reactions were performed using a Biotage Initiator™ Eight microwave synthesizer.

3.4.2 General Procedures

All experimental manipulations were carried out under an atmosphere of dry nitrogen using standard Schlenk techniques and glovebox. Solvents were dried using either an MBraun solvent purification system or distilled under nitrogen using the

appropriated drying agents. Dodecane was used as the internal standard and diethyl ether was used as the solvent for preparation of samples for GC-MS. The analyte concentration was 1×10^{-6} g L^{-1}, $CDCl_3$ with TMS was the solvent for ^1H NMR analysis.

3.4.2.1 Catalytic Method for Microwave assisted

Cross-coupling reactions: In a glove box (50 mg, 0.1 mmol, 5.0 mol% of Fe vs. alkyl halide) of complex **1** and a magnetic stir bar were added to a Biotage™ microwave vial, which was sealed with a septum cap. A solution of alkyl halide (2.00 mmol) in Et_2O was injected into the vial, followed by 4.00 mmol of Grignard reagent in Et_2O (except for Table 3.2, entries 3 and 4 where 8.00 mmol of Grignard was used, and in Table 3.3, entry 3 where 25.0 mmol of 1,4-dichlorobutane was used with 4.00 mmol ArMgBr). The mixture was heated in a Biotage Initiator™ Eight Microwave Synthesizer using the following parameters: time = 10 min; temperature = 100 °C; prestirring = off; absorption level = high; fixed hold time = on. Upon completion, 2.00 mmol of dodecane (internal standard) was added to the mixture followed by 5.0 mL of 1 M HCl(aq) to quench. The organic phase was extracted with Et_2O (1 x 5 mL) and dried over $MgSO_4$.The product yields were quantified by GC-MS (relative to standard curves) and in several cases by ^1H NMR.

3.4.2.2 Catalytic Method at Room Temperature

Catalyst **1** (50 mg, 0.1 mmol, 5.0 mol% vs. alkyl halide) in CH_2Cl_2 (3 mL) was added to the reaction flask followed by removal of the solvent *in vacuo*. To the catalyst

were added Et_2O (5 mL), and the alkyl halide (2.0 mmol). The aryl Grignard (4.0 mmol) was added carefully and the resulting mixture was stirred at room temperature. After 30 min, dodecane (2.0 mmol as internal standard) was added and then the reaction was quenched with HCl (aq., 2 M, 5 mL) and the organic phase was extracted with Et_2O (1 x 5 mL) and dried over $MgSO_4$. The mixture was analyzed by GC-MS and quantified using ^1H NMR and/or GC. NMR samples were prepared by careful removal of solvent under vacuum and dissolving the residue in $CDCl_3$.

3.5 Conclusion

In summary, we have developed a new easily prepared, air-stable, single component Fe^{III} complex that catalyzes the $C(sp^3)$-$C(sp^2)$ bond forming reaction between aryl Grignard reagents and alkyl halides, including primary as well as cyclic or acyclic secondary alkyl chlorides. The system shows improved reactivity for sterically demanding nucleophiles, such as 2,6-dimethylphenylmagnesium bromide, and has demonstrated that diarylmethane motifs can be obtained using both benzyl bromides and chlorides. Lastly, microwave heating of diethyl ether solutions to 100 °C gives improved conversions for several substrate combinations.

3.6 References

(1) Diederich, F., Stang, P. J. *Metal-Catalyzed Cross-Coupling Reactions*, 2nd ed. Wiley-VCH: Weinheim. **2004**.

(2) Càrdenas, D. J. *Angew. Chem. Int. Ed.* **2003**, *42*, 384.

(3) Frisch, A. C.; Beller, M. *Angew. Chem. Int. Ed.* **2005**, *44*, 674.

(4) Netherton, M. R.; Fu, G. C. *Adv. Synth. Catal.* **2004**, *346*, 1525.

(5) Kochi, J. K. *Acc. Chem. Res.* **1974**, *7*, 351.

(6) Czaplik, W. M.; Mayer, M.; Jacobi von Wangelin, A. *Angew. Chem. Int. Ed.* **2009**, *48*, 607.

(7) Fürstner, A. *Angew. Chem. Int. Ed.* **2009**, *48*, 1364.

(8) Rudolph, A.; Lautens, M. *Angew. Chem. Int. Ed.* **2009**, *48*, 2656.

(9) Sherry, B. D.; Fürstner, A. *Acc. Chem. Res.* **2008**, *41*, 1500.

(10) Fürstner, A.; Martin, R. *Chem. Lett.* **2005**, *34*, 624.

(11) Martin, R.; Fürstner, A. *Angew. Chem. Int. Ed.* **2004**, *43*, 3955.

(12) Zhou, J.; Fu, G. C. *J. Am. Chem. Soc.* **2003**, *125*, 12527.

(13) Frisch, A. C.; Shaikh, N.; Zapf, A.; Beller, M. *Angew. Chem. Int. Ed.* **2002**, *41*, 4056.

(14) Kirchhoff, J. H.; Dai, C.; Fu, G. C. *Angew. Chem. Int. Ed.* **2002**, *41*, 1945.

(15) Chowdhury, R. R.; Crane, A. K.; Fowler, C.; Kwong, P.; Kozak, C. M. *Chem. Commun.* **2008**, 94.

(16) Bedford, R. B.; Huwe, M.; Wilkinson, M. C. *Chem. Commun.* **2009**, 600.

(17) Nagano, T.; Hayashi, T. *Org. Lett.* **2004**, *6*, 1297.

(18) Bedford, R. B.; Bruce, D. W.; Frost, R. M.; Goodby, J. W.; Hird, M. *Chem. Commun.* **2004**, 2822.

(19) Fürstner, A.; Leitner, A.; Méndez, M.; Krause, H. *J. Am. Chem. Soc.* **2002**, *124*, 13856.

(20) Fürstner, A.; Leitner, A. *Angew. Chem. Int. Ed.* **2002**, *41*, 609.

(21) Fürstner, A.; Krause, H.; Lehmann, C. W. *Angew. Chem. Int. Ed.* **2006**, *45*, 440.

(22) Bedford, R. B.; Betham, M.; Bruce, D. W.; Danopoulos, A. A.; Frost, R. M.; Hird, M. *J. Org. Chem.* **2006**, *71*, 1104.

(23) Bedford, R. B.; Betham, M.; Bruce, D. W.; Davis, S. A.; Frost, R. M.; Hird, M. *Chem. Commun.* **2006**, 1398.

(24) Bedford, R. B.; Bruce, D. W.; Frost, R. M.; Hird, M. *Chem. Commun.* **2005**, 4161.

(25) Nakamura, M.; Matsuo, K.; Ito, S.; Nakamura, E. *J. Am. Chem. Soc.* **2004**, *126*, 3686.

(26) Cahiez, G.; Habiak, V.; Duplais, C.; Moyeux, A. *Angew. Chem. Int. Ed.* **2007**, *119*, 4442.

(27) Cahiez, G.; Duplais, C.; Moyeux, A. *Org. Lett.* **2007**, *9*, 3253.

(28) Bica, K.; Gaertner, P. *Org. Lett.* **2006**, *8*, 733.

(29) Caddick, S.; Fitzmaurice, R. *Tetrahedron* **2009**, *65*, 3325.

(30) Kappe, C. O. *Chem. Soc. Rev.* **2008**, *37*, 1127.

(31) Appukkuttan, P.; Van Der Eycken, E. *Eur. J. Org. Chem.* **2008**, 1133.

(32) Kappe, C. O. *Angew. Chem. Int. Ed.* **2004**, *43*, 6250.

(33) Strauss, C. R. *Angew. Chem. Int. Ed.* **2002**, *41*, 3589.

(34) Lidström, P.; Tierney, J.; Wathey, B.; Westman, J. *Tetrahedron* **2001**, *57*, 9225.

(35) Walla, P.; Kappe, C. O. *Chem. Commun.* **2004**, *10*, 564.

(36) Hasan, K.; Fowler, C.; Kwong, P.; Crane, A. K.; Collins, J. L.; Kozak, C. M. *Dalton Trans.* **2008**, 2991.

(37) Guérinot, A.; Reymond, S.; Cossy, J. *Angew. Chem. Int. Ed.* **2007**, *46*, 6521.

(38) Kleimark, J.; Hedström, A., Larsson, P.; Johansson, C.; Norrby, P. *ChemCatChem* **2009**, 152.

(39) Noda, D.; Sunada, Y.; Hatakeyama, T.; Nakamura, M.; Nagashima, H. *J. Am. Chem. Soc.* **2009**, *131*, 6078.

(40) Saito, B.; Fu, G. C. *J. Am. Chem. Soc.* **2007**, *129*, 9602.

(41) Son, S.; Fu, G. C. *J. Am. Chem. Soc.* **2008**, *130*, 2756.

(42) Vechorkin, O.; Proust, V.; Hu, X. *J. Am. Chem. Soc.* **2009,** *131*, 9756.

Chapter 4. Iron-catalyzed Double C-Cl Bond Cleavage in Dichloromethane and Chloroform

4.1 Introduction

Transition-metal catalyzed C-C cross-coupling is a powerful tool in organic synthesis and significant advances have been made using aryl and alkenyl halides and pseudohalides as electrophiles.[1] Unactivated alkyl halides, however, continue to pose a challenge,[2,3] and only a few examples of C-C catalysis using alkyl chlorides in particular have been reported.[4-8] Even fewer reports exist of catalytic coupling of di- or polychloroalkanes with organometallic nucleophiles. Particularly noteworthy is the Ni-catalyzed activation of CH_2Cl_2 and $CHCl_3$ leading to selective C-C bond formation with alkyl Grignard reagents (Figure 4.1).[9]

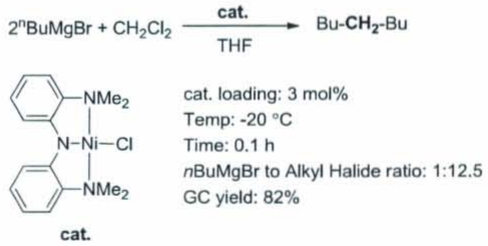

Figure 4.1: Ni-catalyzed activation of CH_2Cl_2 and $CHCl_3$

Related Ni(II) alkyl complexes (Figure 4.2) can react slowly with CH_2Cl_2 (765 equiv), at 110 °C, but no organic product was identified.[10]

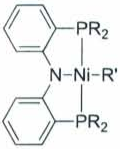

R = Ph, ^{i}Pr, Cy
R' = Me, Et, *n*Bu

Figure 4.2: PNP pincer Ni(II) alkyl complexes

Furthermore, Ag-catalyzed insertion of a carbene into one C-Cl bond of CH_2Cl_2, $CHCl_3$ and CCl_4 forming a new C-C bond has also been reported (Figure 4.3).[11]

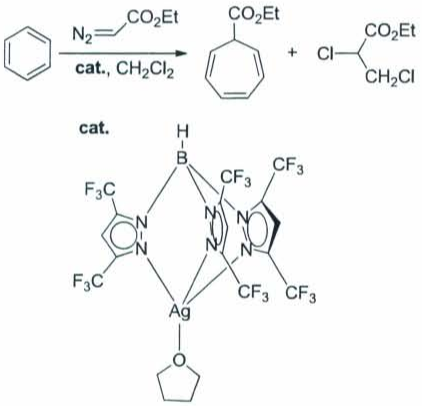

Figure 4.3: Ag-catalyzed insertion of a carbene into one C-Cl bond of CH_2Cl_2

The use of iron for catalytic C-C cross coupling is undergoing a renaissance and various iron-based processes have been described.[4,12-32] Iron is cheap, non-toxic and environmentally benign; therefore, the use of readily prepared iron catalysts that are easily handled is extremely desirable. The ability of iron(III) salts to catalyze cross-

coupling reactions of dichloro systems with Grignard reagents was demonstrated by Tanabe and co-workers using gem-dichlorocyclopropanes as electrophilic partners.[33]

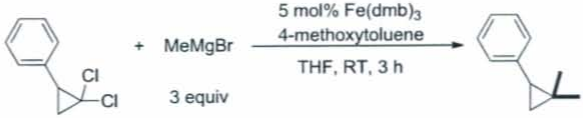

Figure 4.4 Cross-coupling reactions of gem-dichlorocyclopropanes with methyl Grignard reagent

Herein we report the first example of multiple cleavage of C-Cl bonds with aryl/benzyl Grignard reagents by Fe(III) under mild conditions. The products of the cross-coupling are diarylmethanes, but sometimes diarylethanes and other diarylalkanes are obtained as minor products.

4.2 Results & Discussion

4.2.1 General Procedure

Catalytic reactions were performed at either room temperature, or at 100 °C using microwave-assisted heating. An amine-bis-(phenolate) iron complex, $\{FeCl[O_2N]^{BuMenPr}\}_2$ (**1**), or $FeCl_3$ were used initially as catalysts. Different iron salts, ligands and Grignard reagents were then screened, and poor yielding reactions were optimized with respect to different reaction conditions. A catalyst loading of 5 mol% (vs. Grignard reagent) of Fe(III)-complex or $FeCl_3$ was added to flasks followed by CH_2Cl_2 and the Grignard reagent. The best ratio of Grignard reagent to the organohalide was found to be 1:12.5. The reaction mixture was stirred for 30 min at room temperature or 10 min, at 100 °C, after which time it was quenched by adding HCl (aq 2.0 M, 5.0 mL). The

coupled products (Scheme 4.1) were detected using GC-MS and ^{1}H NMR, with dodecane as the internal standard.

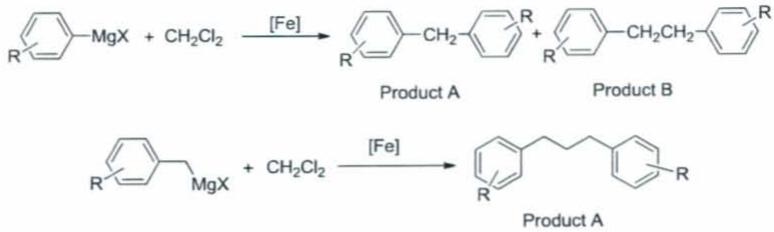

Scheme 4.1 General dichloromethane activation cross-coupling reactions

4.2.2 Catalyst Loading Study

The effect of catalyst loading was investigated (Table 4.1). Increasing the amount of **1** versus the aryl Grignard reagent actually *decreases* the yields of diarylmethane formed (Table 4.1, entries 1 to 3). It has been proposed that iron-catalyzed cross-coupling of Grignard reagents with electrophiles proceeds by the formation of reduced Fe as the active species, which are generated by excess Grignard.[16] Therefore, a higher catalyst loading consumes more Grignard reagent, which is the limiting reagent since the alkyl halide (dichloromethane) is present in large excess.

The optimum loading of **1** was found to be 1.25 mol% versus Grignard (Table 4.1, entry 1) giving 83% yield of cross-coupled product. Lowering the catalyst concentration to 0.5 mol% causes lower yields of diarylmethane (Table 1, entry 4). The absence of **1** gives no cross-coupled products (Table 4.1, entry 5). This optimization was not repeated for $FeCl_3$.

Table 4.6: Condition Optimization: Different [cat] loading

Entry	Catalyst	Loading (mol%)	Grignard Reagent	Ratio[b]	Product A	Product B
1[a]	1	1.25	o-tolyl	1:12.5	83	13
2[a]	"	2.5	"	"	72	7
3[a]	"	5	"	"	69	7
4	"	0.5	"	"	56	7
5	-	-	"	"	0	0

[a] average of two runs. [b] Grignard reagent:CH_2Cl_2

4.2.3 Effects of Nucleophile to Electrophile Ratio, Addition Rate and Temperature

Increasing the CH_2Cl_2-to-Grignard ratio also lowers yield of diarylmethane (Table 4.2, entry 1). A 2:1 loading of Grignard to CH_2Cl_2 results in much lower yields of diarylmethane and no diarylethane (Table 4.2, entry 2). Slow addition of Grignard reagent over a period of 20 minutes using a syringe pump (Table 4.2, entries 3 and 4) decreases the yield of diarylmethane, as does conducting the reaction at 0 °C (Table 4.2, entry 5).

Table 4.7: Condition Optimizing: Nucleophile to Electrophile Ratio, Grignard Addition Rate and Temperature

Entry	Catalyst	Loading (mol%)	Grignard Reagent	Ratio[c]	Product A	Product B
1	**1**	1.25	*o*-tolyl	1:25	51	10
2	"	1.25	"	2:1	27	0
3[a,b]	"	1.25	"	1:12.5	56	10
4[a,b]	"	2.5	"	1:12.5	58	14
5[c]	"	1.25	"	1:12.5	48	9

[a] average of two runs. [b] 3.8 mmol Grignard reagent was added dropwise by syringe pump over 20 min. [c] 0 °C. [c] Grignard reagent:CH_2Cl_2

4.2.4 Variation of Iron Salt and Use of Additives

Interestingly, using $FeBr_3$ gave lower yields of diarylmethane (Table 4.3, entry 1) than the chloride salt (Table 4.4, entry 11), and no diarylethane was observed. The reaction is also strongly dependent upon the Grignard reagent. Using $FeCl_3$ as the catalyst and phenyl Grignard reagent, yields diarylmethane drops significantly and diarylethane was observed in approximately equal yield. Microwave-assisted heating to 100 °C significantly increased the yield when phenyl Grignard reagent reacted with CH_2Cl_2 (Table 4.3, entry 2). Low oxidation state iron is believed to be involved during the catalytic pathway of Fe-catalyzed cross-coupling reactions. Therefore, previous reports have introduced low oxidation iron-catalysts possessing π-carbon type ligands,[34] which

may first react with RMgX and form an anionic complex, then react with alkyl halides. These catalysts are effective for cross-coupling reactions. Thus, we screened different ligands, such as amine or π-carbon type ligands, but from the results we can find they do not give a remarkable increase in the yield of cross-coupling products (Table 4.3, entries 3-6).

The trace impurities of iron(II) salt, copper, palladium and other metal salts have also been shown to strongly influence the yields of cross-coupling reactions where iron(III) salts were used as catalysts,[35] therefore we studied various other simple metal salts for their ability to perform this reaction. Perhaps strangely, $FeCl_2$ shows a poor ability to catalyze cross-coupling (Table 4.3, entry 7), whereas CuCl and $CuBr_2$ (Table 4.3, entry 8 and 9) give no yield of either product A or B. Using $Fe(acac)_3$ with and without TMEDA does not catalyze cross-coupling when phenyl Grignard reagent reacts with CH_2Cl_2, but these conditions are effective when *o*-tolyl Grignard reagent reacts with CH_2Cl_2. Using Pd salts, such as $PdCl_2$ and $Pd(OAc)_2$ gives moderate yields when *o*-tolyl Grignard reagent react with CH_2Cl_2. It is worth noting that Pd catalysts produce product B, diarylethane, as the major products.

Table 4.8: Different Metal Salts and Use of Additives

Entry	Catalyst[d]	Grignard Reagent	Product A	Product B
1	$FeBr_3$	*o*-tolyl	56	0
2	$FeCl_3$	phenyl	21/43[a]	25/27[a]
3[b]	$FeCl_3$ + TMEDA	"	17	25
4[b]	$FeCl_3$ + DMF	"	16	5
5[b]	$FeCl_3$ + 1-Octene	"	33	17
6	$FeCl_3$ + COD	"	25	21
7	$FeCl_2$	*o*-tolyl	12	10
8	CuCl	*o*-tolyl	0	0
9	$CuBr_2$	"	0	0
10	$Fe(acac)_3$	phenyl	trace	trace
11[c]	$Fe(acac)_3$ + TMEDA	"	trace	trace
12	$Fe(acac)_3$	*o*-tolyl	90	trace
13[c]	$Fe(acac)_3$ + TMEDA	"	81	7
14	$Pd(OAc)_2$	"	23	51
15	$PdCl_2$	"	13	31

[a] microwave-assisted 100 °C, 10 min. [b] 1 equiv. ligand to Grignard reagent. [c] 10 mol% additives to Grignard reagent. [d] 2.5 mol% cat. vs. Grignard.

4.2.5 Different Grignard Reagents

A range of Grignard reagents were also screened. When *p*-tolyl- and phenylmagnesium bromide solutions were added to solutions of **1** in CH_2Cl_2 at room temperature only poor yields of diarylmethane were obtained (Table 4.4, entries 1 and 2), but in the case of phenyl Grignard, 1,2-diphenylethane was the major product, albeit in poor yield. The presence of the *ortho*-methyl group may be key to the stability of Fe-aryl intermediates. Use of secondary and primary alkyl Grignard nucleophiles (Table 4.4, entries 3 and 4) gave little or no cross-coupled products, contrary to results obtained using Ni(II) complexes where good yields of cross-coupling products were observed using alkyl nucleophiles but no conversion was shown for aryl nucleophiles.

Entries 7-9 in table 4.4 show that various anisyl Grignards all gave poor yields. It is worth noting that when 4-methoxyphenyl Grignard reagent was reacted with CH_2Cl_2, in addition to diarylmethane and diarylethane, 1,3-diarylpropane and 1,4-diarylbutane were also detected by GC-MS.

When the simple iron salt, $FeCl_3$ was used as the pre-catalyst, *p*-tolyl Grignard reagent gave poorer yields compared to **1**, but *o*-tolyl Girgnard gave better yield of diarylmethane than **1** (Table 4.4, entries 10, 11). Interestingly, when 2,6-dimethylphenyl Grignard reagent was reacted with CH_2Cl_2, only product B, diarylethane was obtained. Microwave-assisted heating to 100 °C could be used to increase the cross-coupling moderately (Table 4.4, entry 12).

Both electron-donating and withdrawing functional group-containing benzyl Grignard reagents were reacted with CH_2Cl_2 and gave good yields of cross-coupling products (Table 4.4, entry 5, 6, 13). For 4-methoxybenzyl Grignard reagent, **1** is a more effective catalyst than $FeCl_3$.

No cross-coupling products were detected when allyl and 2-methylnaphthyl Grignard reagents were reacted with CH_2Cl_2 (Table 4.4, entry 14, 15) using $FeCl_3$. However, 4-Fluorophenyl Grignard reagent reacted with CH_2Cl_2 to give modest yields of diarylmethane and diarylethane products. Heating to 100 °C decreased the yields of these products, and caused a diaryl propane product to form, as shown by GC-MS (Table 4.4, entry 16). 1-Naphthyl Grignard reagent only gaves product A in modest yield (Table 4.4, entry 17).

Table 4.9: Effect of Grignard Reagent on Cross-coupling

Entry	catalyst	Grignard Reagent	Ratio	Product A	Product B
1	**1**	phenyl	1:12.5	11	22
2	"	*p*-tolyl	1:25	21	10
3	"	cyclohexyl	1:12.5	1.3	0.8
4	"	*n*-butyl	"	0	0
5	"	4-methoxybenzyl	"	71	9
6	"	4-flourobenzyl	"	60	0
7	$FeCl_3$	2-methoxyphenyl	"	36	19
8	"	3-methoxyphenyl	"	18	18
9	"	4-methoxyphenyl	"	23	13
10	"	*p*-tolyl	1:25	14	10
11	"	*o*-tolyl	1:12.5	90	trace
12	"	2,6-dimethylphenyl	"	trace	16/40[a]
13	"	4-methoxylbenzyl	"	38	9
14	"	allyl	"	0	0
15	"	2-methylnaphthalyl	"	0	0
16	"	4-fluorophenyl	"	33/18[a]	10/7[a]
17	"	1-naphthyl	"	35	-

[a] microwave-assisted, 100 °C, 10 min.

4.2.6 Results for $CDCl_3$ Activation

Using chloroform as the electrophile, only 1,2-dichloro-1,2-diarylethane was obtained as the main product. Complex **1** and $FeCl_3$ gave similar results with *o*-tolyl Grignard (Table 4.5 entries 1 and 3) whereas *p*-tolyl Grignard reagent again gave a lower yield (entry 2). This trend in yields is similar to that observed for CH_2Cl_2 activation. While the chloroform reacted with the hindered Grignard reagent 2,6-dimethylphenyl magnesium bromide, 1,2-diarylethene was obtained as the product (entry 4). All the yields are quite poor.

Table 4.10: Results for $CDCl_3$ Activation

Entry	Catalyst	Grignard Reagent	Ratio	Product	Yield %
1	**1**	*o*-tolyl	1:12.5	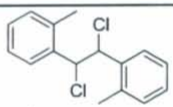	12
2	**1**	*p*-tolyl	1:25	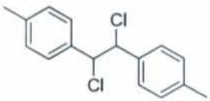	6
3	$FeCl_3$	*o*-tolyl	1:12.5	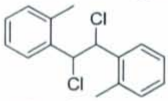	11
4	$FeCl_3$	2,6-dimethylphenyl	1:12.5	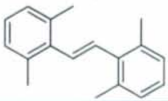	5

4.3 Conclusions

Iron complex **1** and simple iron salts ($FeCl_3$ and $Fe(acac)_3$) can catalyze multiple C-Cl bond activations in CH_2Cl_2 and $CHCl_3$. This is the first report in this field. The effect of varying the type of the Grignard reagent on cross-coupling yields was screened. However, only *o*-tolyl and benzyl type Grignard reagents gave good results for double cross-coupling. For the remaining Grignards attempted, the biaryl homocoupling products were obtained in high yields. The results suggest that the cross-coupling reactions and homo-coupling reactions are very competitive during the catalytic cycle. When the Grignard reagent is too bulky to form the homo-coupling by-product, it will be prone to react with CH_2Cl_2 and give the cross-coupling product. These results indicate a delicate balance of steric influence, since *o*-tolyl appears well suited to giving the cross-coupled product whereas 2,6-dimethylphenyl is too hindered for double cross-coupling and instead gives the diarylethane product preferentially. Furthermore, increasing the nucleophilicity will be prone to give a long chain cross-coupling product, as conducted at high temperature (Table 4.4, entries 9 and 16).

The formation of diarylethane in the cross-coupling of CH_2Cl_2 with some Grignard reagents suggests the formation of an arylmethyl radical, which subsequently undergoes radical coupling. Since yields of the diarylmethane products are favoured under optimized conditions, the reaction of arylmethyl radicals with aryl nucleophiles proceeds faster than homocoupling, particularly if the concentration of Grignard *vs.* Fe (and alkyl radical) is high. In the cross-coupling of aryl Grignards with chloroform, biaryl formation dominates. Since no Ar-$CDCl_2$ product is observed, it must therefore react

upon formation with Fe to generate Ar-CDCl$^{\bullet}$ radical, which undergoes homocoupling to give the 1,2-dichloro-1,2-diarylethane product. Further studies to extend the scope of this methodology and to gain detailed mechanistic insight are currently underway in our laboratory.

Another hypothesis that may be proposed is during the catalytic cycle a carbene intermediate (H_2C:) may occur since GC-MS can detect 1,3-diarylpropane and 1,4-diarylbutane as products (for example, Table 4.3, entry 2; Table 4.4 entries 9 and 16). Moreover, in the presence of strong base, such as potassium *t*-butoxide, organolithium or Grignard reagents, chloroform undergoes α-H elimination and may lose one Cl^- to form a carbine (Figure 4.4).[12]

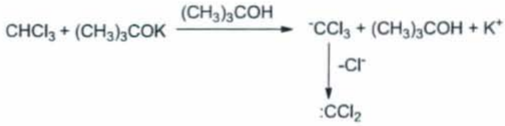

Figure 4.5: Carbene formed from chloroform under basic conditions

Dihalomethanes also give similar reactions that form zinc or copper carbenoids. As shown in Figure 4.5.[36-40]

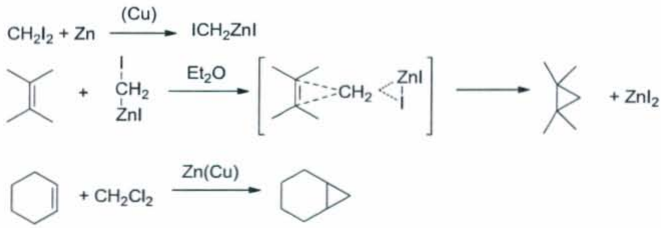

Figure 4.6: Dihalomethane insertion reactions via carbene

Thus, it is proposed that dichloromethane may react with the Grignard reagent and form a Mg carbenoid. This intermediate may react with the low oxidation state iron intermediate, as shown in a hypothetical mechanistic model shown in Equation 1. This model may also explain why a redox catalyst such as Fe is important and why adding the Grignard reagent slowly will decrease the yield (Table 4.2).

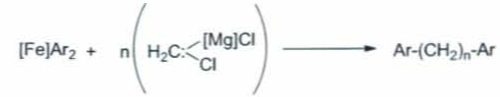

(Eq.1)

4.4 Experimental

4.4.1 Instrumentation

NMR spectra were recorded in $CDCl_3$ on a Bruker Avance-500 spectrometer. Gas chromatography mass spectrometry (GC-MS) analyses were performed using an Agilent Technologies 7890 GC system coupled to an Agilent Technologies 5975C mass selective detector (MSD). The chromatograph is equipped with electronic pressure control, split/splitless and on-column injectors, and an HP5-MS column. All catalytic reactions were performed on a Radleys Carousel Reactor™. Twelve 45 mL reaction tubes were fitted with threaded Teflon caps equipped with valves for connection to the inert gas or vacuum supply of Schlenk apparatus, and septa for the introduction of reagents. Microwave-heated reactions were performed using a Biotage Initiator™ Eight microwave synthesizer.

4.4.2 General Procedures

Unless otherwise stated, all manipulations were performed under an atmosphere of dry oxygen-free nitrogen by means of standard Schlenk or glove box techniques. Anhydrous diethyl ether and THF were stored over sieves and distilled from sodium benzophenone ketyl under nitrogen in the case of THF or purified by an MBraun Solvent Purification System in the case of diethylether. Reagents were purchased either from Aldrich, Alfa Aesar or STREM and used without further purification. Grignard reagents were analyzed by GC-MS after being quenched with dilute HCl(aq) to quantify biaryl complexes or other impurities present prior to their use in catalyst runs. Anhydrous $FeCl_3$ (97%), $FeBr_3$ (99%), $FeCl_2$ (99%) were purchased from Aldrich. $Pd(OAc)_2$ (99%), $PdCl_2$ (99%) were purchased from Precious Metals Online, Monash University, Australia.

4.4.2.1 Catalytic Method at Room Temperature

Catalyst **1** (0.05 mmol, 1.25 mol% vs. Grignard reagent, per Fe atom) or $FeCl_3$ (97% purity, 0.02g, 2.5 mol% to Grignard reagent) in CH_2Cl_2 (3 mL) was added to the reaction flask, and a solution of Grignard reagent was added dropwise under vigorous stirring. The resulting mixture was stirred for 30 minutes, then quenched with 5 mL 2 M HCl (aq.). The organic phase was extracted with Et_2O (5 mL) and dried over $MgSO_4$. The mixture was analyzed by GC-MS and ^1H NMR. ^1H NMR samples were prepared by careful removal of solvent under vacuum and dissolving the residue in $CDCl_3$.

4.4.2.2 Catalytic Method for Microwave Heating

In a glove box 1.25 mol% **1** or 2.5 mol% $FeCl_3$ and a magnetic stir bar were added to a Biotage™ microwave vial, which was sealed with a septum cap. 1.5 mL CH_2Cl_2 (25 mmol) was injected into the vial. 1.9 mmol of Grignard reagent was injected slowly. The mixture was heated in a Biotage Initiator™ Eight Microwave Synthesizer using the following parameters: time = 10 min; temperature = 100 °C; prestirring = off; absorption level = high; fixed hold time = on. Upon completion, 1.9 mmol of dodecane was added to the mixture followed by 5 mL of 1 M HCl (aq). The product yields were quantified by GC-MS and in some cases by ^{1}H NMR.

4.4.2.3 Catalytic Method at 0 °C

Catalyst **1** (0.05 mmol, 2.5 mol% to Grignard reagent) or $FeCl_3$ (97% purity, 0.02 g, 5 mol% vs. Grignard reagent) in CH_2Cl_2 (3 mL) was added to the reaction flask. The solution was stirred at 0 °C for 10 min, and the Grignard reagent was added slowly. The work-up procedure is the same as for the room temperature reaction.

4.5 References

(1) de Meijere, A.; Diederich, F. Eds. *Metal-Catalyzed Cross-Coupling Reactions*. 2nd ed.; Wiley-VCH: Weinheim, **2004**.

(2) Frisch, A.C.; Beller, M. *Angew. Chem. Int. Ed.* **2005**, *44*, 674.

(3) Netherton, M.R.; Fu, G.C. *Adv. Synth. Catal.* **2004**, *346*, 1525.

(4) Martin, R.; Fürstner, A. *Angew. Chem. Int. Ed.* **2004**, *43*, 3955.

(5) Zhou, J.R.; Fu, G.C. *J. Am. Chem. Soc.* **2003**, *125*, 12527.

(6) Frisch, A.C.; Shaikh, N.; Zapf, A.; Beller, M. *Angew. Chem. Int. Ed.* **2002**, *41*, 4056.

(7) Kirchhoff, J.H.; Dai, C.Y.; Fu, G.C. *Angew. Chem. Int. Ed.* **2002**, *41*, 1945.

(8) Terao, J.; Watanabe, H.; Ikumi, A.; Kuniyasu, H.; Kambe, N. *J. Am. Chem. Soc.* **2002**, *124*, 4222.

(9) Csok, Z.; Vechorkin, O.; Harkins, S.B.; Scopelliti, R.; Hu, X. L. *J. Am. Chem. Soc.* **2008**, *130*, 8156.

(10) Liang, L. C.; Chien, P. S.; Lin, J. M.; Huang, M. H.; Huang, Y.L.; Liao, J. H. *Organometallics* **2006**, *25*, 1399.

(11) Dias, H. V. R.; Browning, R. G.; Polach, S. A.; Diyabalanage, H. V. K.; Lovely, C. J. *J. Am. Chem. Soc.* **2003**, *125*, 9270.

(12) Czaplik, W. M.; Mayer, M.; Cvengros, J.; von Wangelin, A. J. *ChemSusChem* **2009**, *2*, 396.

(13) Sherry, B. D.; Fürstner, A. *Acc. Chem. Res.* **2008**, *41*, 1500.

(14) Fürstner, A. *Angew. Chem. Int. Ed.* **2009**, *48*, 1364.

(15) Czaplik, W.M.; Mayer, M.; von Wangelin, A.J. *Angew. Chem. Int. Ed.* **2009**, *48*, 607.

(16) Fürstner, A.; Martin, R.; Krause, H.; Seidel, G.; Goddard, R.; Lehmann, C.W. *J. Am. Chem. Soc.* **2008**, *130*, 8773.

(17) Fürstner, A.; Martin, R. *Chem. Lett.* **2005**, *34*, 624.

(18) Fürstner, A.; Krause, H.; Lehmann, C.W. *Angew. Chem. Int. Ed.* **2006**, *45*, 440.

(19) Scheiper, B.; Bonnekessel, M.; Krause, H.; Fürstner, A. *J. Org. Chem.* **2004**, *69*, 3943.

(20) Seidel, G.; Laurich, D.; Fürstner, A. *J. Org. Chem.* **2004**, *69*, 3950.

(21) Neumann, S.M.; Kochi, J.K. *J. Org. Chem.* **1975**, *40*, 599.

(22) Tamura, M.; Kochi, J. *J. Am. Chem. Soc.* **1971**, *93*, 1487.

(23) Tamura, M.; Kochi, J. *Synthesis* **1971**, 303.

(24) Nakamura, M.; Matsuo, K.; Ito, S.; Nakamura, B. *J. Am. Chem. Soc.* **2004**, *126*, 3686.

(25) Bedford, R.B.; Bruce, D.W.; Frost, R.M.; Goodby, J.W.; Hird, M. *Chem. Commun.* **2004**, 2822.

(26) Bedford, R.B.; Bruce, D.W.; Frost, R.M.; Hird, M. *Chem. Commun.* **2005**, 4161.

(27) Bedford, R.B.; Betham, M.; Bruce, D.W.; Danopoulos, A.A.; Frost, R.M.; Hird, M. *J. Org. Chem.* **2006**, *71*, 1104.

(28) Nagano, T.; Hayashi, T. *Org. Lett.* **2004**, *6*, 1297.

(29) Bica, K.; Gaertner, P. *Org. Lett.* **2006**, *8*, 733.

(30) Cahiez, G.; Habiak, V.; Duplais, C.; Moyeux, A. *Angew. Chem. Int. Ed.* **2007**, *46*, 4364.

(31) Cahiez, G.; Chaboche, C.; Mahuteau-Betzer, F.; Ahr, M. *Org. Lett.* **2005**, *7*, 1943.

(32) Chowdhury, R.R.; Crane, A.K.; Fowler, C.; Kwong, P.; Kozak, C.M. *Chem. Commun.* **2008**, 94.

(33) Nishii, Y.; Wakasugi, K.; Tanabe, Y. *Synlett.* **1998**, 67.

(34) Terao, J.; Kambe, N. *Acc. Chem. Res.* **2008**, *41*, 1545.

(35) Bedford, R.B.; Nakamura, M.; Gower, N.J.; Haddow, M.F.; Hall, M.A.; Huwe, M.; Hashimoto, T.; Okopie, R.A., *Tetrahedron Lett.* **2009**, *50*, 6110.

(36) Yves, J. *Molecular Orbitals of Transition Metal Complexes*. Oxford, New York, **2005** ; p 275.

(37) Grasse, P. B.; Brauer, B. E.; Zupancic, J. J.; Kaufmann, K. J.; Schuster, G. B. *J. Am. Chem. Soc.* **1983**, *105*, 6833.

(38) Nemirowski, A.; Schreiner, P. *J. Org. Chem.* **2007**, *72*, 9533.

(39) Skell, P. S.; Woodworth, R. C. *J. Am. Chem. Soc.* **1956**, *78*,4496.

(40) Von E. Doering, W.; Hoffmann, A. K. *J. Am. Chem. Soc.* **1954**, *76*,6162.

Chapter 5. Future Work

5.1 Introduction

Iron-catalyzed cross-coupling reactions have matured to an advanced stage and show a versatile range of organic synthesis routes.[1] Although iron is the most abundant metal and iron salts are quite cheap, researchers have started working in depth in this area very recently. This chapter deals with the discussion of some current topics related to iron catalysis.

5.2 Further Studies of Iron-Catalyzed CH_2Cl_2 Activation Reactions

As the iron-catalyzed CH_2Cl_2 reactions show interesting results, further optimization of the reaction conditions to obtain better yields of the coupled products should be pursued. Even though it may be difficult to find a general catalytic system for a variety of Grignard reagents, information regarding the mechanism of iron-catalyzed C-C cross-coupling reactions may be revealed through trying different iron salts, ligands and temperatures.

Iron salts (or complexes), such as $Fe(dbm)_3$ (dbm = dibenzoylmethido) or the iron(-II) complex $[Li(tmeda)]_2[Fe(C_2H_4)_4]$ should be investigated because they show efficient catalytic ability for cross-coupling reactions of gem-dichlorocyclopropanes with methyl Grignard reagent[2] and alkylation of aryl Grignard reagents,[3] respectively. Some other kinds of low-valent iron complexes may be also worth investigating.[4] This work

may illustrate new vistas in iron catalysis, which is currently a "hot area" of research due to the cheap, non-toxic nature of iron and its diverse applications.

5.3 Iron-catalyzed Sonogashira C-C cross-coupling reaction

Aryl alkynes are very important compounds in chemical industry and pharmaceuticals.[5-9] The Sonogashira-Hagihara reaction has been known as the most straightforward and efficient method to form $C(sp^2)$-C(sp) bonds. Although transition-metal free Sonogashira-Hagihara reactions have been previously reported, they require very high temperature and phase-transfer catalysts. Milder conditions can be achieved by using Pd or Ni catalysts in the presence of a ligand and a copper co-catalyst. However, chemists will never cease to find a cheaper and non-toxic catalytic system that requires mild conditions. In this respect, iron catalysts stand out as valuable alternative candidates used in Sonogashira coupling reactions.

Several outstanding reports have been published already in the field of iron-catalyzed Sonogashira reactions of aryl iodides with terminal alkynes. One is from Bolm and co-workers, who found the simple iron salt, $FeCl_3$, when combined with the non-toxic and cheap amine, dmeda, in the presence of Cs_2CO_3, could couple aryl iodides and terminal alkynes efficiently (Figure 5.1).[10]

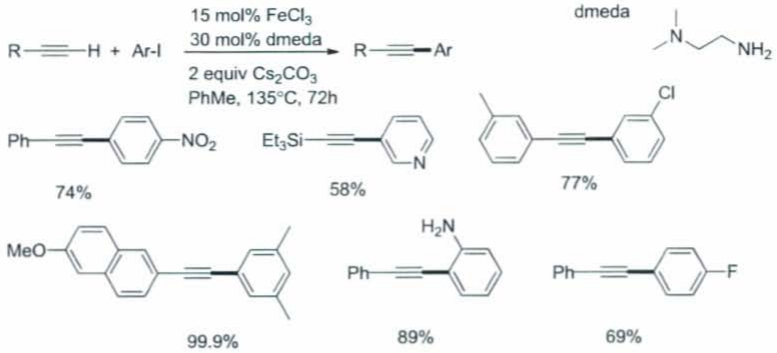

Scheme 5.1: Iron-catalyzed Sonogashira reactions by Bolm *et al.*

Another report is from Vogel *et al.*, who developed an efficient catalytic system using $Fe(acac)_3$ and CuI as catalyst (Figure 5.2). No toxic/expensive ligand is required, but NMP, DMSO or DMF that were used as solvents may also have played the role of ligand.[11] Furthermore, microwave heating can be employed efficiently to shorten the reaction time sharply, whilst keeping the high yield. Mao *et al.* also reported a similar catalytic system to Vogel's.[12] However they replaced the base Cs_2CO_3 with K_3PO_4, but also achieved excellent yields (up to 99%). It should be noted that Vogel showed that the unique catalytic reactivity of $Fe(acac)_3$ compared to other iron salts, such like $FeCl_2$ and $FeCl_3$.

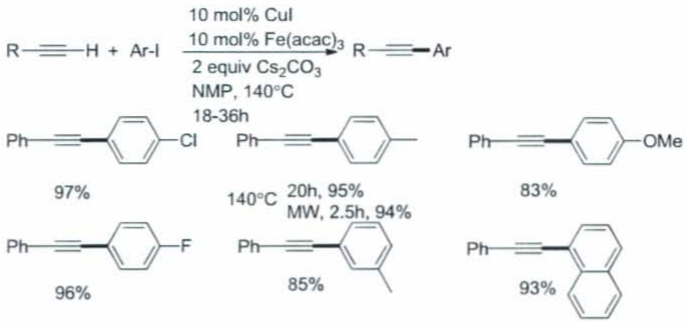

Scheme 5.2: Iron-catalyzed Sonogashira reactions by Vogel *et al.*

As previously mentioned, the iron complex is an efficient catalyst for use in Kumada cross-coupling reactions, therefore, they may be useful for the Sonogashira reaction. More studies may focus on the role of solvent and the choice of base. Also microwave heating may be a valuable tool for shortening the reaction time and increasing the yields. Moreover, for some unactive substrates, such as C-Cl bond activation, the easy-handled amine-bis(phenolate) iron complex may have potencial catalytic reactivity.

5.4 C-H Functionalization

Direct C-C and C-heteroatom bond formation via C-H bond activation is always of interest to chemists because of its inherently atom-efficient nature. However, this task is primarily achieved through the use of the rare and expensive transition metals such as Pd, Rh and Ru.[13-15] In the quest for cheaper and greener methods, more and more chemists are exploring iron-catalyzed C-H functionalization. Some desirable results have been discovered that showed iron has some unique properties.[13-15] This cheap metal can perform noble tasks, and even broaden some new routes for C-H activation that cannot be

achieved by others. However, the development of efficient iron-catalyzed C-C functionalization is still limited to activated substrates, such as those containing heteroatoms or directing groups.

Nakamura *et al.* developed an iron-catalyzed C-C bond-forming reaction through initial C-H bond activation.[16] The overall synthetic transformation formally represents the nucleophilic displacement of the *ortho*hydrogen atom by an arylzinc nucleophile. Phenanthroline is used as ligand. 1,2-dichloro-2-methylpropane maybe acts as an electron acceptor. It was also note that TMEDA was indispensable additive for obtaining desired yields.

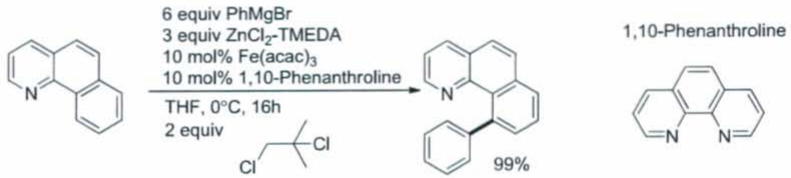

Scheme 5.3: Iron-catalyzed C-H activation by Nakamura *et al.*

Shi and co-workers developed a novel iron-catalyzed $C(sp^3)$-$C(sp^3)$ bond-forming reaction between alcohols and olefins through direct $C(sp^3)$-H functionalization, and various substrates proved to be well tolerated.[17] This protocol provides an economical and convenient strategy for efficient access to structurally diverse secondary alcohols.

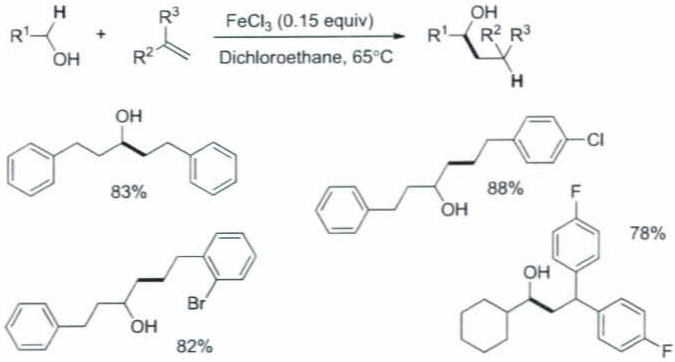

Scheme 5.4: Iron-catalyzed C-H activation by Shi *et al.*

Another novel and useful method to construct C-C bonds via iron-catalyzed direct benzylic C-H transformations with functionalized olefins was reported.[18] DTBP acts as an oxidant and provides a significant effect on the catalytic cycle.

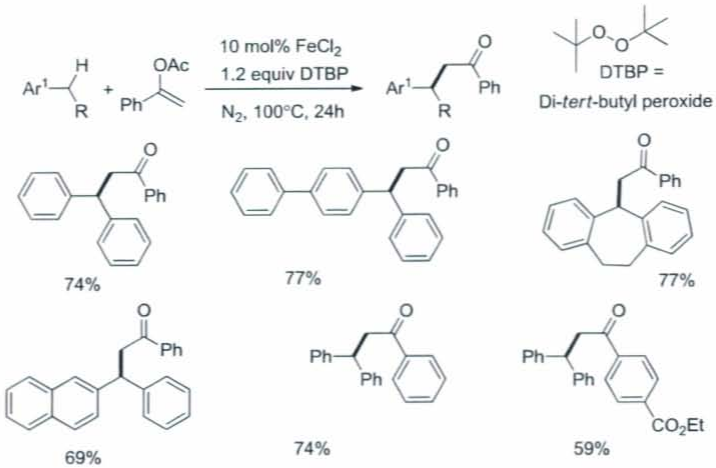

Scheme 5.5: Iron-catalyzed C-H activation by Shi *et al.*

As there have been some excellent reports that showed C-H activation of unactivated substrates is possible,[13-15] it is of possibilities that a rich variety of hydrocarbons can be used as feedstocks for the synthesis of value-added compounds. Iron catalysts will undoubtedly become an indispensable tool for sustainable syntheses of complex molecules.

5.5 References

(1) Plietker, B. *Iron catalysis in organic chemistry: reactions and applications;* Wiley-VCH: Weinheim, **2008**.

(2) Nishii, Y.; Wakasugi, K.; Tanabe, Y. *Synlett* **1998**, 67.

(3) Martin, R.; Fürstner, A. *Angew. Chem. Int. Ed.* **2004**, *43*, 3955.

(4) Fürstner, A.; Martin, R.; Krause, H.; Seidel, G.; Goddard, R.; Lehmann, C. W. *J. Am. Chem. Soc.* **2008**, *130*, 8773.

(5) Chinchilla, R.; Nájera, C. *Chem. Rev.* **2007**, *107*, 874.

(6) Li, C. C.; Xie, Z. X.; Zhang, Y. D.; Chen, J. H.; Yang, Z. *J. Org. Chem.* **2003**, *68*, 8500.

(7) Hiroya, K.; Matsumoto, S.; Sakamoto, T. *Org. Lett.* **2004**, *6*, 2953.

(8) Nicolaou, K. C.; Bulger, P. G.; Sarlah, D. *Angew. Chem. Int. Ed.* **2005**, *44*, 4442.

(9) Odlo, K.; Klaveness, J.; Rongved, P.; Hansen, T. V. *Tetrahedron Lett.* **2006**, *47*, 1101.

(10) Carril, M.; Correa, A.; Bolm, C. *Angew. Chem. Int. Ed.* **2008**, *47*, 4862.

(11) Rao Volla, C. M.; Vogel, P. *Tetrahedron Lett.* **2008**, *49*, 5961.

(12) Mao, J.; Xie, G.; Wu, M.; Guo, J.; Ji, S. *Adv. Synth. Catal.* **2008**, *350*, 2477.

(13) Godula, K.; Sames, D. *Science* **2006**, *312*, 67.

(14) Bergman, R. G. *Nature* **2007**, *446*, 391.

(15) Davies, H. M. L.; Manning, J. R. *Nature* **2008**, *451*, 417.

(16) Norinder, J.; Matsumoto, A.; Yoshikai, N.; Nakamura, E. *J. Am. Chem. Soc.* **2008**, *130*, 5858.

(17) Zhang, S.; Tu, Y.; Fan, C.; Zhang, F.; Shi, L. *Angew. Chem. Int. Ed.* **2009**, *48*, 8761.

(18) Song, C. X.; Cai, G. X.; Farrell, T. R.; Jiang, Z. P.; Li, H.; Gan, L. B.; Shi, Z. J. *Chem. Commun.* **2009**, 6002.

Appendix

Figure A1: ^{1}H NMR spectrum for L1.

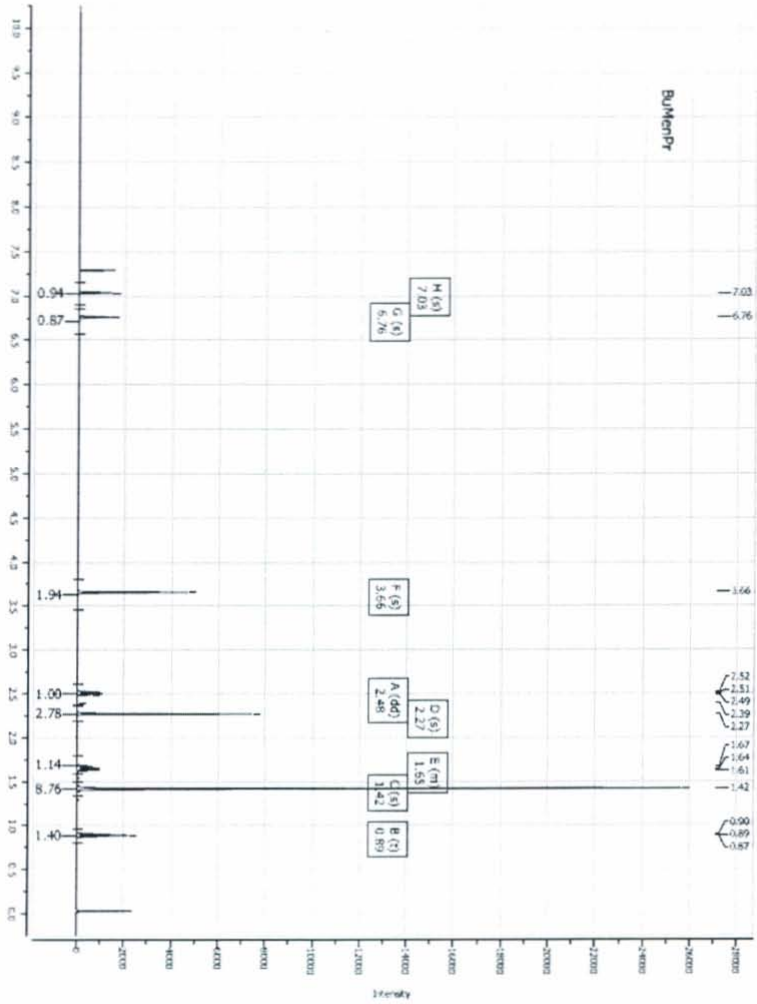

Figure A2: ^{1}H NMR spectrum for L2.

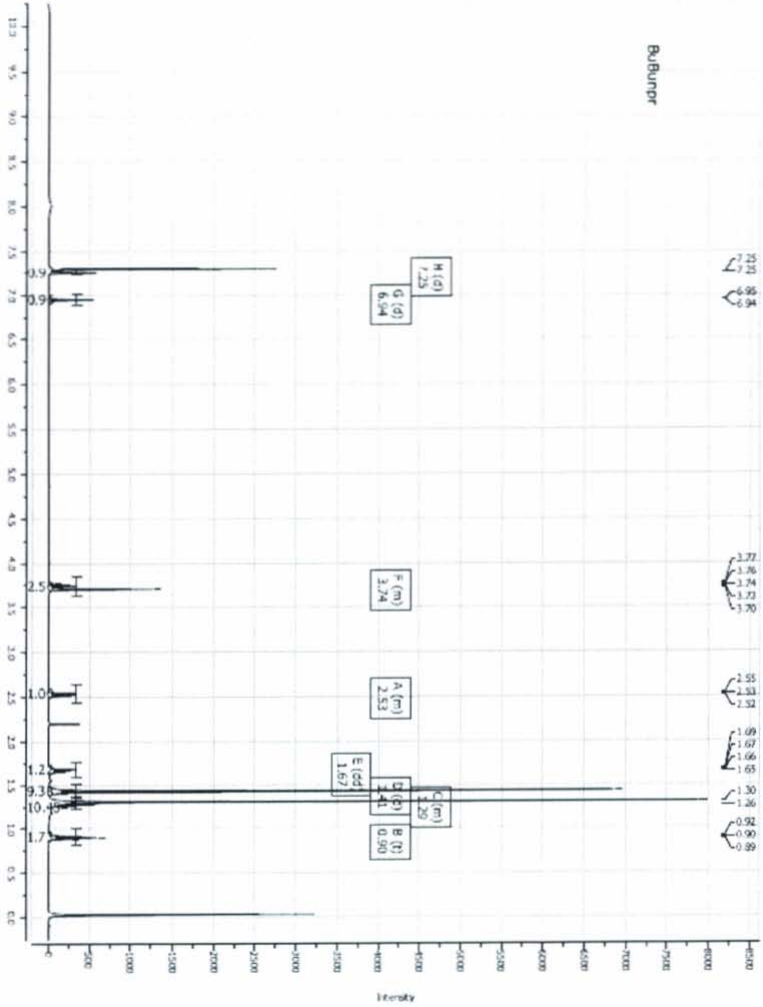

Figure A3: ^{1}H NMR spectrum for L3.

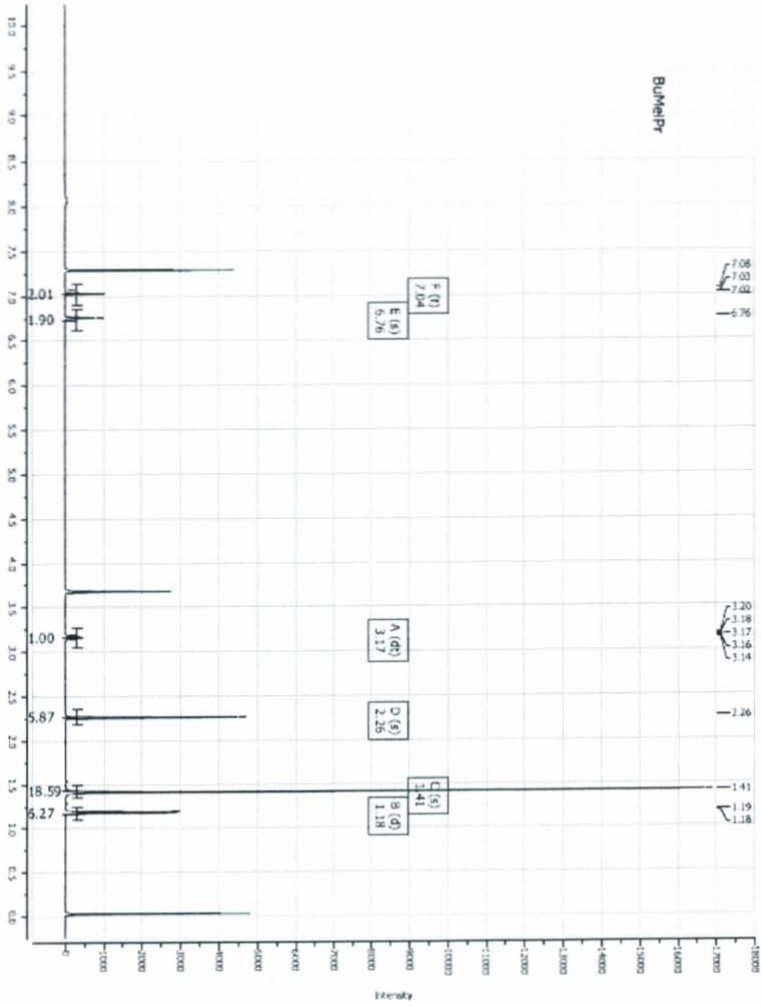

Figure A4: ^{1}H NMR spectrum for L4.

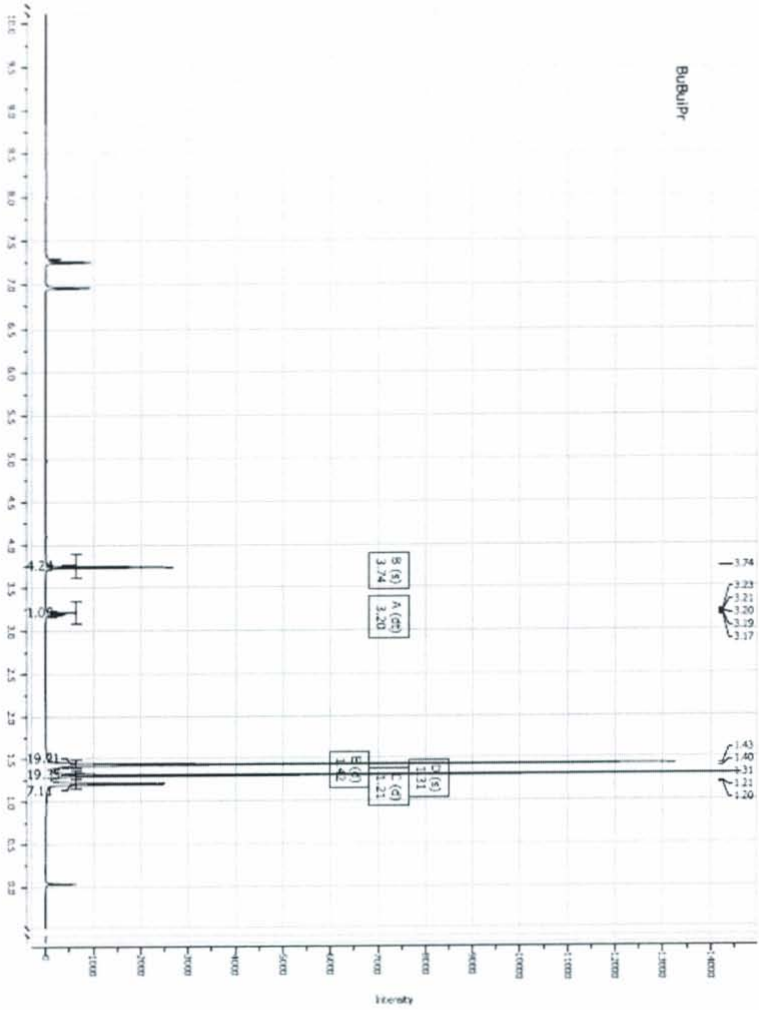

Figure A5: ^{1}H NMR spectrum for L6.

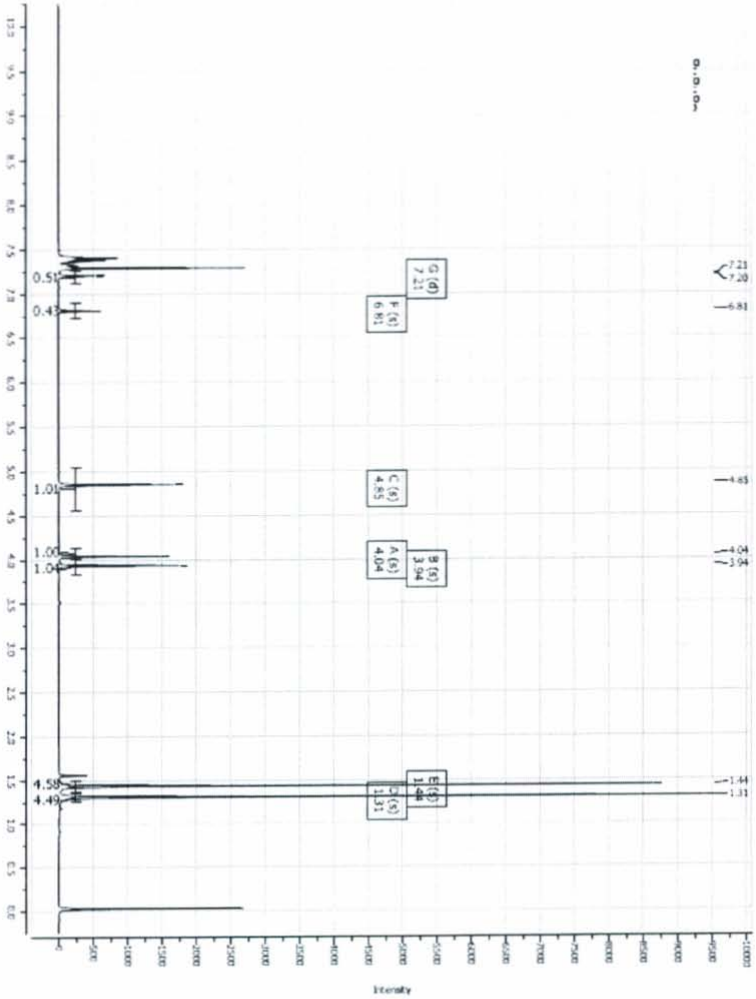

Figure A6:: ^{1}H NMR spectrum for L7.

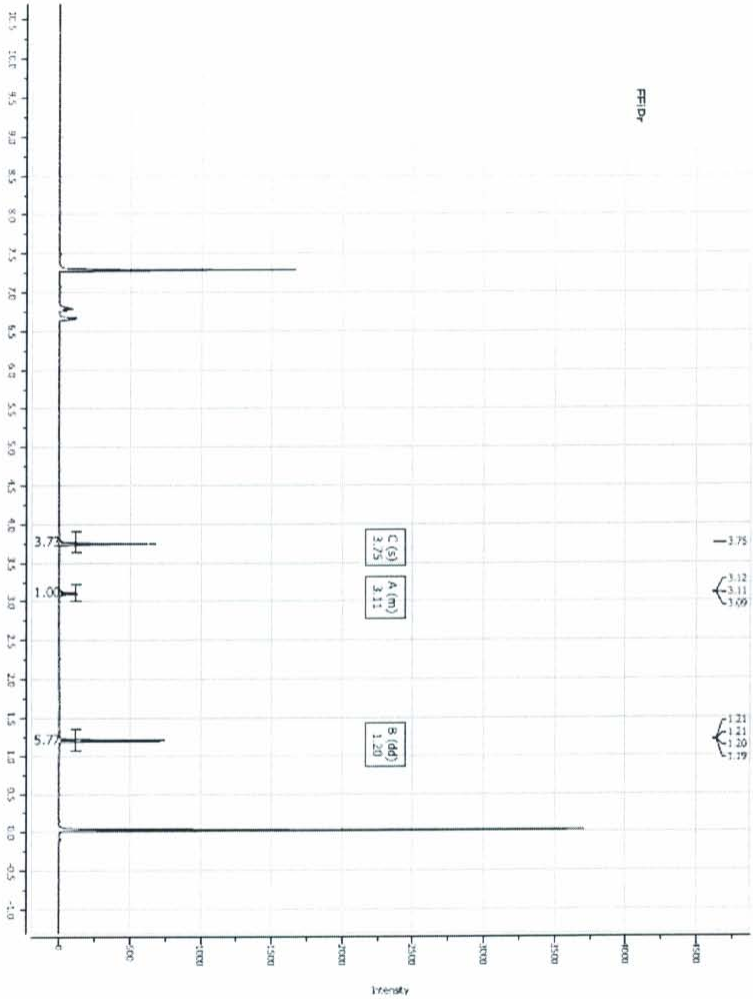

Figure A7: MALDI-TOF spectrum for $\{FeCl[O_2N]^{BuBu\mathit{n}Pr}\}_2$(2)

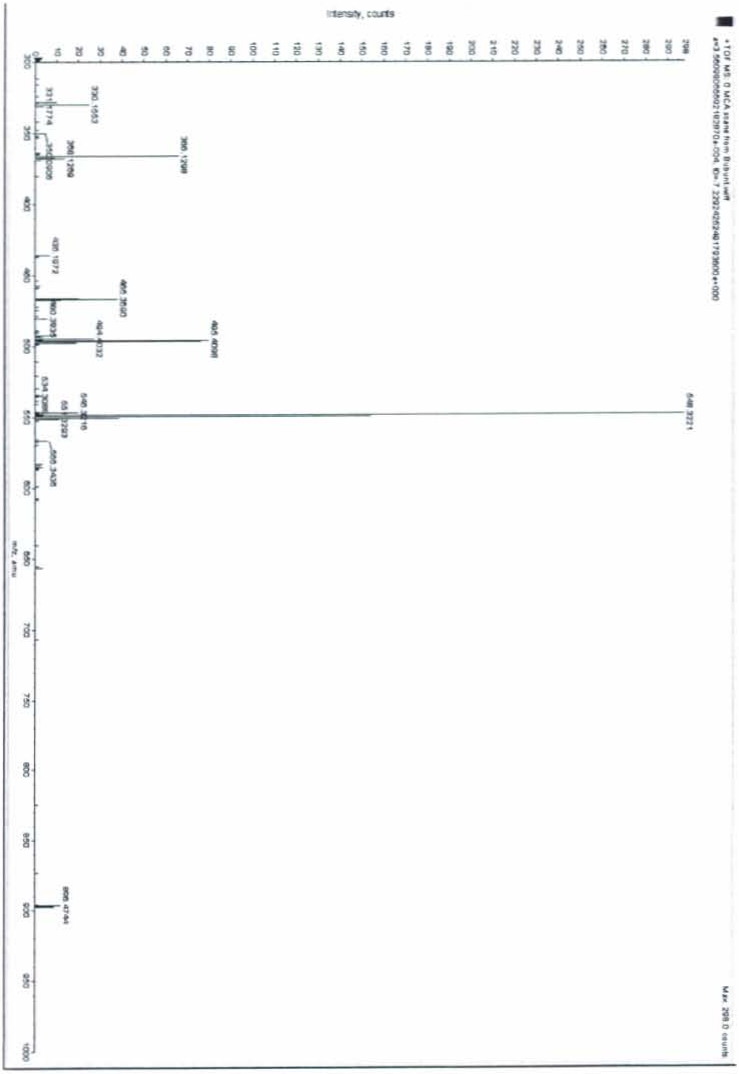

Figure A8: MALDI-TOF spectrum for $\{FeCl[O_2N]^{BuMe/Pr}\}_2$ (3)

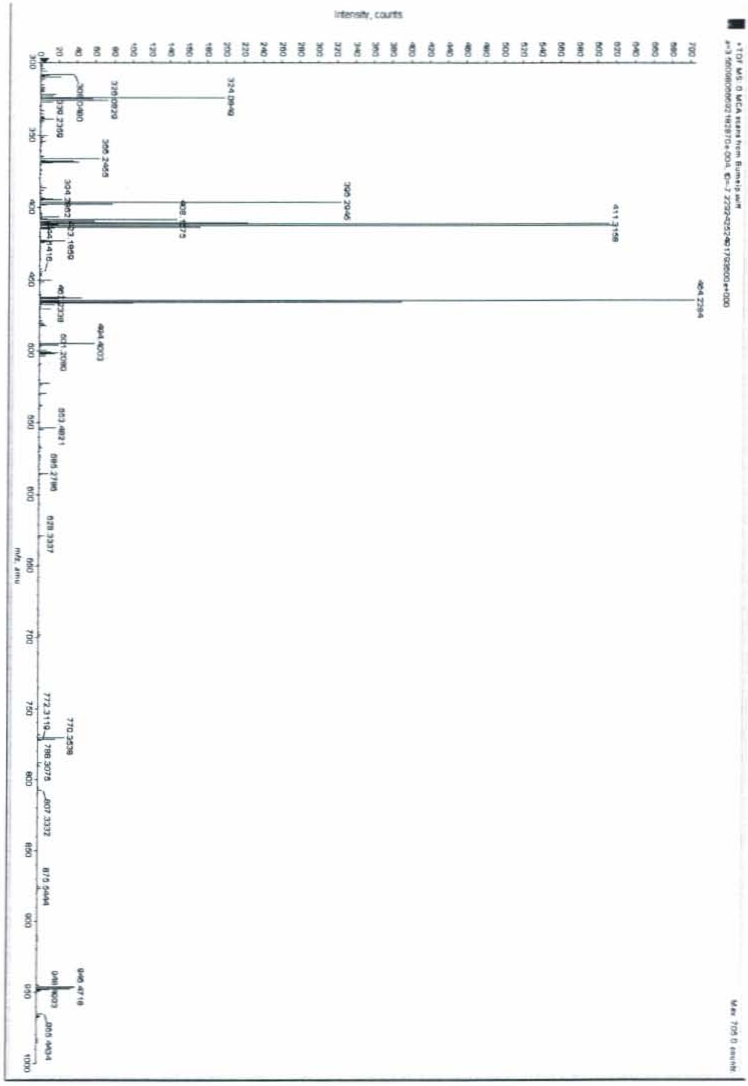

Figure A9: MALDI-TOF spectrum for $\{FeCl[O_2N]^{BuBu/Pr}\}$(4)

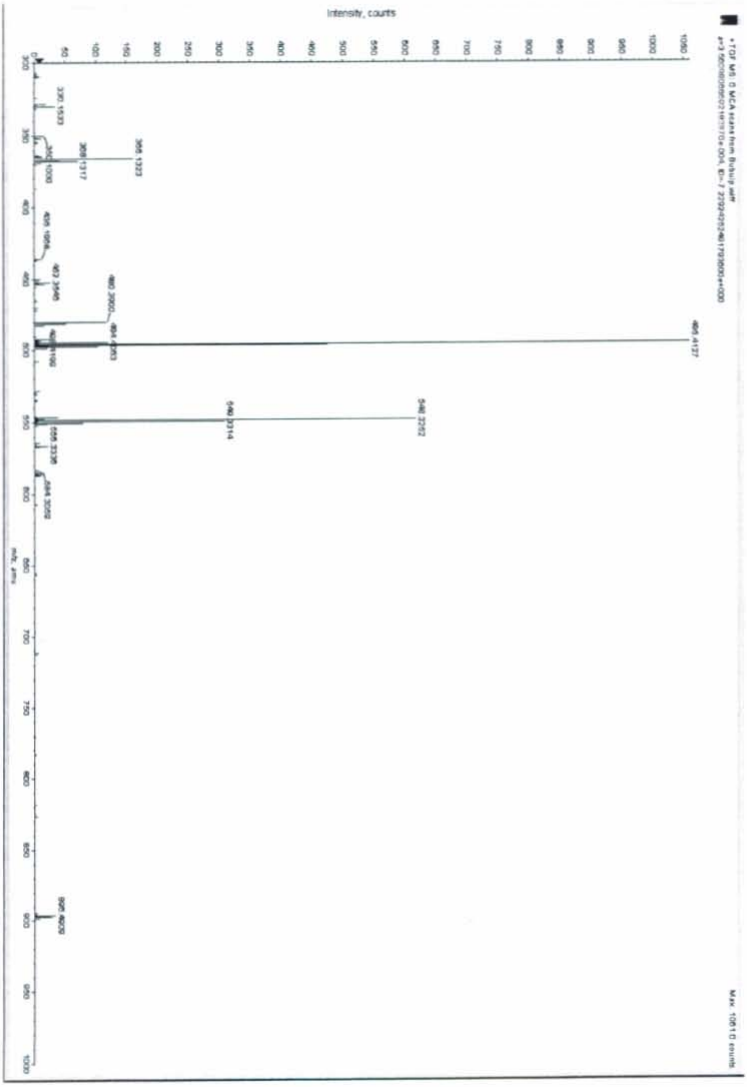

Figure A10: MALDI-TOF spectrum for $\{FeCl[O_2N]BuBuBn\}_2$(6)

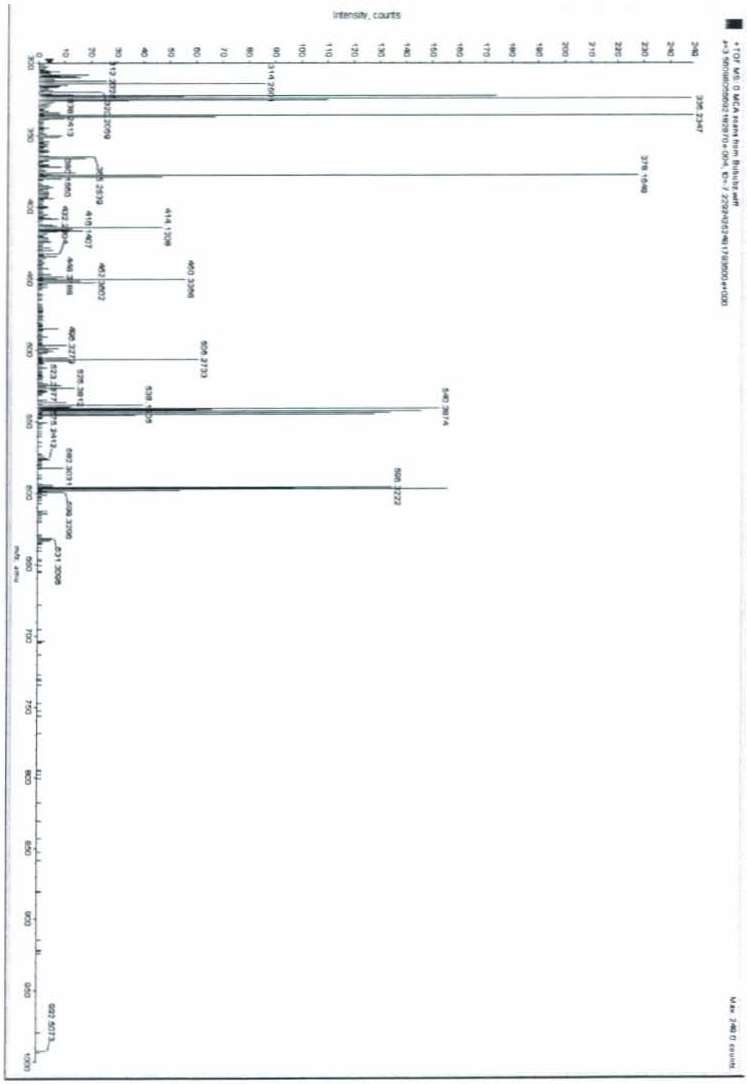

Figure A11: MALDI-TOF spectrum for $\{FeCl[O_2N]^{FF\mathit{i}Pr}\}_2$(7)

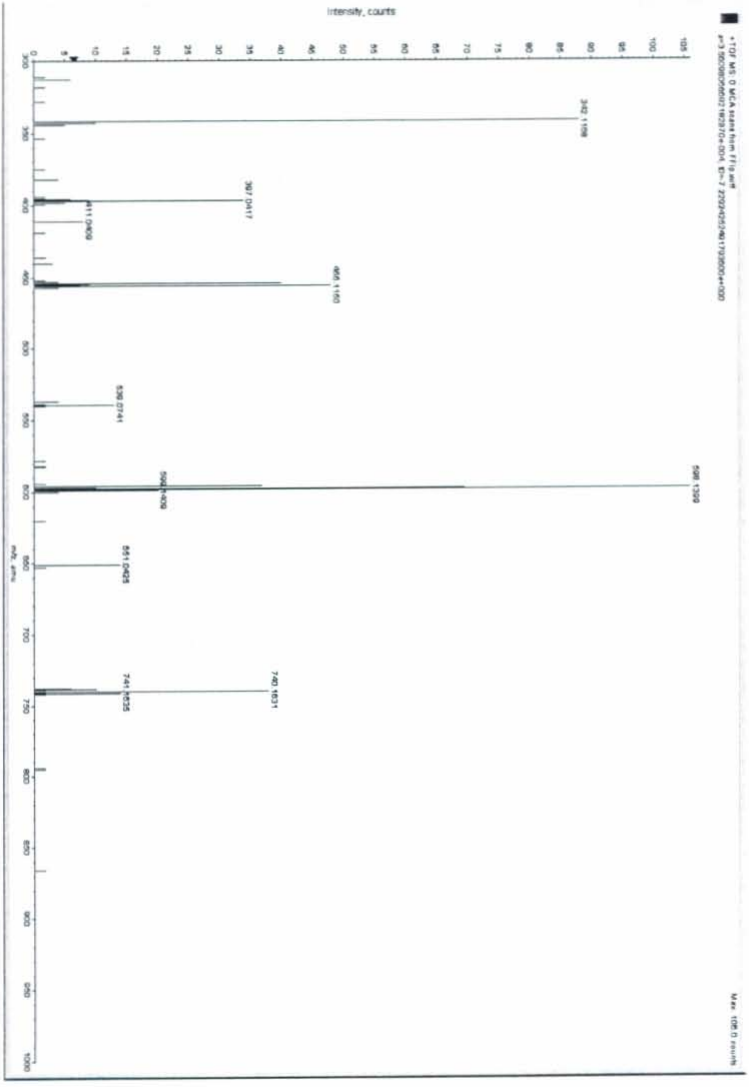

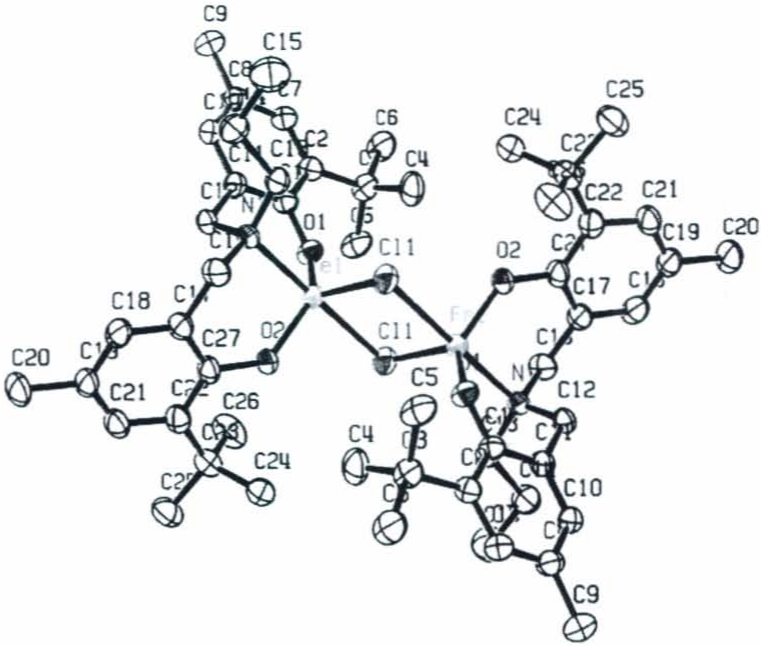

Figure A12: Molecular structure (ORTEP) and complete atom labeling of $\{FeCl[O_2N]^{BuMe\mathit{n}Pr}\}_2$. Ellipsoids shown at 50% probability.

Hydrogen atoms omitted for clarity.

Table A1: Bond lengths (Å) for $\{FeCl[O_2N]^{BuMe\mathit{n}Pr}\}_2$

atom	atom	distance	atom	atom	distance
Fe(1)	Cl(1)	2.2976(12)	Fe(1)	Cl(1)$^{1)}$	2.4912(14)
Fe(1)	O(1)	1.818(2)	Fe(1)	O(2)	1.817(2)
Fe(1)	N(1)	2.183(3)	O(1)	C(1)	1.336(4)
O(2)	C(27)	1.350(4)	N(1)	C(12)	1.489(5)
N(1)	C(13)	1.484(5)	N(1)	C(16)	1.487(4)
C(1)	C(2)	1.402(5)	C(1)	C(11)	1.390(6)
C(2)	C(3)	1.534(6)	C(2)	C(7)	1.381(6)
C(3)	C(4)	1.516(6)	C(3)	C(5)	1.529(7)

C(3)	C(6)	1.527(6)	C(7)	C(8)	1.382(7)
C(8)	C(9)	1.498(6)	C(8)	C(10)	1.374(5)
C(10)	C(11)	1.385(5)	C(11)	C(12)	1.480(5)
C(13)	C(14)	1.516(8)	C(14)	C(15)	1.515(9)
C(16)	C(17)	1.497(6)	C(17)	C(18)	1.393(5)
C(17)	C(27)	1.394(7)	C(18)	C(19)	1.373(7)
C(19)	C(20)	1.520(6)	C(19)	C(21)	1.371(8)
C(21)	C(22)	1.409(6)	C(22)	C(23)	1.515(8)
C(22)	C(27)	1.396(6)	C(23)	C(24)	1.528(6)
C(23)	C(25)	1.531(6)	C(23)	C(26)	1.534(7)

Symmetry Operators: (1) -x + 1, -y + 1, -z + 1

Table A2: Bond angles (°) for $\{FeCl[O_2N]^{BuMenPr}\}_2$

atom	atom	atom	angle	atom	atom	atom	angle
Cl(1)	Fe(1)	Cl(1)$^{1)}$	87.36(4)	Cl(1)	Fe(1)	O(1)	122.07(9)
Cl(1)	Fe(1)	O(2)	113.18(9)	Cl(1)	Fe(1)	N(1)	93.92(9)
Cl(1)$^{1)}$	Fe(1)	O(1)	89.41(11)	Cl(1)$^{1)}$	Fe(1)	O(2)	89.86(11)
Cl(1)$^{1)}$	Fe(1)	N(1)	178.32(9)	O(1)	Fe(1)	O(2)	124.63(13)
O(1)	Fe(1)	N(1)	89.00(13)	O(2)	Fe(1)	N(1)	90.63(13)
Fe(1)	Cl(1)	Fe(1)$^{1)}$	92.64(5)	Fe(1)	O(1)	C(1)	135.5(3)
Fe(1)	O(2)	C(27)	134.6(2)	Fe(1)	N(1)	C(12)	105.3(2)
Fe(1)	N(1)	C(13)	111.0(2)	Fe(1)	N(1)	C(16)	106.3(2)
C(12)	N(1)	C(13)	112.7(3)	C(12)	N(1)	C(16)	111.3(2)
C(13)	N(1)	C(16)	110.0(3)	O(1)	C(1)	C(2)	120.3(4)
O(1)	C(1)	C(11)	118.5(3)	C(2)	C(1)	C(11)	121.2(3)
C(1)	C(2)	C(3)	120.8(3)	C(1)	C(2)	C(7)	116.8(4)
C(3)	C(2)	C(7)	122.5(3)	C(2)	C(3)	C(4)	108.8(4)
C(2)	C(3)	C(5)	109.7(3)	C(2)	C(3)	C(6)	111.2(3)
C(4)	C(3)	C(5)	111.4(4)	C(4)	C(3)	C(6)	108.1(3)
C(5)	C(3)	C(6)	107.6(4)	C(2)	C(7)	C(8)	123.4(3)
C(7)	C(8)	C(9)	120.2(3)	C(7)	C(8)	C(10)	118.2(3)
C(9)	C(8)	C(10)	121.6(4)	C(8)	C(10)	C(11)	121.2(4)
C(1)	C(11)	C(10)	119.3(3)	C(1)	C(11)	C(12)	120.2(3)
C(10)	C(11)	C(12)	120.5(4)	N(1)	C(12)	C(11)	112.8(2)
N(1)	C(13)	C(14)	115.5(3)	C(13)	C(14)	C(15)	110.3(4)
N(1)	C(16)	C(17)	114.4(4)	C(16)	C(17)	C(18)	120.5(4)
C(16)	C(17)	C(27)	120.5(3)	C(18)	C(17)	C(27)	119.0(4)
C(17)	C(18)	C(19)	120.7(5)	C(18)	C(19)	C(20)	119.8(5)
C(18)	C(19)	C(21)	119.3(4)	C(20)	C(19)	C(21)	120.9(4)
C(19)	C(21)	C(22)	123.0(4)	C(21)	C(22)	C(23)	122.4(4)
C(21)	C(22)	C(27)	116.0(4)	C(23)	C(22)	C(27)	121.5(3)
C(22)	C(23)	C(24)	110.3(4)	C(22)	C(23)	C(25)	112.4(4)

C(22)	C(23)	C(26)	109.9(4)	C(24)	C(23)	C(25)	107.3(3)
C(24)	C(23)	C(26)	109.6(4)	C(25)	C(23)	C(26)	107.2(4)
O(2)	C(27)	C(17)	117.8(3)	O(2)	C(27)	C(22)	120.1(4)
C(17)	C(27)	C(22)	122.1(3)				

Symmetry Operators: (1) -x + 1, -y + 1, -z + 1

Table A3: Torsion angles (°) $\{FeCl[O_2N]^{BuMenPr}\}_2$

atom1	atom2	atom3	atom4	angle	atom1	atom2	atom3	atom4	angle
Cl(1)	Fe(1)	O(1)	C(1)	85.6(3)	O(1)	Fe(1)	Cl(1)	Fe(1)$^{1)}$	87.64(14)
Cl(1)	Fe(1)	O(2)	C(27)	-110.0(3)	O(2)	Fe(1)	Cl(1)	Fe(1)$^{1)}$	-88.72(12)
Cl(1)	Fe(1)	N(1)	C(12)	-159.64(18)	Cl(1)	Fe(1)	N(1)	C(13)	-37.4(2)
Cl(1)	Fe(1)	N(1)	C(16)	82.1(2)	N(1)	Fe(1)	Cl(1)	Fe(1)$^{1)}$	178.92(7)
Cl(1)$^{1)}$	Fe(1)	O(1)	C(1)	172.1(3)	O(1)	Fe(1)	Cl(1)$^{1)}$	Fe(1)$^{1)}$	-122.15(9)
Cl(1)$^{1)}$	Fe(1)	O(2)	C(27)	163.0(4)	O(2)	Fe(1)	Cl(1)$^{1)}$	Fe(1)$^{1)}$	113.21(9)
Cl(1)$^{1)}$	Fe(1)	N(1)	C(12)	-20(2)	Cl(1)$^{1)}$	Fe(1)	N(1)	C(13)	102(2)
Cl(1)$^{1)}$	Fe(1)	N(1)	C(16)	-138(2)	N(1)	Fe(1)	Cl(1)$^{1)}$	Fe(1)$^{1)}$	-140(2)
O(1)	Fe(1)	O(2)	C(27)	73.8(4)	O(2)	Fe(1)	O(1)	C(1)	-98.5(3)
O(1)	Fe(1)	N(1)	C(12)	-37.6(2)	O(1)	Fe(1)	N(1)	C(13)	84.7(2)
O(1)	Fe(1)	N(1)	C(16)	-155.8(2)	N(1)	Fe(1)	O(1)	C(1)	-8.4(3)
O(2)	Fe(1)	N(1)	C(12)	87.1(2)	O(2)	Fe(1)	N(1)	C(13)	-150.7(2)
O(2)	Fe(1)	N(1)	C(16)	-31.2(2)	N(1)	Fe(1)	O(2)	C(27)	-15.4(4)
Fe(1)	O(1)	C(1)	C(2)	-149.3(3)	Fe(1)	O(1)	C(1)	C(11)	29.2(5)
Fe(1)	O(2)	C(27)	C(17)	32.7(5)	Fe(1)	O(2)	C(27)	C(22)	-146.4(3)
Fe(1)	N(1)	C(12)	C(11)	69.7(4)	Fe(1)	N(1)	C(13)	C(14)	-171.4(3)
Fe(1)	N(1)	C(16)	C(17)	65.2(3)	C(12)	N(1)	C(13)	C(14)	-53.6(4)
C(13)	N(1)	C(12)	C(11)	-51.4(5)	C(12)	N(1)	C(16)	C(17)	-49.0(5)
C(16)	N(1)	C(12)	C(11)	-175.5(4)	C(13)	N(1)	C(16)	C(17)	-174.6(3)
C(16)	N(1)	C(13)	C(14)	71.2(4)	O(1)	C(1)	C(2)	C(3)	0.7(6)
O(1)	C(1)	C(2)	C(7)	179.6(3)	O(1)	C(1)	C(11)	C(10)	-179.4(3)
O(1)	C(1)	C(11)	C(12)	1.3(6)	C(2)	C(1)	C(11)	C(10)	-0.9(6)
C(2)	C(1)	C(11)	C(12)	179.8(3)	C(11)	C(1)	C(2)	C(3)	-177.7(4)
C(11)	C(1)	C(2)	C(7)	1.2(6)	C(1)	C(2)	C(3)	C(4)	62.7(5)
C(1)	C(2)	C(3)	C(5)	-59.4(5)	C(1)	C(2)	C(3)	C(6)	-178.3(4)
C(1)	C(2)	C(7)	C(8)	-1.0(6)	C(3)	C(2)	C(7)	C(8)	177.9(4)
C(7)	C(2)	C(3)	C(4)	-116.1(4)	C(7)	C(2)	C(3)	C(5)	121.8(4)
C(7)	C(2)	C(3)	C(6)	2.9(6)	C(2)	C(7)	C(8)	C(9)	-177.9(4)
C(2)	C(7)	C(8)	C(10)	0.6(6)	C(7)	C(8)	C(10)	C(11)	-0.2(5)
C(9)	C(8)	C(10)	C(11)	178.2(4)	C(8)	C(10)	C(11)	C(1)	0.4(6)
C(8)	C(10)	C(11)	C(12)	179.7(4)	C(1)	C(11)	C(12)	N(1)	-55.6(5)
C(10)	C(11)	C(12)	N(1)	125.1(4)	N(1)	C(13)	C(14)	C(15)	-174.9(4)
N(1)	C(16)	C(17)	C(18)	126.3(4)	N(1)	C(16)	C(17)	C(27)	-56.2(5)
C(16)	C(17)	C(18)	C(19)	178.0(4)	C(16)	C(17)	C(27)	O(2)	2.7(5)

C(16)	C(17)	C(27)	C(22)	-178.2(3)	C(18)	C(17)	C(27)	O(2)	-179.7(3)
C(18)	C(17)	C(27)	C(22)	-0.6(6)	C(27)	C(17)	C(18)	C(19)	0.5(6)
C(17)	C(18)	C(19)	C(20)	179.1(4)	C(17)	C(18)	C(19)	C(21)	0.3(6)
C(18)	C(19)	C(21)	C(22)	-0.8(7)	C(20)	C(19)	C(21)	C(22)	-179.7(4)
C(19)	C(21)	C(22)	C(23)	179.6(4)	C(19)	C(21)	C(22)	C(27)	0.7(6)
C(21)	C(22)	C(23)	C(24)	122.1(4)	C(21)	C(22)	C(23)	C(25)	2.4(5)
C(21)	C(22)	C(23)	C(26)	-116.9(4)	C(21)	C(22)	C(27)	O(2)	179.2(3)
C(21)	C(22)	C(27)	C(17)	0.1(4)	C(23)	C(22)	C(27)	O(2)	0.2(5)
C(23)	C(22)	C(27)	C(17)	-178.9(3)	C(27)	C(22)	C(23)	C(24)	-59.0(5)
C(27)	C(22)	C(23)	C(25)	-178.7(3)	C(27)	C(22)	C(23)	C(26)	62.0(5)

Symmetry Operators: (1) -x + 1, -y + 1, -z + 1

The sign is positive if when looking from atom 2 to atom 3 a clock-wise motion of atom 1 would superimpose it on atom 4.

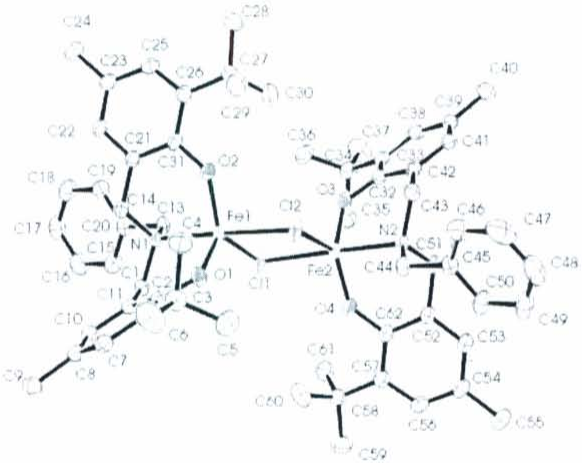

Figure A13: Molecular structure (ORTEP) and complete atom labeling of $\{FeCl[O_2N]^{BuMeBn}\}_2$. Ellipsoids shown at 50% probability. Hydrogen atoms omitted for clarity.

Table A4: Bond lengths (Å) for $\{FeCl[O_2N]^{BuMeBn}\}_2$

atom	atom	distance	atom	atom	distance

Fe(1)	Cl(1)	2.3290(4)	Fe(1)	Cl(2)	2.5025(3)
Fe(1)	O(1)	1.8276(13)	Fe(1)	O(2)	1.8222(12)
Fe(1)	N(1)	2.1819(10)	Fe(2)	Cl(1)	2.5023(3)
Fe(2)	Cl(2)	2.3305(5)	Fe(2)	O(3)	1.8228(13)
Fe(2)	O(4)	1.8282(13)	Fe(2)	N(2)	2.1771(10)
O(1)	C(1)	1.344(2)	O(2)	C(31)	1.3499(17)
O(3)	C(32)	1.346(2)	O(4)	C(62)	1.3489(17)
N(1)	C(12)	1.495(2)	N(1)	C(13)	1.513(2)
N(1)	C(20)	1.497(2)	N(2)	C(43)	1.502(2)
N(2)	C(44)	1.506(2)	N(2)	C(51)	1.494(2)
C(1)	C(2)	1.414(2)	C(1)	C(11)	1.400(2)
C(2)	C(3)	1.540(2)	C(2)	C(7)	1.394(2)
C(3)	C(4)	1.538(3)	C(3)	C(5)	1.531(2)
C(3)	C(6)	1.533(3)	C(7)	C(8)	1.393(2)
C(8)	C(9)	1.512(2)	C(8)	C(10)	1.394(2)
C(10)	C(11)	1.396(2)	C(11)	C(12)	1.516(2)
C(13)	C(14)	1.5123(18)	C(14)	C(15)	1.391(2)
C(14)	C(19)	1.392(2)	C(15)	C(16)	1.388(2)
C(16)	C(17)	1.377(2)	C(17)	C(18)	1.377(3)
C(18)	C(19)	1.386(2)	C(20)	C(21)	1.507(2)
C(21)	C(22)	1.3975(19)	C(21)	C(31)	1.399(2)
C(22)	C(23)	1.384(2)	C(23)	C(24)	1.509(2)
C(23)	C(25)	1.391(2)	C(25)	C(26)	1.396(2)
C(26)	C(27)	1.534(2)	C(26)	C(31)	1.413(2)
C(27)	C(28)	1.535(3)	C(27)	C(29)	1.544(2)
C(27)	C(30)	1.538(2)	C(32)	C(33)	1.413(2)
C(32)	C(42)	1.4052(19)	C(33)	C(34)	1.537(2)
C(33)	C(38)	1.398(2)	C(34)	C(35)	1.534(2)
C(34)	C(36)	1.534(2)	C(34)	C(37)	1.532(3)
C(38)	C(39)	1.394(2)	C(39)	C(40)	1.515(2)
C(39)	C(41)	1.390(2)	C(41)	C(42)	1.395(2)
C(42)	C(43)	1.513(2)	C(44)	C(45)	1.5141(18)
C(45)	C(46)	1.388(2)	C(45)	C(50)	1.386(2)
C(46)	C(47)	1.382(2)	C(47)	C(48)	1.379(3)
C(48)	C(49)	1.372(3)	C(49)	C(50)	1.387(2)
C(51)	C(52)	1.506(2)	C(52)	C(53)	1.3942(19)
C(52)	C(62)	1.404(2)	C(53)	C(54)	1.382(2)
C(54)	C(55)	1.508(2)	C(54)	C(56)	1.392(2)
C(56)	C(57)	1.389(2)	C(57)	C(58)	1.534(2)
C(57)	C(62)	1.418(2)	C(58)	C(59)	1.533(3)
C(58)	C(60)	1.535(2)	C(58)	C(61)	1.532(2)

Table A5: Bond angles (°) for $\{FeCl[O_2N]^{BuMeBn}\}_2$

atom	atom	atom	angle	atom	atom	atom	angle
Cl(1)	Fe(1)	Cl(2)	84.341(14)	Cl(1)	Fe(1)	O(1)	114.96(4)
Cl(1)	Fe(1)	O(2)	125.52(4)	Cl(1)	Fe(1)	N(1)	93.59(3)
Cl(2)	Fe(1)	O(1)	88.91(3)	Cl(2)	Fe(1)	O(2)	92.60(3)
Cl(2)	Fe(1)	N(1)	177.28(3)	O(1)	Fe(1)	O(2)	119.36(5)
O(1)	Fe(1)	N(1)	90.38(4)	O(2)	Fe(1)	N(1)	90.03(4)
Cl(1)	Fe(2)	Cl(2)	84.316(14)	Cl(1)	Fe(2)	O(3)	91.63(3)
Cl(1)	Fe(2)	O(4)	89.53(3)	Cl(1)	Fe(2)	N(2)	177.64(4)
Cl(2)	Fe(2)	O(3)	109.27(4)	Cl(2)	Fe(2)	O(4)	129.40(4)
Cl(2)	Fe(2)	N(2)	94.23(3)	O(3)	Fe(2)	O(4)	121.10(6)
O(3)	Fe(2)	N(2)	90.60(5)	O(4)	Fe(2)	N(2)	89.97(4)
Fe(1)	Cl(1)	Fe(2)	95.384(14)	Fe(1)	Cl(2)	Fe(2)	95.341(15)
Fe(1)	O(1)	C(1)	134.96(8)	Fe(1)	O(2)	C(31)	136.27(9)
Fe(2)	O(3)	C(32)	134.55(8)	Fe(2)	O(4)	C(62)	136.88(10)
Fe(1)	N(1)	C(12)	106.53(7)	Fe(1)	N(1)	C(13)	110.51(8)
Fe(1)	N(1)	C(20)	106.63(8)	C(12)	N(1)	C(13)	110.29(12)
C(12)	N(1)	C(20)	110.37(13)	C(13)	N(1)	C(20)	112.28(11)
Fe(2)	N(2)	C(43)	106.94(7)	Fe(2)	N(2)	C(44)	108.61(9)
Fe(2)	N(2)	C(51)	107.00(8)	C(43)	N(2)	C(44)	111.34(12)
C(43)	N(2)	C(51)	109.95(13)	C(44)	N(2)	C(51)	112.72(11)
O(1)	C(1)	C(2)	119.87(12)	O(1)	C(1)	C(11)	118.82(15)
C(2)	C(1)	C(11)	121.31(14)	C(1)	C(2)	C(3)	121.34(15)
C(1)	C(2)	C(7)	116.34(14)	C(3)	C(2)	C(7)	122.30(17)
C(2)	C(3)	C(4)	109.38(14)	C(2)	C(3)	C(5)	111.29(15)
C(2)	C(3)	C(6)	111.36(15)	C(4)	C(3)	C(5)	109.28(15)
C(4)	C(3)	C(6)	107.02(17)	C(5)	C(3)	C(6)	108.39(16)
C(2)	C(7)	C(8)	123.66(17)	C(7)	C(8)	C(9)	120.61(17)
C(7)	C(8)	C(10)	118.06(16)	C(9)	C(8)	C(10)	121.32(14)
C(8)	C(10)	C(11)	120.73(13)	C(1)	C(11)	C(10)	119.43(16)
C(1)	C(11)	C(12)	121.01(14)	C(10)	C(11)	C(12)	119.53(13)
N(1)	C(12)	C(11)	114.96(14)	N(1)	C(13)	C(14)	116.95(13)
C(13)	C(14)	C(15)	120.49(14)	C(13)	C(14)	C(19)	120.77(15)
C(15)	C(14)	C(19)	118.60(13)	C(14)	C(15)	C(16)	120.34(16)
C(15)	C(16)	C(17)	120.36(18)	C(16)	C(17)	C(18)	119.85(14)
C(17)	C(18)	C(19)	120.15(17)	C(14)	C(19)	C(18)	120.64(17)
N(1)	C(20)	C(21)	114.41(14)	C(20)	C(21)	C(22)	119.49(13)
C(20)	C(21)	C(31)	121.20(12)	C(22)	C(21)	C(31)	119.27(16)
C(21)	C(22)	C(23)	121.36(13)	C(22)	C(23)	C(24)	121.18(14)
C(22)	C(23)	C(25)	117.94(13)	C(24)	C(23)	C(25)	120.88(17)
C(23)	C(25)	C(26)	123.55(17)	C(25)	C(26)	C(27)	122.18(16)
C(25)	C(26)	C(31)	116.71(13)	C(27)	C(26)	C(31)	121.05(13)
C(26)	C(27)	C(28)	111.64(13)	C(26)	C(27)	C(29)	108.50(16)

C(26)	C(27)	C(30)	111.50(15)	C(28)	C(27)	C(29)	108.03(17)
C(28)	C(27)	C(30)	107.41(18)	C(29)	C(27)	C(30)	109.71(14)
O(2)	C(31)	C(21)	119.07(15)	O(2)	C(31)	C(26)	119.86(12)
C(21)	C(31)	C(26)	121.06(13)	O(3)	C(32)	C(33)	119.63(12)
O(3)	C(32)	C(42)	118.82(16)	C(33)	C(32)	C(42)	121.54(15)
C(32)	C(33)	C(34)	121.01(15)	C(32)	C(33)	C(38)	116.51(13)
C(34)	C(33)	C(38)	122.44(16)	C(33)	C(34)	C(35)	109.92(13)
C(33)	C(34)	C(36)	110.80(15)	C(33)	C(34)	C(37)	111.25(15)
C(35)	C(34)	C(36)	109.35(15)	C(35)	C(34)	C(37)	107.37(17)
C(36)	C(34)	C(37)	108.06(15)	C(33)	C(38)	C(39)	123.34(17)
C(38)	C(39)	C(40)	120.15(17)	C(38)	C(39)	C(41)	118.27(16)
C(40)	C(39)	C(41)	121.57(13)	C(39)	C(41)	C(42)	121.20(13)
C(32)	C(42)	C(41)	118.97(16)	C(32)	C(42)	C(43)	120.66(15)
C(41)	C(42)	C(43)	120.36(12)	N(2)	C(43)	C(42)	114.41(14)
N(2)	C(44)	C(45)	118.72(14)	C(44)	C(45)	C(46)	120.48(14)
C(44)	C(45)	C(50)	120.81(15)	C(46)	C(45)	C(50)	118.21(14)
C(45)	C(46)	C(47)	120.45(19)	C(46)	C(47)	C(48)	120.7(2)
C(47)	C(48)	C(49)	119.60(17)	C(48)	C(49)	C(50)	119.85(18)
C(45)	C(50)	C(49)	121.19(19)	N(2)	C(51)	C(52)	115.18(14)
C(51)	C(52)	C(53)	119.70(13)	C(51)	C(52)	C(62)	121.08(12)
C(53)	C(52)	C(62)	119.13(16)	C(52)	C(53)	C(54)	121.57(14)
C(53)	C(54)	C(55)	121.05(14)	C(53)	C(54)	C(56)	117.87(13)
C(55)	C(54)	C(56)	121.05(17)	C(54)	C(56)	C(57)	123.62(17)
C(56)	C(57)	C(58)	121.99(16)	C(56)	C(57)	C(62)	116.79(13)
C(58)	C(57)	C(62)	121.20(12)	C(57)	C(58)	C(59)	112.24(12)
C(57)	C(58)	C(60)	111.02(15)	C(57)	C(58)	C(61)	109.28(16)
C(59)	C(58)	C(60)	107.51(18)	C(59)	C(58)	C(61)	106.98(16)
C(60)	C(58)	C(61)	109.72(14)	O(4)	C(62)	C(52)	119.10(15)
O(4)	C(62)	C(57)	120.11(12)	C(52)	C(62)	C(57)	120.78(12)

Table A6: Torsion angles (°) for $\{FeCl[O_2N]^{BuMeBn}\}_2$

atom1	atom2	atom3	atom4	angle	atom1	atom2	atom3	atom4	angle
Cl(1)	Fe(1)	Cl(2)	Fe(2)	6.18(2)	Cl(2)	Fe(1)	Cl(1)	Fe(2)	-5.75(2)
Cl(1)	Fe(1)	O(1)	C(1)	-102.38(15)	O(1)	Fe(1)	Cl(1)	Fe(2)	-91.90(3)
Cl(1)	Fe(1)	O(2)	C(31)	92.34(17)	O(2)	Fe(1)	Cl(1)	Fe(2)	83.40(3)
Cl(1)	Fe(1)	N(1)	C(12)	78.89(10)	Cl(1)	Fe(1)	N(1)	C(13)	-40.93(10)
Cl(1)	Fe(1)	N(1)	C(20)	-163.22(10)	N(1)	Fe(1)	Cl(1)	Fe(2)	176.01(4)
Cl(2)	Fe(1)	O(1)	C(1)	174.37(15)	O(1)	Fe(1)	Cl(2)	Fe(2)	121.39(4)
Cl(2)	Fe(1)	O(2)	C(31)	177.24(16)	O(2)	Fe(1)	Cl(2)	Fe(2)	-119.26(4)
Cl(2)	Fe(1)	N(1)	C(12)	38.7(9)	Cl(2)	Fe(1)	N(1)	C(13)	-81.2(9)
Cl(2)	Fe(1)	N(1)	C(20)	156.5(8)	N(1)	Fe(1)	Cl(2)	Fe(2)	46.6(9)
O(1)	Fe(1)	O(2)	C(31)	-92.54(17)	O(2)	Fe(1)	O(1)	C(1)	82.00(15)
O(1)	Fe(1)	N(1)	C(12)	-36.14(10)	O(1)	Fe(1)	N(1)	C(13)	-155.96(10)

O(1)	Fe(1)	N(1)	C(20)	81.74(11)	N(1)	Fe(1)	O(1)	C(1)	-8.25(15)
O(2)	Fe(1)	N(1)	C(12)	-155.51(10)	O(2)	Fe(1)	N(1)	C(13)	84.67(10)
O(2)	Fe(1)	N(1)	C(20)	-37.62(11)	N(1)	Fe(1)	O(2)	C(31)	-2.09(17)
Cl(1)	Fe(2)	Cl(2)	Fe(1)	-5.749(19)	Cl(2)	Fe(2)	Cl(1)	Fe(1)	6.18(2)
Cl(1)	Fe(2)	O(3)	C(32)	-169.45(15)	O(3)	Fe(2)	Cl(1)	Fe(1)	-103.03(4)
Cl(1)	Fe(2)	O(4)	C(62)	-178.84(17)	O(4)	Fe(2)	Cl(1)	Fe(1)	135.87(4)
Cl(1)	Fe(2)	N(2)	C(43)	-126.6(9)	Cl(1)	Fe(2)	N(2)	C(44)	-6.4(10)
Cl(1)	Fe(2)	N(2)	C(51)	115.6(9)	N(2)	Fe(2)	Cl(1)	Fe(1)	58.0(9)
Cl(2)	Fe(2)	O(3)	C(32)	106.01(15)	O(3)	Fe(2)	Cl(2)	Fe(1)	83.99(3)
Cl(2)	Fe(2)	O(4)	C(62)	-96.59(17)	O(4)	Fe(2)	Cl(2)	Fe(1)	-90.45(4)
Cl(2)	Fe(2)	N(2)	C(43)	-74.96(10)	Cl(2)	Fe(2)	N(2)	C(44)	45.30(10)
Cl(2)	Fe(2)	N(2)	C(51)	167.25(10)	N(2)	Fe(2)	Cl(2)	Fe(1)	176.11(4)
O(3)	Fe(2)	O(4)	C(62)	89.54(18)	O(4)	Fe(2)	O(3)	C(32)	-79.01(16)
O(3)	Fe(2)	N(2)	C(43)	34.41(11)	O(3)	Fe(2)	N(2)	C(44)	154.68(10)
O(3)	Fe(2)	N(2)	C(51)	-83.37(11)	N(2)	Fe(2)	O(3)	C(32)	11.32(15)
O(4)	Fe(2)	N(2)	C(43)	155.51(11)	O(4)	Fe(2)	N(2)	C(44)	-84.22(10)
O(4)	Fe(2)	N(2)	C(51)	37.73(11)	N(2)	Fe(2)	O(4)	C(62)	-1.14(18)
Fe(1)	O(1)	C(1)	C(2)	-149.42(12)	Fe(1)	O(1)	C(1)	C(11)	30.4(2)
Fe(1)	O(2)	C(31)	C(21)	20.7(2)	Fe(1)	O(2)	C(31)	C(26)	-159.75(14)
Fe(2)	O(3)	C(32)	C(33)	146.82(13)	Fe(2)	O(3)	C(32)	C(42)	-32.4(2)
Fe(2)	O(4)	C(62)	C(52)	-15.8(2)	Fe(2)	O(4)	C(62)	C(57)	164.52(14)
Fe(1)	N(1)	C(12)	C(11)	64.70(12)	Fe(1)	N(1)	C(13)	C(14)	-178.35(11)
Fe(1)	N(1)	C(20)	C(21)	65.44(13)	C(12)	N(1)	C(13)	C(14)	64.12(16)
C(13)	N(1)	C(12)	C(11)	-175.33(10)	C(12)	N(1)	C(20)	C(21)	-179.24(11)
C(20)	N(1)	C(12)	C(11)	-50.69(13)	C(13)	N(1)	C(20)	C(21)	-55.73(15)
C(20)	N(1)	C(13)	C(14)	-59.43(18)	Fe(2)	N(2)	C(43)	C(42)	-64.64(13)
Fe(2)	N(2)	C(44)	C(45)	179.93(12)	Fe(2)	N(2)	C(51)	C(52)	-64.68(13)
C(43)	N(2)	C(44)	C(45)	-62.57(17)	C(44)	N(2)	C(43)	C(42)	176.86(10)
C(43)	N(2)	C(51)	C(52)	179.52(11)	C(51)	N(2)	C(43)	C(42)	51.20(14)
C(44)	N(2)	C(51)	C(52)	54.65(15)	C(51)	N(2)	C(44)	C(45)	61.54(19)
O(1)	C(1)	C(2)	C(3)	8.5(2)	O(1)	C(1)	C(2)	C(7)	-173.16(14)
O(1)	C(1)	C(11)	C(10)	174.08(14)	O(1)	C(1)	C(11)	C(12)	-3.7(2)
C(2)	C(1)	C(11)	C(10)	-6.1(2)	C(2)	C(1)	C(11)	C(12)	176.15(14)
C(11)	C(1)	C(2)	C(3)	-171.28(15)	C(11)	C(1)	C(2)	C(7)	7.0(2)
C(1)	C(2)	C(3)	C(4)	55.0(2)	C(1)	C(2)	C(3)	C(5)	-65.8(2)
C(1)	C(2)	C(3)	C(6)	173.11(16)	C(1)	C(2)	C(7)	C(8)	-2.2(2)
C(3)	C(2)	C(7)	C(8)	176.09(16)	C(7)	C(2)	C(3)	C(4)	-123.17(18)
C(7)	C(2)	C(3)	C(5)	115.98(19)	C(7)	C(2)	C(3)	C(6)	-5.1(2)
C(2)	C(7)	C(8)	C(9)	177.23(16)	C(2)	C(7)	C(8)	C(10)	-3.5(2)
C(7)	C(8)	C(10)	C(11)	4.6(2)	C(9)	C(8)	C(10)	C(11)	-176.17(15)
C(8)	C(10)	C(11)	C(1)	0.1(2)	C(8)	C(10)	C(11)	C(12)	177.86(15)
C(1)	C(11)	C(12)	N(1)	-48.59(18)	C(10)	C(11)	C(12)	N(1)	133.66(14)
N(1)	C(13)	C(14)	C(15)	-87.8(2)	N(1)	C(13)	C(14)	C(19)	96.6(2)
C(13)	C(14)	C(15)	C(16)	-178.66(19)	C(13)	C(14)	C(19)	C(18)	177.69(18)
C(15)	C(14)	C(19)	C(18)	2.0(3)	C(19)	C(14)	C(15)	C(16)	-2.9(3)

C(14)	C(15)	C(16)	C(17)	2.0(3)	C(15)	C(16)	C(17)	C(18)	-0.0(2)
C(16)	C(17)	C(18)	C(19)	-0.9(3)	C(17)	C(18)	C(19)	C(14)	-0.0(2)
N(1)	C(20)	C(21)	C(22)	130.61(15)	N(1)	C(20)	C(21)	C(31)	-51.8(2)
C(20)	C(21)	C(22)	C(23)	179.10(17)	C(20)	C(21)	C(31)	O(2)	3.6(2)
C(20)	C(21)	C(31)	C(26)	-175.95(16)	C(22)	C(21)	C(31)	O(2)	-178.85(16)
C(22)	C(21)	C(31)	C(26)	1.6(2)	C(31)	C(21)	C(22)	C(23)	1.5(2)
C(21)	C(22)	C(23)	C(24)	176.83(18)	C(21)	C(22)	C(23)	C(25)	-2.6(2)
C(22)	C(23)	C(25)	C(26)	0.7(3)	C(24)	C(23)	C(25)	C(26)	-178.76(19)
C(23)	C(25)	C(26)	C(27)	-175.22(18)	C(23)	C(25)	C(26)	C(31)	2.3(2)
C(25)	C(26)	C(27)	C(28)	-3.0(2)	C(25)	C(26)	C(27)	C(29)	116.0(2)
C(25)	C(26)	C(27)	C(30)	-123.1(2)	C(25)	C(26)	C(31)	O(2)	177.09(16)
C(25)	C(26)	C(31)	C(21)	-3.4(2)	C(27)	C(26)	C(31)	O(2)	-5.4(2)
C(27)	C(26)	C(31)	C(21)	174.13(17)	C(31)	C(26)	C(27)	C(28)	179.65(18)
C(31)	C(26)	C(27)	C(29)	-61.4(2)	C(31)	C(26)	C(27)	C(30)	59.5(2)
O(3)	C(32)	C(33)	C(34)	-5.3(2)	O(3)	C(32)	C(33)	C(38)	176.77(14)
O(3)	C(32)	C(42)	C(41)	-176.99(14)	O(3)	C(32)	C(42)	C(43)	2.3(2)
C(33)	C(32)	C(42)	C(41)	3.8(2)	C(33)	C(32)	C(42)	C(43)	-176.83(15)
C(42)	C(32)	C(33)	C(34)	173.83(15)	C(42)	C(32)	C(33)	C(38)	-4.1(2)
C(32)	C(33)	C(34)	C(35)	-57.7(2)	C(32)	C(33)	C(34)	C(36)	63.2(2)
C(32)	C(33)	C(34)	C(37)	-176.52(16)	C(32)	C(33)	C(38)	C(39)	1.1(2)
C(34)	C(33)	C(38)	C(39)	-176.82(16)	C(38)	C(33)	C(34)	C(35)	120.05(19)
C(38)	C(33)	C(34)	C(36)	-118.97(19)	C(38)	C(33)	C(34)	C(37)	1.3(2)
C(33)	C(38)	C(39)	C(40)	-178.62(16)	C(33)	C(38)	C(39)	C(41)	2.1(2)
C(38)	C(39)	C(41)	C(42)	-2.4(2)	C(40)	C(39)	C(41)	C(42)	178.33(16)
C(39)	C(41)	C(42)	C(32)	-0.5(2)	C(39)	C(41)	C(42)	C(43)	-179.79(15)
C(32)	C(42)	C(43)	N(2)	50.33(19)	C(41)	C(42)	C(43)	N(2)	-130.36(15)
N(2)	C(44)	C(45)	C(46)	96.8(2)	N(2)	C(44)	C(45)	C(50)	-91.5(2)
C(44)	C(45)	C(46)	C(47)	171.5(2)	C(44)	C(45)	C(50)	C(49)	-173.42(19)
C(46)	C(45)	C(50)	C(49)	-1.5(3)	C(50)	C(45)	C(46)	C(47)	-0.5(3)
C(45)	C(46)	C(47)	C(48)	1.6(4)	C(46)	C(47)	C(48)	C(49)	-0.8(4)
C(47)	C(48)	C(49)	C(50)	-1.1(4)	C(48)	C(49)	C(50)	C(45)	2.3(3)
N(2)	C(51)	C(52)	C(53)	-131.47(16)	N(2)	C(51)	C(52)	C(62)	51.8(2)
C(51)	C(52)	C(53)	C(54)	-178.20(17)	C(51)	C(52)	C(62)	O(4)	-6.1(2)
C(51)	C(52)	C(62)	C(57)	173.54(16)	C(53)	C(52)	C(62)	O(4)	177.17(16)
C(53)	C(52)	C(62)	C(57)	-3.2(2)	C(62)	C(52)	C(53)	C(54)	-1.4(2)
C(52)	C(53)	C(54)	C(55)	-173.86(18)	C(52)	C(53)	C(54)	C(56)	4.1(2)
C(53)	C(54)	C(56)	C(57)	-2.3(3)	C(55)	C(54)	C(56)	C(57)	175.68(19)
C(54)	C(56)	C(57)	C(58)	176.18(19)	C(54)	C(56)	C(57)	C(62)	-2.1(3)
C(56)	C(57)	C(58)	C(59)	-1.1(2)	C(56)	C(57)	C(58)	C(60)	119.2(2)
C(56)	C(57)	C(58)	C(61)	-119.64(19)	C(56)	C(57)	C(62)	O(4)	-175.52(17)
C(56)	C(57)	C(62)	C(52)	4.8(2)	C(58)	C(57)	C(62)	O(4)	6.2(2)
C(58)	C(57)	C(62)	C(52)	-173.47(17)	C(62)	C(57)	C(58)	C(59)	177.07(18)
C(62)	C(57)	C(58)	C(60)	-62.6(2)	C(62)	C(57)	C(58)	C(61)	58.6(2)

The sign is positive if when looking from atom 2 to atom 3 a clock-wise motion of atom 1

would superimpose it on atom 4.

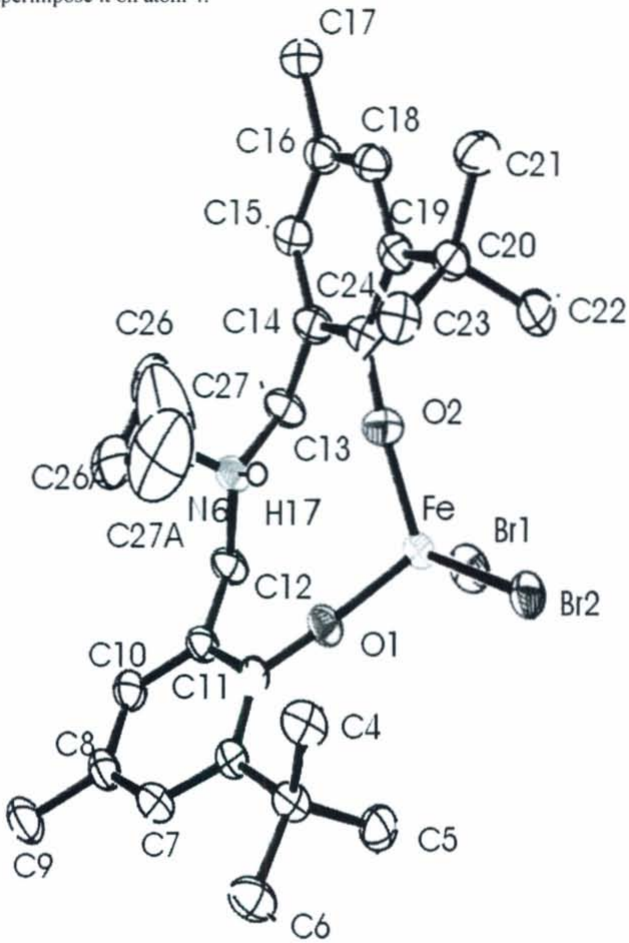

Figure A14: Molecular structure (ORTEP) and complete atom labeling of $FeBr_2[O_2NH]^{BuMenPr}$. Ellipsoids shown at 50% probability.

Hydrogen atoms omitted for clarity.

Table A7: Bond lengths (Å) for $FeBr_2[O_2NH]^{BuMe\mathit{n}Pr}$

atom	atom	distance	atom	atom	distance
Br(1)	Fe(1)	2.3569(7)	Br(2)	Fe(1)	2.3723(7)
Fe(1)	O(1)	1.828(3)	Fe(1)	O(2)	1.836(3)
O(1)	C(1)	1.337(5)	O(2)	C(24)	1.357(5)
N(6)	C(12)	1.509(6)	N(6)	C(13)	1.517(5)
N(6)	C(25)	1.516(6)	C(1)	C(2)	1.417(5)
C(1)	C(11)	1.413(5)	C(2)	C(3)	1.532(5)
C(2)	C(7)	1.394(6)	C(3)	C(4)	1.548(6)
C(3)	C(5)	1.539(6)	C(3)	C(6)	1.538(6)
C(7)	C(8)	1.398(6)	C(8)	C(9)	1.513(6)
C(8)	C(10)	1.386(6)	C(10)	C(11)	1.389(6)
C(11)	C(12)	1.498(6)	C(13)	C(14)	1.493(6)
C(14)	C(15)	1.396(6)	C(14)	C(24)	1.411(6)
C(15)	C(16)	1.391(6)	C(16)	C(17)	1.520(7)
C(16)	C(18)	1.376(6)	C(18)	C(19)	1.412(6)
C(19)	C(20)	1.535(6)	C(19)	C(24)	1.412(6)
C(20)	C(21)	1.546(7)	C(20)	C(22)	1.528(6)
C(20)	C(23)	1.540(6)	C(25)	C(26)	1.581(17)
C(25)	C(26A)	1.507(11)	C(26)	C(27)	1.56(4)
C(26)	C(26A)	1.24(2)	C(26)	C(27A)	1.19(3)
C(27)	C(26A)	1.51(5)	C(27)	C(27A)	0.48(5)
C(28)	C(29)	1.358(19)	C(29)	C(30)	1.413(11)
C(29)	C(31)[1)]	1.396(13)	C(30)	C(31)	1.376(13)
C(26A)	C(27A)	1.50(3)			

Table A8: Bond angles (°) for $FeBr_2[O_2NH]^{BuMe\mathit{n}Pr}$

atom	atom	atom	angle	atom	atom	atom	angle
Br(1)	Fe(1)	Br(2)	109.54(2)	Br(1)	Fe(1)	O(1)	110.72(9)
Br(1)	Fe(1)	O(2)	112.87(10)	Br(2)	Fe(1)	O(1)	109.42(10)
Br(2)	Fe(1)	O(2)	108.93(9)	O(1)	Fe(1)	O(2)	105.24(15)
Fe(1)	O(1)	C(1)	166.7(2)	Fe(1)	O(2)	C(24)	159.6(2)
C(12)	N(6)	C(13)	109.7(3)	C(12)	N(6)	C(25)	113.5(3)
C(13)	N(6)	C(25)	112.7(3)	O(1)	C(1)	C(2)	122.0(3)
O(1)	C(1)	C(11)	118.2(3)	C(2)	C(1)	C(11)	119.8(3)
C(1)	C(2)	C(3)	121.7(3)	C(1)	C(2)	C(7)	116.8(3)
C(3)	C(2)	C(7)	121.6(3)	C(2)	C(3)	C(4)	109.6(3)
C(2)	C(3)	C(5)	109.9(3)	C(2)	C(3)	C(6)	111.7(3)
C(4)	C(3)	C(5)	110.8(3)	C(4)	C(3)	C(6)	107.6(3)
C(5)	C(3)	C(6)	107.2(4)	C(2)	C(7)	C(8)	124.2(4)
C(7)	C(8)	C(9)	121.5(4)	C(7)	C(8)	C(10)	117.7(4)

C(9)	C(8)	C(10)	120.9(4)	C(8)	C(10)	C(11)	120.9(4)
C(1)	C(11)	C(10)	120.7(3)	C(1)	C(11)	C(12)	118.9(3)
C(10)	C(11)	C(12)	120.4(3)	N(6)	C(12)	C(11)	112.7(3)
N(6)	C(13)	C(14)	112.2(3)	C(13)	C(14)	C(15)	120.5(4)
C(13)	C(14)	C(24)	119.6(4)	C(15)	C(14)	C(24)	119.9(4)
C(14)	C(15)	C(16)	120.9(4)	C(15)	C(16)	C(17)	120.4(4)
C(15)	C(16)	C(18)	118.0(4)	C(17)	C(16)	C(18)	121.5(4)
C(16)	C(18)	C(19)	124.3(4)	C(18)	C(19)	C(20)	121.6(4)
C(18)	C(19)	C(24)	116.2(4)	C(20)	C(19)	C(24)	122.2(4)
C(19)	C(20)	C(21)	111.8(4)	C(19)	C(20)	C(22)	110.0(3)
C(19)	C(20)	C(23)	109.3(3)	C(21)	C(20)	C(22)	106.8(3)
C(21)	C(20)	C(23)	107.9(3)	C(22)	C(20)	C(23)	111.1(4)
O(2)	C(24)	C(14)	117.4(4)	O(2)	C(24)	C(19)	121.9(3)
C(14)	C(24)	C(19)	120.6(4)	N(6)	C(25)	C(26)	109.0(7)
N(6)	C(25)	C(26A)	115.0(5)	C(26)	C(25)	C(26A)	47.1(8)
C(25)	C(26)	C(27)	115(2)	C(25)	C(26)	C(26A)	63.3(8)
C(25)	C(26)	C(27A)	126(2)	C(27)	C(26)	C(26A)	64(2)
C(27)	C(26)	C(27A)	13(2)	C(26A)	C(26)	C(27A)	77(2)
C(26)	C(27)	C(26A)	47.4(16)	C(26)	C(27)	C(27A)	33(6)
C(26A)	C(27)	C(27A)	80(7)	C(28)	C(29)	C(30)	121.4(10)
C(28)	C(29)	C(31)[1)]	120.6(9)	C(30)	C(29)	C(31)[1)]	117.8(8)
C(29)	C(30)	C(31)	122.5(8)	C(29)[1)]	C(31)	C(30)	119.7(7)
C(25)	C(26A)	C(26)	69.6(9)	C(25)	C(26A)	C(27)	124(2)
C(25)	C(26A)	C(27A)	110.6(14)	C(26)	C(26A)	C(27)	69(2)
C(26)	C(26A)	C(27A)	50.2(16)	C(27)	C(26A)	C(27A)	18(2)
C(26)	C(27A)	C(27)	134(8)	C(26)	C(27A)	C(26A)	53.1(15)
C(27)	C(27A)	C(26A)	81(7)				

Table A9: Torsion angles (°) for $FeBr_2[O_2NH]^{BuMe\mathit{n}Pr}$

atom1	atom2	atom3	atom4	angle	atom1	atom2	atom3	atom4	angle
Br(1)	Fe(1)	O(1)	C(1)	-152.7(13)	Br(1)	Fe(1)	O(2)	C(24)	124.0(8)
Br(2)	Fe(1)	O(1)	C(1)	-31.9(13)	Br(2)	Fe(1)	O(2)	C(24)	2.1(9)
O(1)	Fe(1)	O(2)	C(24)	-115.1(8)	O(2)	Fe(1)	O(1)	C(1)	85.0(13)
Fe(1)	O(1)	C(1)	C(2)	152.5(11)	Fe(1)	O(1)	C(1)	C(11)	-27.8(15)
Fe(1)	O(2)	C(24)	C(14)	56.1(10)	Fe(1)	O(2)	C(24)	C(19)	-126.3(7)
C(12)	N(6)	C(13)	C(14)	-162.1(3)	C(13)	N(6)	C(12)	C(11)	162.1(3)
C(12)	N(6)	C(25)	C(26)	139.7(8)	C(12)	N(6)	C(25)	C(26A)	89.1(6)
C(25)	N(6)	C(12)	C(11)	-70.9(4)	C(13)	N(6)	C(25)	C(26)	-94.8(8)
C(13)	N(6)	C(25)	C(26A)	-145.4(6)	C(25)	N(6)	C(13)	C(14)	70.4(4)
O(1)	C(1)	C(2)	C(3)	-2.5(6)	O(1)	C(1)	C(2)	C(7)	178.0(3)
O(1)	C(1)	C(11)	C(10)	-178.3(4)	O(1)	C(1)	C(11)	C(12)	4.7(6)
C(2)	C(1)	C(11)	C(10)	1.4(6)	C(2)	C(1)	C(11)	C(12)	-175.7(3)

C(11)	C(1)	C(2)	C(3)	177.8(3)	C(11)	C(1)	C(2)	C(7)	-1.6(6)
C(1)	C(2)	C(3)	C(4)	61.9(4)	C(1)	C(2)	C(3)	C(5)	-60.2(5)
C(1)	C(2)	C(3)	C(6)	-179.0(4)	C(1)	C(2)	C(7)	C(8)	1.4(6)
C(3)	C(2)	C(7)	C(8)	-178.1(4)	C(7)	C(2)	C(3)	C(4)	-118.7(4)
C(7)	C(2)	C(3)	C(5)	119.2(4)	C(7)	C(2)	C(3)	C(6)	0.4(5)
C(2)	C(7)	C(8)	C(9)	178.6(4)	C(2)	C(7)	C(8)	C(10)	-0.8(7)
C(7)	C(8)	C(10)	C(11)	0.4(6)	C(9)	C(8)	C(10)	C(11)	-178.9(4)
C(8)	C(10)	C(11)	C(1)	-0.8(6)	C(8)	C(10)	C(11)	C(12)	176.2(4)
C(1)	C(11)	C(12)	N(6)	-67.2(5)	C(10)	C(11)	C(12)	N(6)	115.8(4)
N(6)	C(13)	C(14)	C(15)	-121.2(4)	N(6)	C(13)	C(14)	C(24)	60.5(5)
C(13)	C(14)	C(15)	C(16)	-177.1(4)	C(13)	C(14)	C(24)	O(2)	-2.8(6)
C(13)	C(14)	C(24)	C(19)	179.6(3)	C(15)	C(14)	C(24)	O(2)	178.9(3)
C(15)	C(14)	C(24)	C(19)	1.2(6)	C(24)	C(14)	C(15)	C(16)	1.2(6)
C(14)	C(15)	C(16)	C(17)	178.9(4)	C(14)	C(15)	C(16)	C(18)	-2.6(6)
C(15)	C(16)	C(18)	C(19)	1.8(6)	C(17)	C(16)	C(18)	C(19)	-179.8(4)
C(16)	C(18)	C(19)	C(20)	-176.8(4)	C(16)	C(18)	C(19)	C(24)	0.5(6)
C(18)	C(19)	C(20)	C(21)	-1.0(5)	C(18)	C(19)	C(20)	C(22)	-119.4(4)
C(18)	C(19)	C(20)	C(23)	118.4(4)	C(18)	C(19)	C(24)	O(2)	-179.6(3)
C(18)	C(19)	C(24)	C(14)	-2.0(6)	C(20)	C(19)	C(24)	O(2)	-2.3(6)
C(20)	C(19)	C(24)	C(14)	175.3(3)	C(24)	C(19)	C(20)	C(21)	-178.1(4)
C(24)	C(19)	C(20)	C(22)	63.4(5)	C(24)	C(19)	C(20)	C(23)	-58.8(5)
N(6)	C(25)	C(26)	C(27)	-68(2)	N(6)	C(25)	C(26)	C(26A)	-106.9(9)
N(6)	C(25)	C(26)	C(27A)	-60(2)	N(6)	C(25)	C(26A)	C(26)	93.2(10)
N(6)	C(25)	C(26A)	C(27)	49(2)	N(6)	C(25)	C(26A)	C(27A)	63.6(17)
C(26)	C(25)	C(26A)	C(27)	-44(2)	C(26)	C(25)	C(26A)	C(27A)	-29.6(17)
C(26A)	C(25)	C(26)	C(27)	38(2)	C(26A)	C(25)	C(26)	C(27A)	47(2)
C(25)	C(26)	C(27)	C(26A)	-38(2)	C(25)	C(26)	C(27)	C(27A)	149(11)
C(25)	C(26)	C(26A)	C(27)	141(2)	C(25)	C(26)	C(26A)	C(27A)	142.9(19)
C(25)	C(26)	C(27A)	C(27)	-35(12)	C(25)	C(26)	C(27A)	C(26A)	-41.9(18)
C(27)	C(26)	C(26A)	C(25)	-141(2)	C(27)	C(26)	C(26A)	C(27A)	2(2)
C(26A)	C(26)	C(27)	C(27A)	-173(11)	C(27)	C(26)	C(27A)	C(26A)	-7(10)
C(27A)	C(26)	C(27)	C(26A)	173(11)	C(26A)	C(26)	C(27A)	C(27)	7(10)
C(27A)	C(26)	C(26A)	C(25)	-142.9(19)	C(27A)	C(26)	C(26A)	C(27)	-2(2)
C(26)	C(27)	C(26A)	C(25)	45(2)	C(26)	C(27)	C(26A)	C(27A)	-4(5)
C(26)	C(27)	C(27A)	C(26A)	5(8)	C(26A)	C(27)	C(27A)	C(26)	-5(8)
C(27A)	C(27)	C(26A)	C(25)	49(8)	C(27A)	C(27)	C(26A)	C(26)	4(5)
C(28)	C(29)	C(30)	C(31)	-174.5(11)	C(28)	C(29)	C(31)[1)]	C(30)[1)]	174.5(11)
C(30)	C(29)	C(31)[1)]	C(30)[1)]	0.0(12)	C(31)[1)]	C(29)	C(30)	C(31)	-0.0(12)
C(29)	C(30)	C(31)	C(29)[1)]	0.0(12)	C(25)	C(26A)	C(27A)	C(26)	37.1(19)
C(25)	C(26A)	C(27A)	C(27)	-138(7)	C(26)	C(26A)	C(27A)	C(27)	-175(7)
C(27)	C(26A)	C(27A)	C(26)	175(7)					

The sign is positive if when looking from atom 2 to atom 3 a clock-wise motion of atom 1 would superimpose it on atom 4.

^{1}H NMR data of cross-coupled products and radical clock experiments (for Chapter 3)

Table 3.1, Entry 1: 1-cyclohexylbenzene. ^{1}H NMR (500 MHz, $CDCl_3$, δ): 2.44 (m, 1H, Ar*CH*); 1.36-1.80 (m, 10H, CH_2).

Table 3.1, Entry 2: 1-cyclohexyl-3-methoxybenzene. ^{1}H NMR (500 MHz, $CDCl_3$, δ): 3.79 (s, 3H, OCH_3); 2.47 (m, H, Ar*CH*); 1.46-1.86 (m, 10H).

Table 3.1, Entry 3: 1-cyclohexyl-4-fluorobenzene. ^{1}H NMR (500 MHz, $CDCl_3$, δ): 2.47 (m, 1H, Ar*CH*); 1.39-1.84 (m, 10H, CH_2).

Table 3.1, Entry 5: 1-cyclohexylnaphthalene. ^{1}H NMR (500 MHz, $CDCl_3$, δ): 3.32 (m, 1H, Ar*CH*); 1.55-2.03 (m, 10H, CH_2).

Table 3.1, Entry 6: 1-cyclohexyl-4-methylbenzene. ^{1}H NMR (500 MHz, $CDCl_3$, δ): 7.08 (m, 4H); 2.45 (m, 1H, Ar*CH*); 2.30 (s, 3H, $ArCH_3$); 1.81 (m, 5H CH_2); 1.27 (m, 5H, CH_2).

Table 3.1, Entry 7: 1-cyclohexyl-2-methylbenzene. ^{1}H NMR (500 MHz, $CDCl_3$, δ): 7.14 (m, 4H, Ar*H*); 2.70 (m, 1H, Ar*CH*); 2.33 (s, 3H, $ArCH_3$); 2.15 (m, 5H, CH_2); 1.53 (m, 2H, CH_2); 1.39 (m, 3H, CH_2).

Table 3.1, Entry 8: 1-cyclohexyl-4-methoxybenzene. ^{1}H NMR (500 MHz, $CDCl_3$, δ): 7.13 (d, 2H); 6.84 (d, 2H); 3.79 (s, 3H, OCH_3); 2.44 (m, 1H, Ar*CH*); 1.81 (m, 5H, CH_2); 1.30 (m, 5H, CH_2).

Table 3.2, Entry 1: 1-benzyl-2-methylbenzene. ^{1}H NMR (500 MHz, $CDCl_3$, δ): 3.79 (s, 2H, CH_2); 2.33 (s, 3H, $ArCH_3$).

Table 3.2, Entry 2: 2-benzyl-1,3-dimethylbenzene. ^{1}H NMR (500 MHz, $CDCl_3$, δ): 4.05 (s, 2H, $ArCH_2Ar$); 2.23 (s, 6H, $ArCH_3$).

Table 3.2, Entry 3: 1,3-bis(2-methylbenzyl)benzene. ^{1}H NMR (500 MHz, $CDCl_3$, δ): 3.93 (s, 4H, $ArCH_2Ar$); 2.23 (s, 6H, $ArCH_3$).

Table 3.2, Entry 4: 1,3-bis(2,6-dimethylbenzyl)benzene. ^{1}H NMR (500 MHz, $CDCl_3$, δ): 3.74 (s, 4H, CH_2); 2.24 (s, 6H, $ArCH_3$).

Table 3.3, Entry 1: 1-(3-chloropropyl)-2-methylbenzene. ^{1}H NMR (500 MHz, $CDCl_3$, δ): 3.51 (t, 2H, CH_2Cl); 2.70 (t, 2H, $ArCH_2$); 2.33 (s, 3H, $ArCH_3$); 1.84 (m, 2H, $ArCH_2CH_2$).

Table 3.3, Entry 2: 1-(3-chloropropyl)-4-fluorobenzene. ^{1}H NMR (500 MHz, $CDCl_3$, δ): 3.51 (dd, 2H, CH_2Cl); 2.75 (t, 2H, $ArCH_2$); 2.05 (t, 2H, CH_2).

Table 3.3, Entry 3: 1-(4-chlorobutyl)-2-methylbenzene. ^{1}H NMR (500 MHz, $CDCl_3$, δ): 3.56 (m, 2H, CH_2Cl); 2.62 (m, 2H, $ArCH_2$); 1.81 (m, 2H, CH_2CH_2Cl); 1.69 (m, 2H, $ArCH_2CH_2$).

Table 3.3, Entry 4: 1-methyl-2-octylbenzene. ^{1}H NMR (500 MHz, $CDCl_3$, δ): 7.41 (s, br, 4H, Ar*H*); 2.71 (t, 2H, ArCH_2); 2.45 (s, 3H, ArCH_3); 1.74 (m, 2H, CH_2CH_3); 1.44 (m, 10H, CH_2); 1.03 (t, 3H, CH_2CH_3).

Table 3.3, Entry 5: 1,3-dimethyl-2-octylbenzene. ^{1}H NMR (500 MHz, $CDCl_3$, δ): 2.58 (m, 2H, ArCH_2), 2.34 (s, 6H, ArCH_3); 1.89 (m, 2H, ArCH_2CH_2); 1.28 (s, 10H, CH_2); 0.88 (dd, 3H, CH_3).

Table 3.3, Entry 6: 1-methyl-2-propylbenzene. ^{1}H NMR (500 MHz, $CDCl_3$, δ): 2.58 (m, 2H, ArCH_2); 2.29 (s, 3H, ArCH_3); 1.60 (dt, 2H, ArCH_2); 0.98 (m, 2H, CH_3).

Table 3.3, Entry 7: 1-fluoro-4-propylbenzene. ^{1}H NMR (500 MHz, $CDCl_3$, δ): 2.60 (t, 2H, ArCH_2); 1.66 (m, 2H, CH_2); 0.92 (t, 3H, CH_3).

Table 3.3, Entry 8: 1,3-dimethyl-2-propylbenzene. ^{1}H NMR (500 MHz, $CDCl_3$, δ): 2.41 (t, 2H, ArCH_2); 2.32 (s, 6H, ArCH_3); 1.45(m, 2H, ArCH_2CH_2); 0.92 (t, 3H, CH_3).

Table 3.4, Entry 2: 1-sec-butyl-4-methoxybenzene. ^{1}H NMR (500 MHz, $CDCl_3$, δ): 3.78 (s, 3H, OCH_3); 2.27 (m, 1H, Ar*CH*); 1.42 (dt, 2H, $CHCH_2$); 1.12 (t, 3H, $CHCH_3$); 0.87 (t, 3H, CH_2CH_3).

Table 3.4, Entry 3: 1-sec-butyl-2-methylbenzene. ^{1}H NMR (500 MHz, $CDCl_3$, δ): 2.33 (m, H, Ar*CH*); 2.09 (s, 3H, ArCH_3); 1.46 (m, 2H, ArCH_2); 1.29 (m, 3H, $CHCH_3$); 0.92 (t, 3H, CH_2CH_3).

Table 3.4, Entry 4: sec-butylbenzene. ^{1}H NMR (500 MHz, $CDCl_3$, δ): 2.35 (m, H, Ar*CH*); 1.45 (m, 2H, $CHCH_2$); 1.33 (m, 3H, $CHCH_3$); 0.95 (t, 3H, CH_2CH_3).

Table 3.4, Entry 5: 1-sec-butyl-4-methylbenzene. ^{1}H NMR (500 MHz, $CDCl_3$, δ): 2.38 (s, 3H, ArCH_3); 2.34 (m, H, Ar*CH*); 1.55 (m, 2H, $CHCH_2$); 1.26 (m, 3H, $CHCH_3$); 0.88 (m, 3H, CH_2CH_3).

Table 3.5, Entry 1: 2-(2-methylphenethyl)-1,3-dioxane. ^{1}H NMR (500 MHz, $CDCl_3$, δ): 4.52 (t, H, C*H*); 4.12(m, 2H, O*CH*); 3.75(m, 2H, O*CH*); 2.71 (m, 2H, ArCH_2); 2.31(s, 3H, ArCH_3); 2.01 (m, 2H, CH_2CH_2CH); 1.87(m, 2H, $CH_2CH_2CH_2$).

Table 3.5, Entry 3: ethyl 6-o-tolylhexanoate. ^{1}H NMR (500 MHz, $CDCl_3$, δ): 4.12 (q, 2H, CH_2CH_3); 2.89 (t, 2H, ArCH_2); 2.59 (dd, 2H, CH_2CO); 2.30 (s, 3H, ArCH_3); 1.66 (m, 2H, ArCH_2CH_2; 2H, CH_2CH_2 CO); 1.40 (dt, 3H, CH_3).

Table 3.5, Entry 4: ethyl 6-(4-fluorophenyl)hexanoate. ^{1}H NMR (500 MHz, $CDCl_3$, δ): 4.15 (qq, 2H, OCH_2); 2.61 (m, 2H, ArCH_2); 2.32 (m, 2H, CH_2CO); 1.65 (m, 2H, ArCH_2CH_2; 2H, CH_2CH_2 CO); 1.30 (m, 2H, Ar$CH_2CH_2CH_2$; m, 3H, CH_3).

Table 3.5, Entry 7: 2-phenylbicyclo[2.2.1]heptane. ^{1}H NMR (500 MHz, $CDCl_3$, δ): 2.73 (m, H, Ar*CH*); 2.33 (t, 2H, $CHCH_2CH$); 1.42-1.78 (m, 8H).

NMR Data for "Radical Clock" Experiments

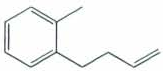

1-(but-3-enyl)-2-methylbenzene (500 MHz, $CDCl_3$, δ): 5.81(ddt, =CH, 1H,); 4.97(m, $=CH_2$, 2H,); 2.59(m, CH_2, 2H,); 2.29(s, CH_3, 3H,); 2.09(m, CH_2, 2H,).

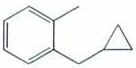

1-(cyclopropylmethyl)-2-methylbenzene (500 MHz, $CDCl_3$, δ): 2.61(m, CH_2, 2H,); 2.30(s, CH_3, 3H,); ~1.5(m, C_3H_5, 5H).

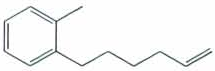

1-(hex-5-enyl)-2-methylbenzene (500 MHz, $CDCl_3$, δ): 5.88(m, =CH, 1H,); 5.02(dd, $=CH_2$, 2H,); 2.69(m, CH_2, 2H,); 2.30(s, CH_3, 3H,); 2.14(m, CH_2, 2H,).

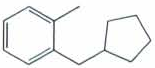

1-(cyclopentylmethyl)-2-methylbenzene (500 MHz, $CDCl_3$, δ): 2.33(m, CH_2, 2H,); 2.30(s, CH_3, 3H,); 2.01(m, CH, 1H).

GC Traces and Mass Spectra of Selected Products Given in Chapter 3

Table 3.1, Entry 1: Dodecane internal standard: R_t = 7.202 min. Cyclohexylbenzene: R_t = 8.211 min. By-product, biphenyl: R_t = 8.623 min.

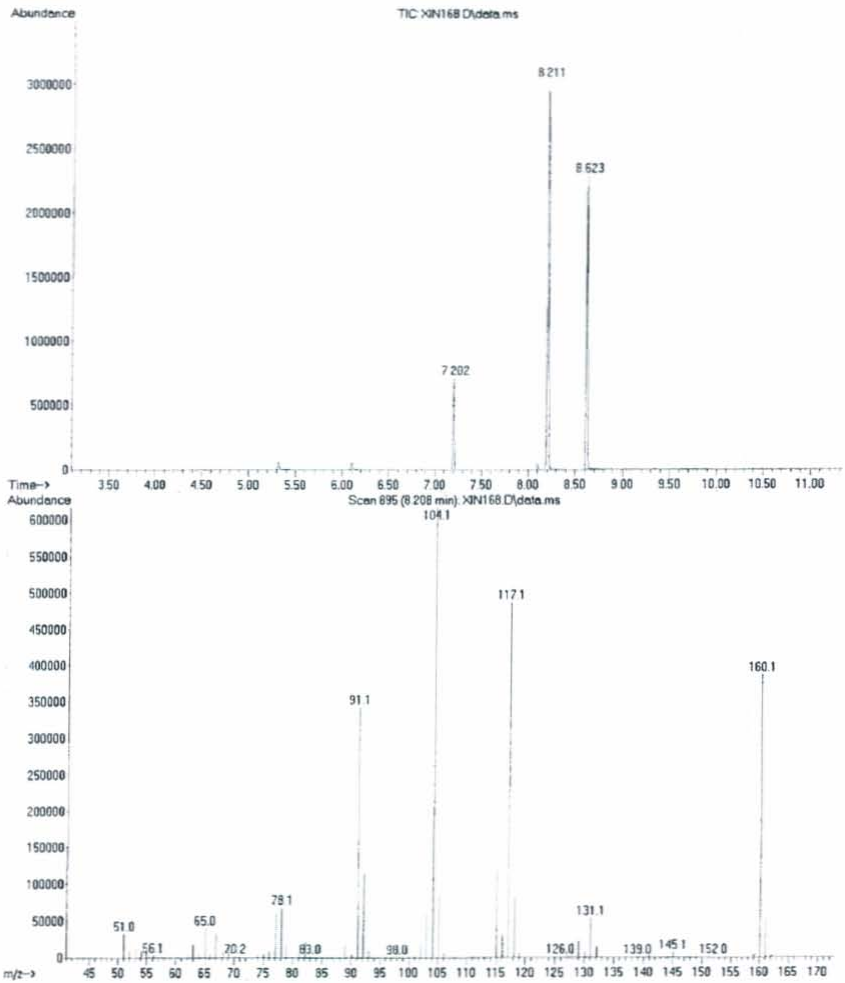

Table 3.1, Entry 2: Dodecane internal standard: R_t = 7.204 min. 1-cyclohexyl-3-methoxybenzene: R_t = 9.881 min. By-product, 3,3'-dimethoxybiphenyl, R_t = 12.839 min.

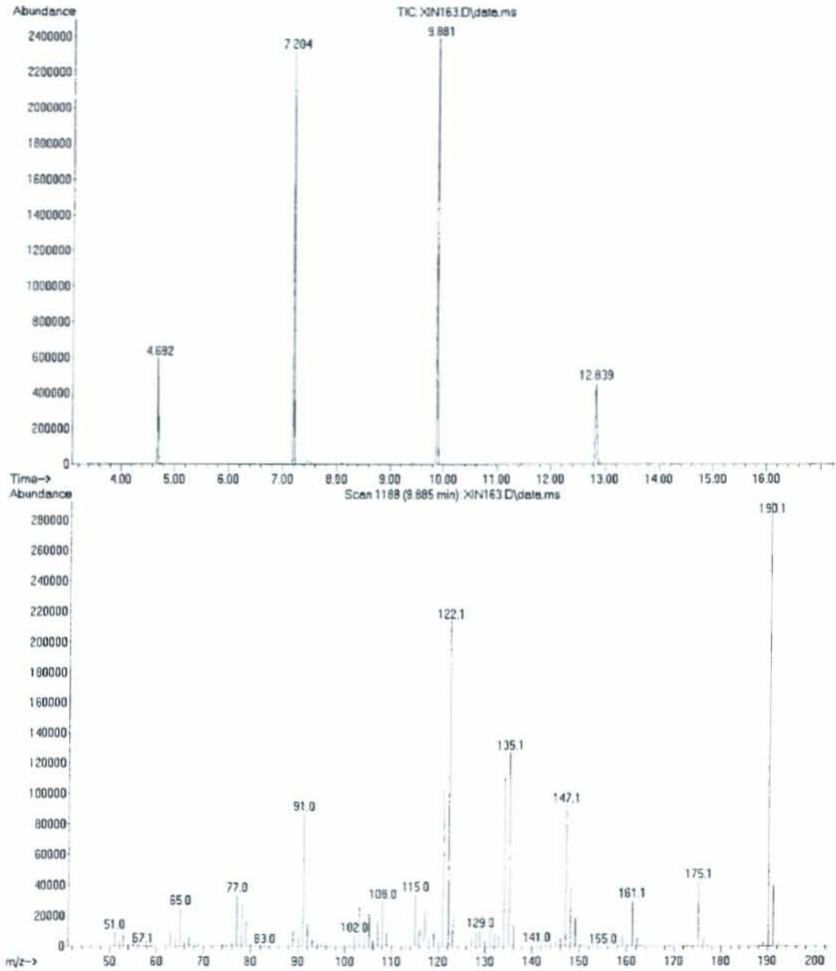

Table 3.1, Entry 3: Dodecane internal standard: R_t = 7.202 min. 1-cyclohexyl-4-fluorobenzene: R_t = 8.282 min. By-product, 4,4'-difluorobiphenyl: R_t = 8.594 min.

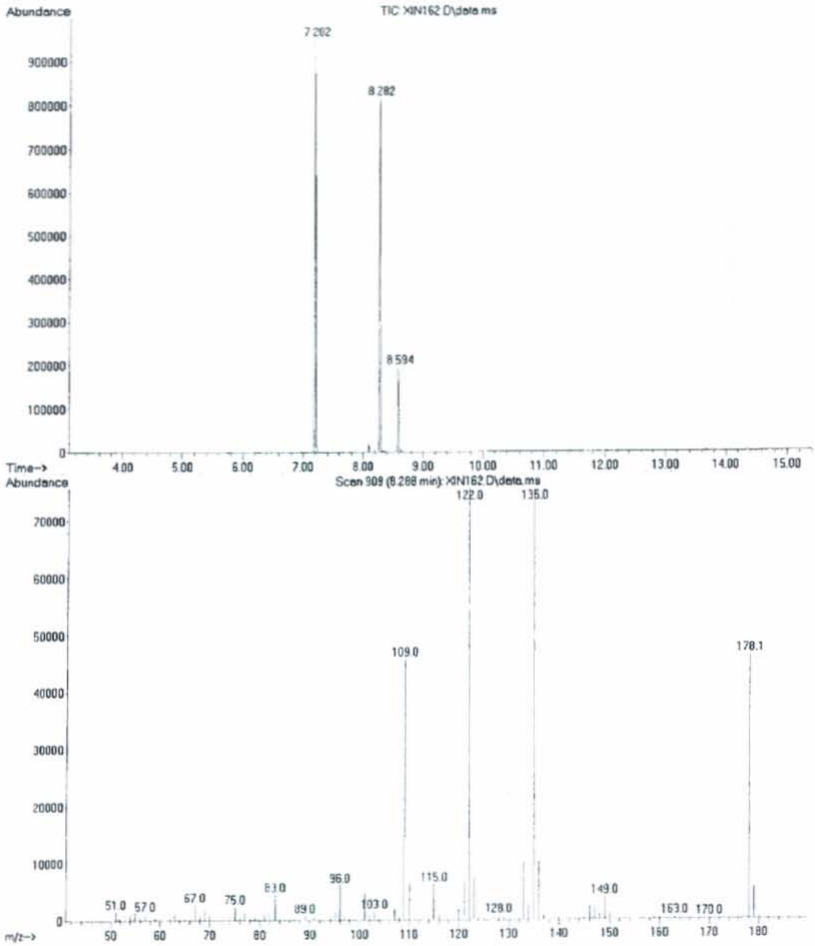

Table 3.1, Entry 4 (MW method): Dodecane internal standard: $R_t = 7.203$ min. Cyclohexene: $R_t = 5.286$ min. Starting material, cyclohexyl bromide: $R_t = 4.174$ min.

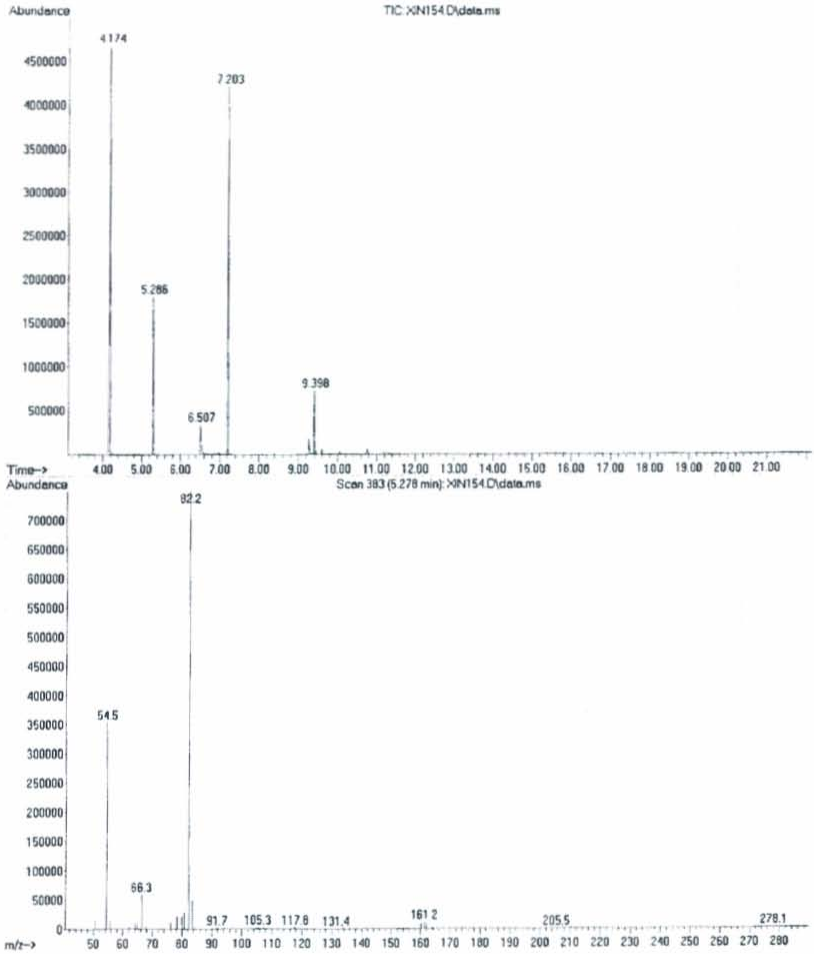

Table 3.1, Entry 5: Dodecane internal standard: $R_t = 7.204$ min. 1-cyclohexylnaphthalene: $R_t = 12.915$ min.

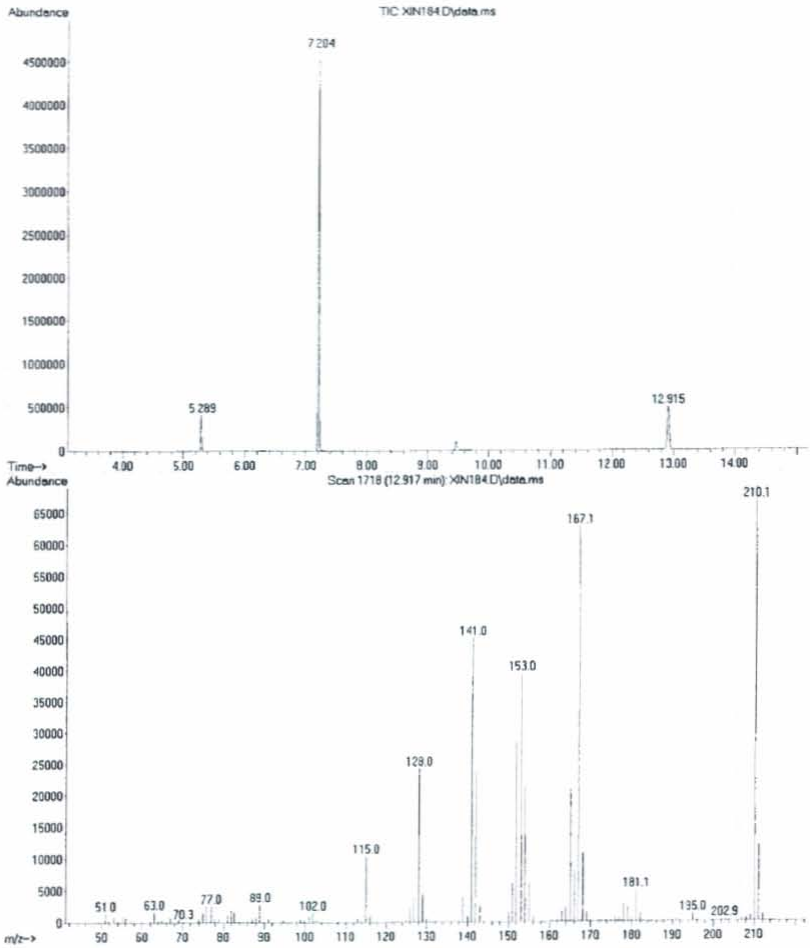

Table 3.1, Entry 6: Dodecane internal standard: R_t = 6.694 min. 1-cyclohexyl-4-methylbenzene: R_t = 8.440 min. By-product, 4,4'-dimethylbiphenyl: R_t = 9.588 min.

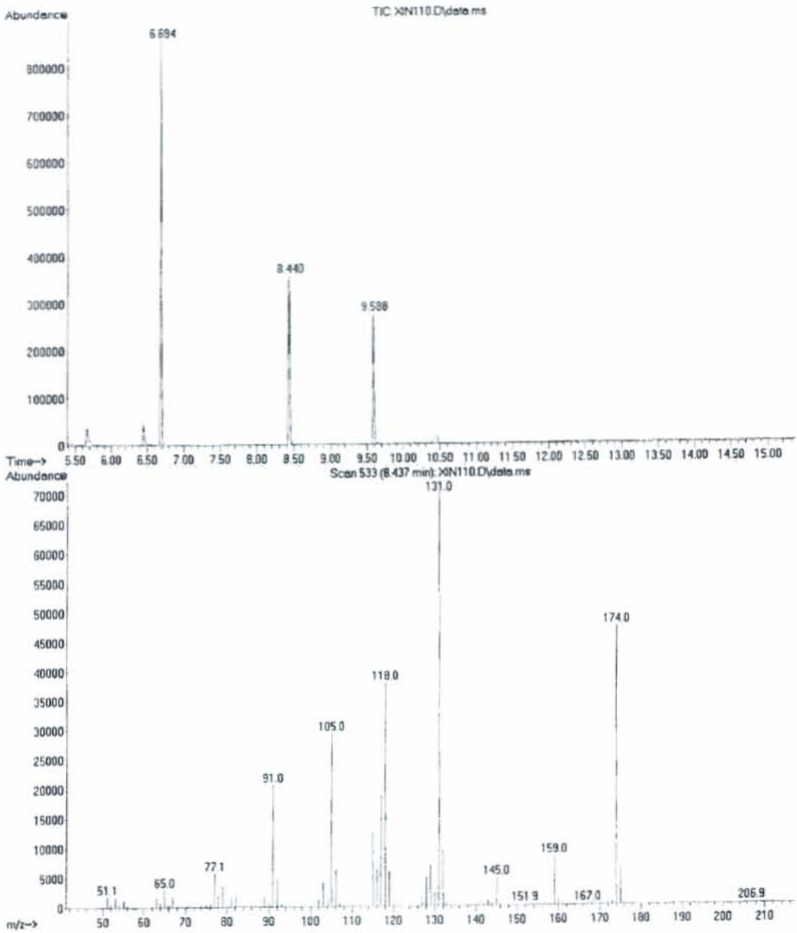

Table 3.1, Entry 7: Dodecane internal standard: R_t = 6.726 min. 1-cyclohexyl-2-methylbenzene: R_t = 8.444 min.

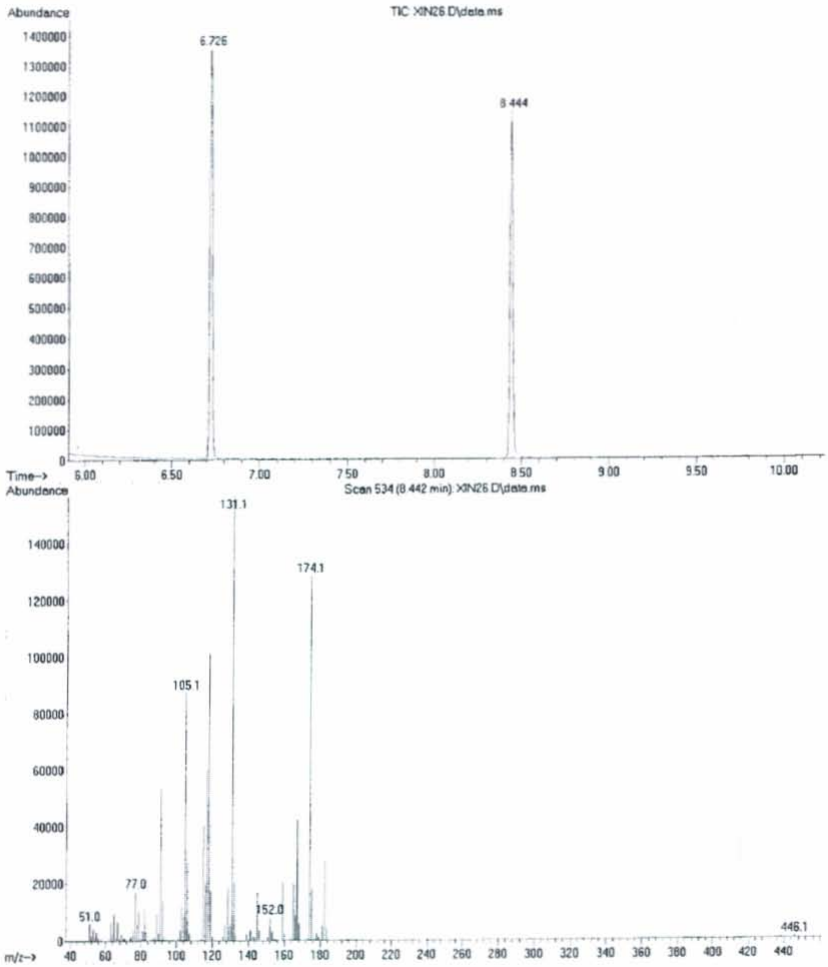

Table 3.1, Entry 8 (Heated to 40 °C): Dodecane internal standard: R_t = 7.203 min. 1-cyclohexyl-4-methoxy- benzene: R_t = 9.965 min. Starting material, cyclohexyl chloride: R_t = 4.413 min.

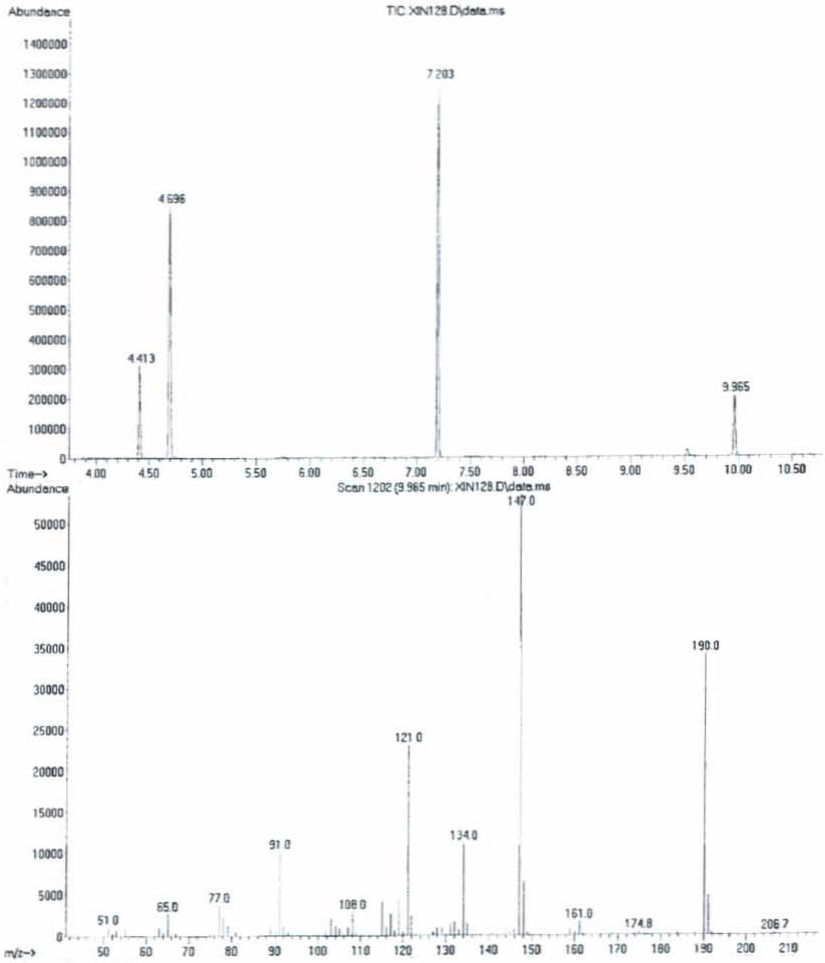

Table 3.1, Entry 8 (MW method): Dodecane internal standard: R_t = 7.206 min. 1-cyclohexyl-4-methoxybenzene, R_t = 9.967 min. By-product: 4,4'-dimethoxybiphenyl, R_t = 13.468 min.

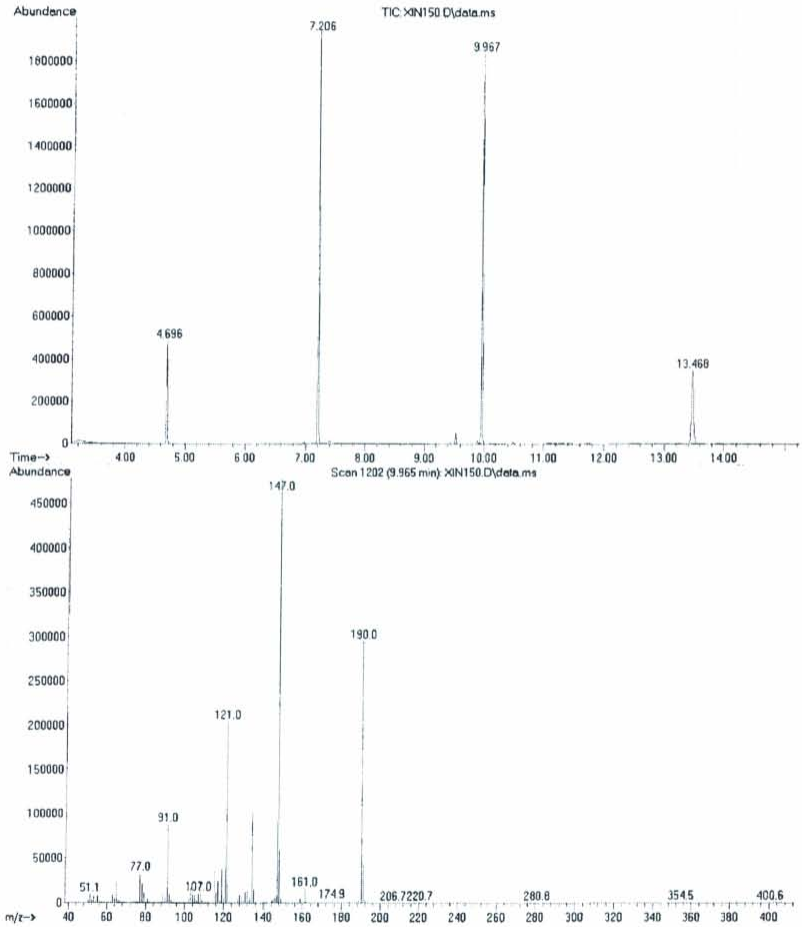

Table 3.2, Entry 1: Dodecane internal standard R_t = 6.724 min. 1-benzyl-2-methylbenzene, R_t = 9.155 min. By-product: 2,2'-dimethylbiphenyl, R_t = 8.447 min.

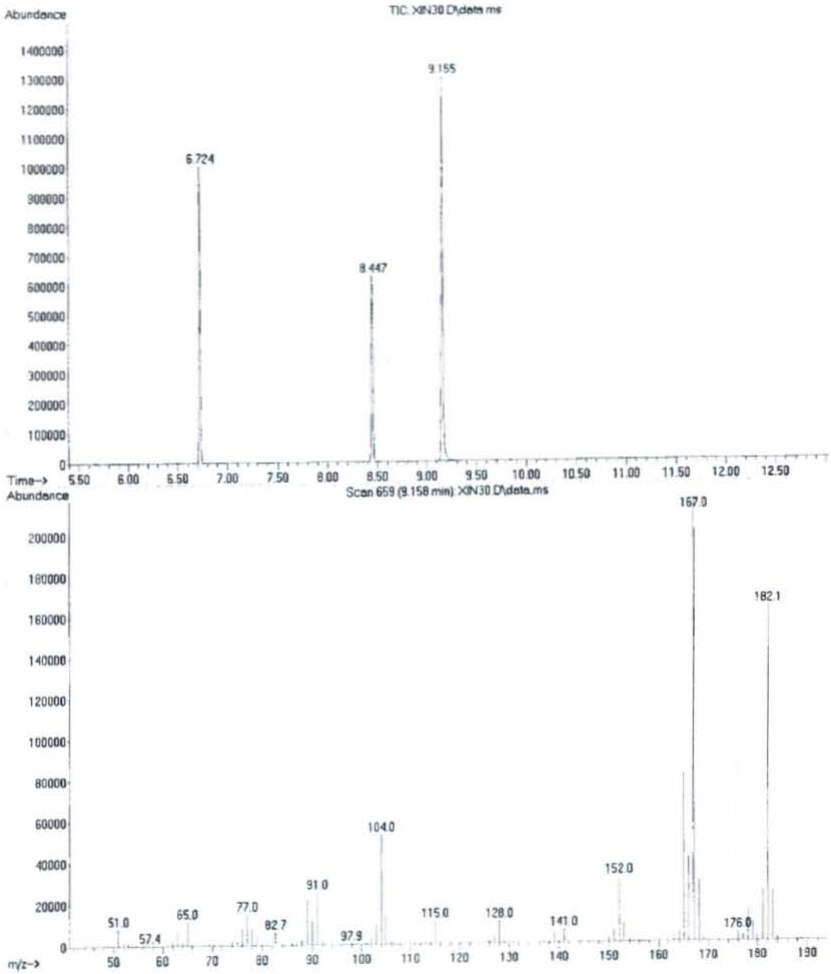

Table 3.2, Entry 2: Dodecane internal standard R_t = 6.694 min. 2-benzyl-1,3-dimethylbenzene, R_t = 9.630 min. By-product: 2,2',6,6'-tetramethylbiphenyl, R_t = 8.910 min. 1,2-diphenylethane, R_t = 9.062 min.

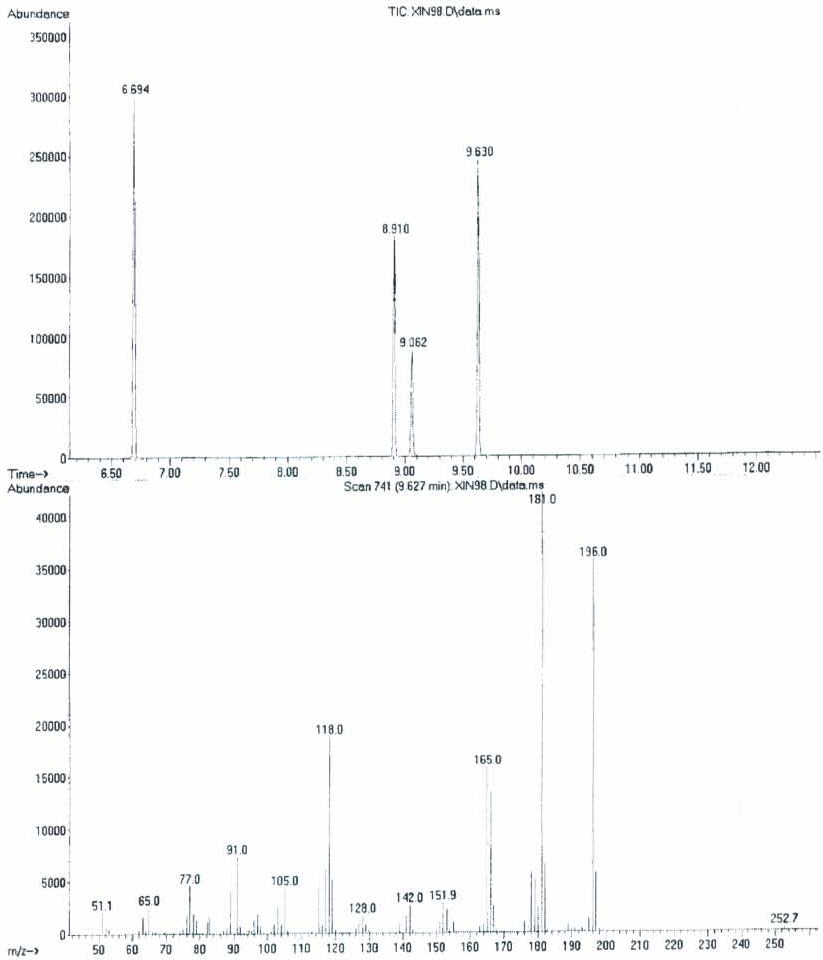

Table 3.2, Entry 3: Dodecane internal standard R_t = 6.689 min. 1,3-bis(2-methylbenzyl)benzene, R_t = 14.067 min. By-product: 2,2'-dimethylbiphenyl, R_t = 8.411 min.

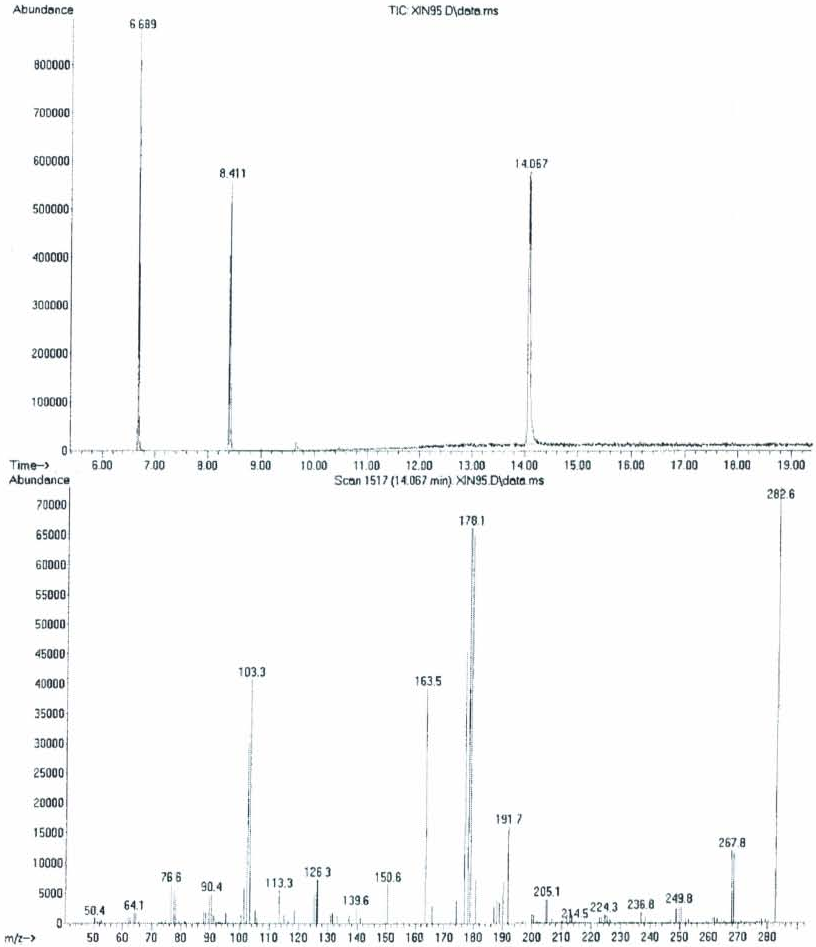

Table 3.3, Entry 1: Dodecane internal standard R_t = 6.461 min. 1-(3-chloropropyl)-2-methylbenzene, R_t = 7.520 min. By-product: 2,2'-dimethylbiphenyl, R_t = 8.195 min.

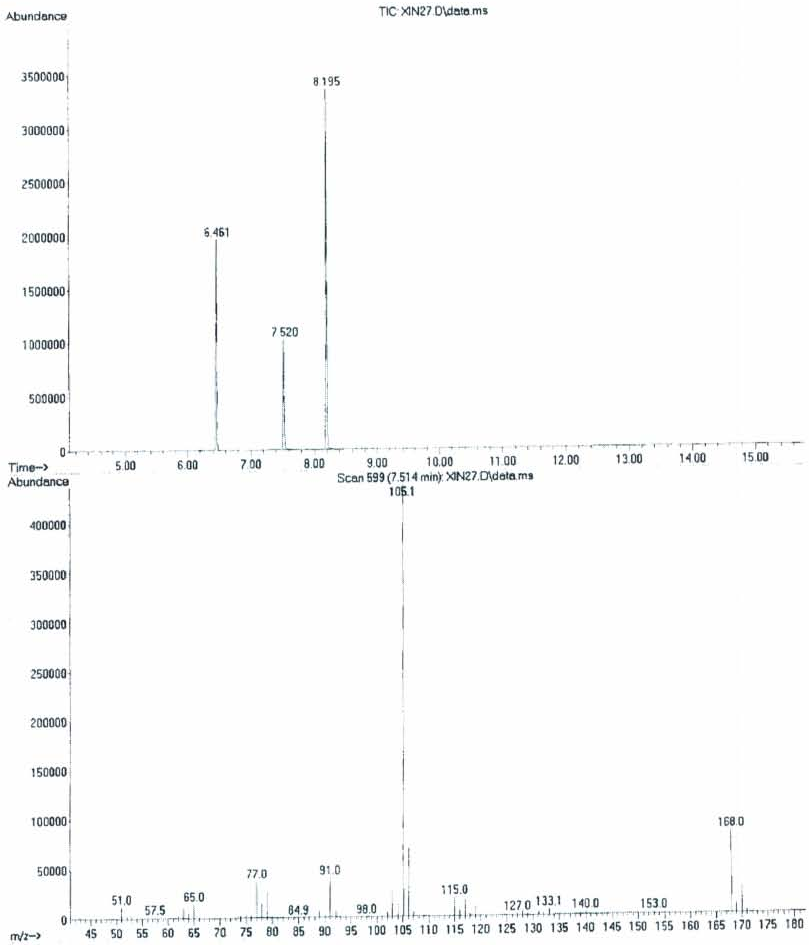

Table 3.3, Entry 2 (MW method): Dodecane internal standard R_t = 7.213 min. 1-(3-chloropropyl)-4-fluoro- benzene, R_t = 7.501 min. By-product: 4,4'-difluorobiphenyl, R_t = 8.599 min.

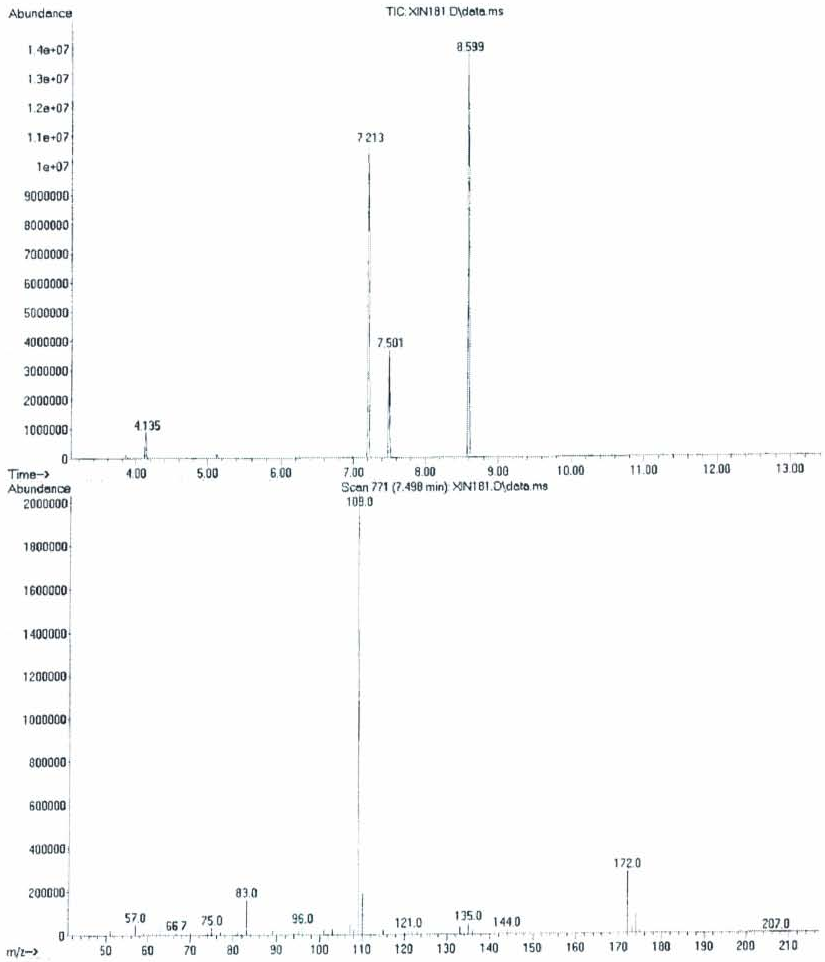

Table 3.3, Entry 3: Dodecane internal standard R_t = 6.693 min. 1-(4-chlorobutyl)-2-methylbenzene, R_t = 8.513 min. By-product: 2,2'-dimethylbiphenyl, R_t = 8.416 min.

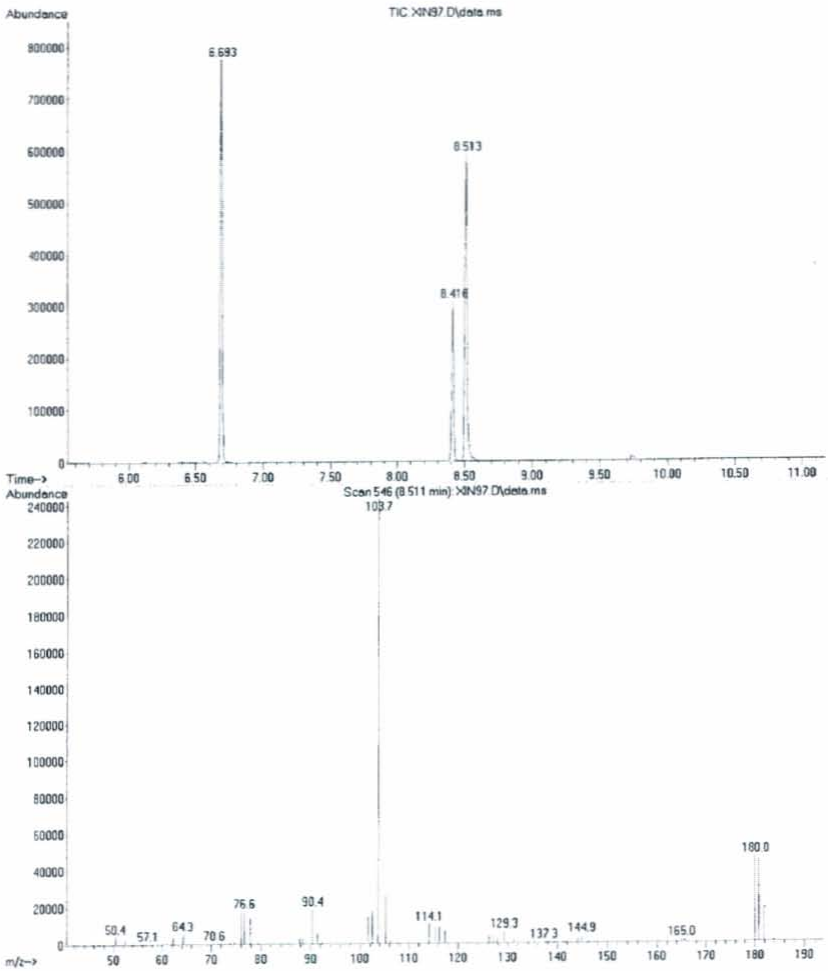

Table 3.3, Entry 4: Dodecane internal standard R_t = 7.206 min. 1-methyl-2-octylbenzene, R_t = 9.832 min. By-product: 2,2'-dimethylbiphenyl, R_t = 8.908 min.

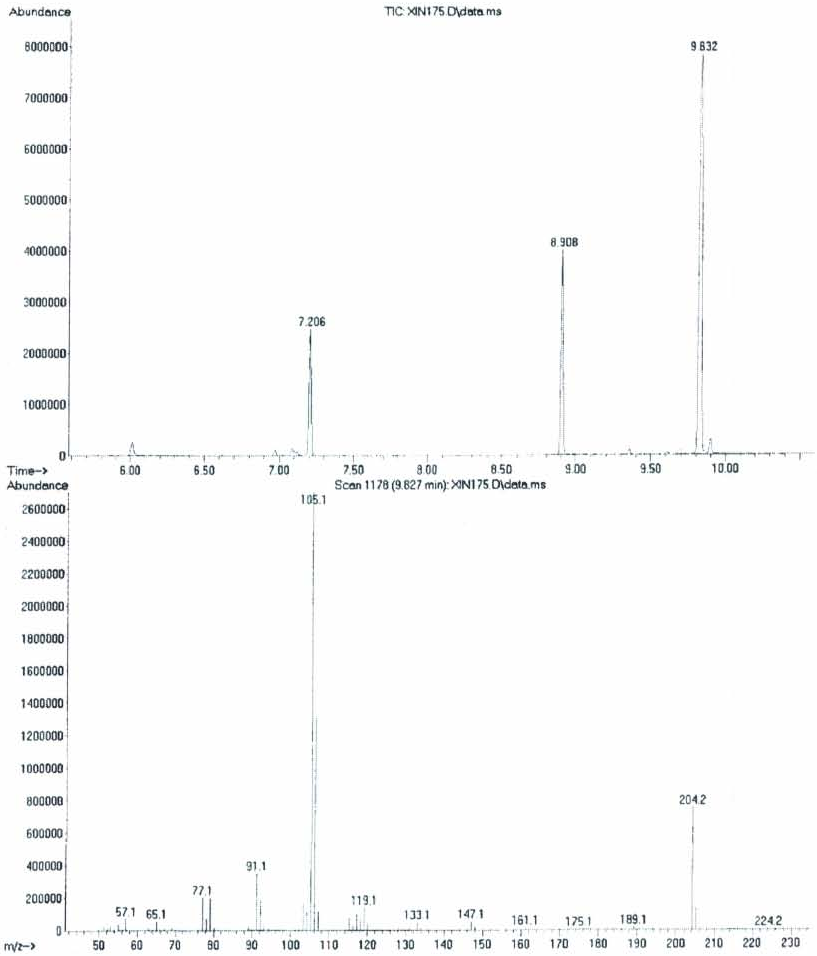

Table 3.3, Entry 5 (MW method): Dodecane internal standard R_t = 7.203 min. 1,3-dimethyl-2-octylbenzene, R_t = 10.576 min. By-product: 2,2',6,6'-tetramethylbiphenyl, R_t = 9.400 min.

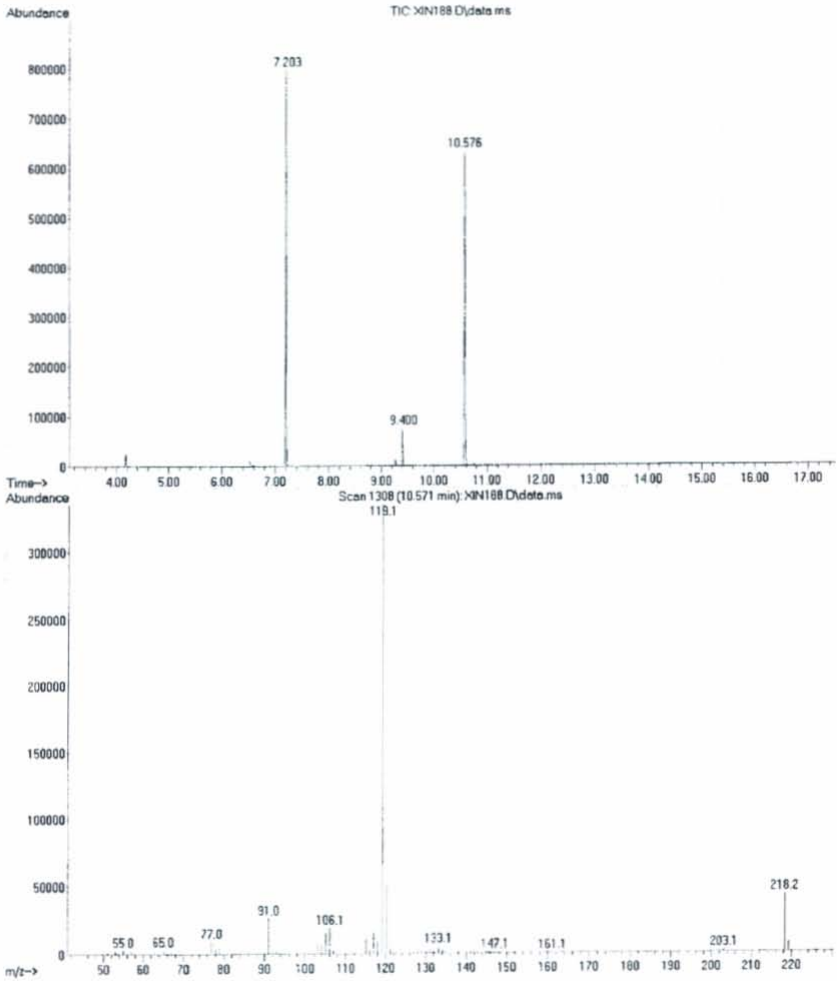

Table 3.3, Entry 6: Dodecane internal standard R_t = 7.202 min. 1-methyl-2-propylbenzene, R_t = 6.166 min. By-product: 2,2'-dimethylbiphenyl, R_t = 8.906 min.

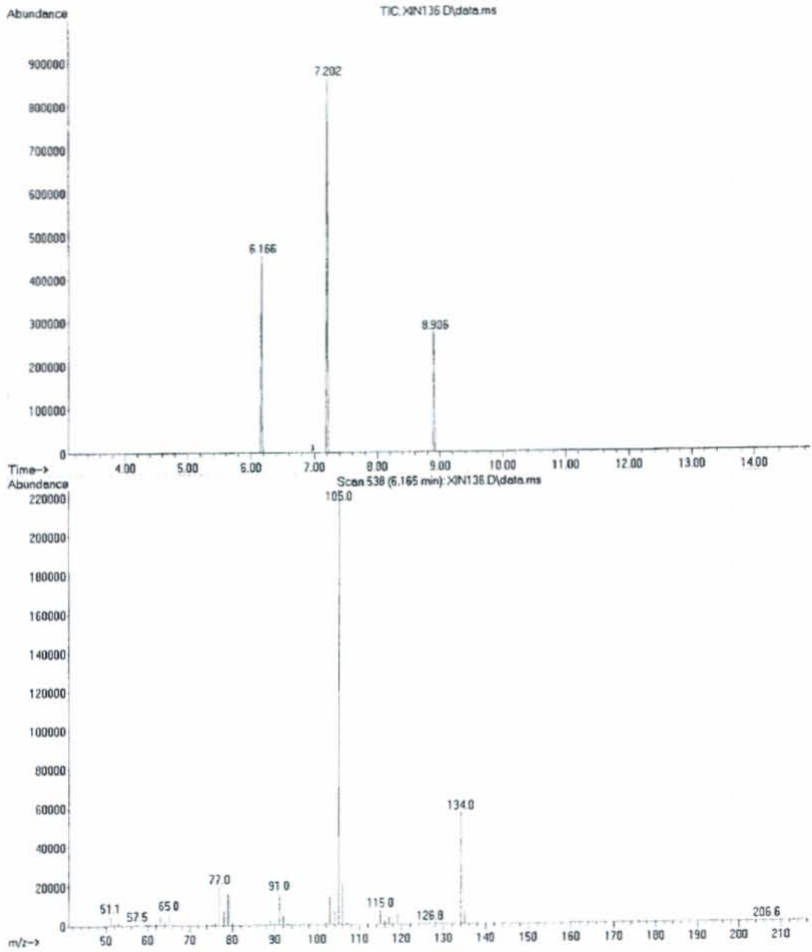

Table 3.3, Entry 7: Dodecane internal standard R_t = 7.204 min. 1-fluoro-4-propylbenzene, R_t = 5.224 min. By-product: 4,4'-difluorobiphenyl, R_t = 8.594 min.

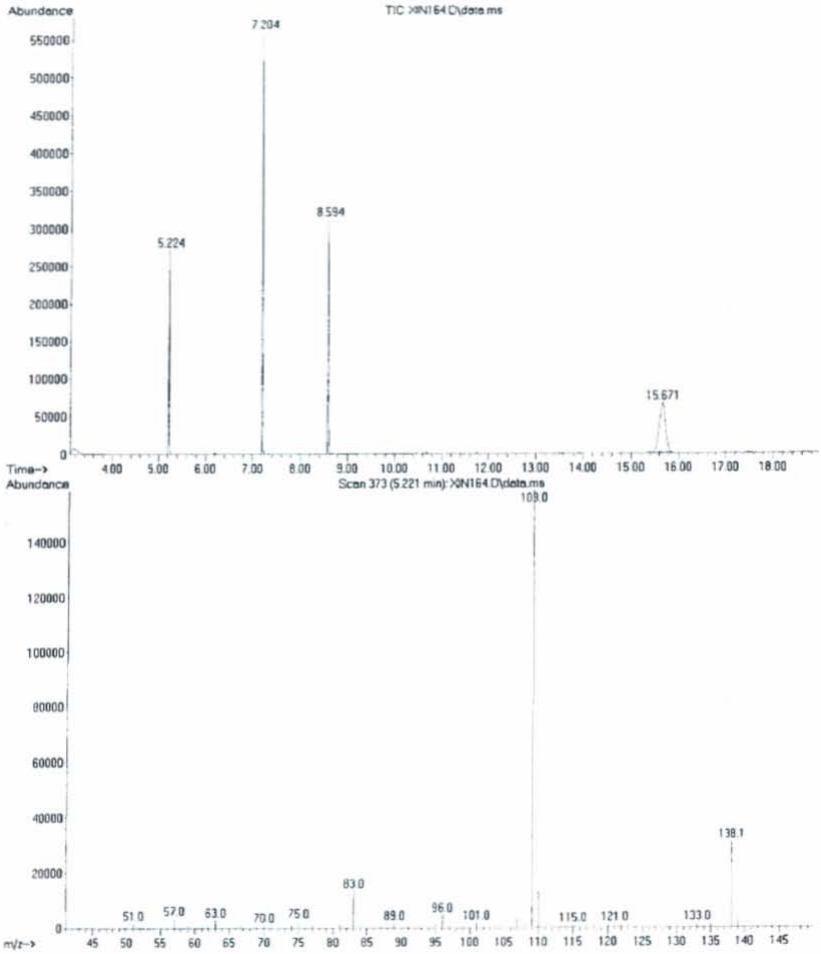

Table 3.3, Entry 8 (MW method): Dodecane internal standard R_t = 7.207 min. 1,3-dimethyl-2-propylbenzene, R_t = 7.079 min. By-product: 2,2',6,6'-tetramethylbiphenyl, R_t = 9.399 min.

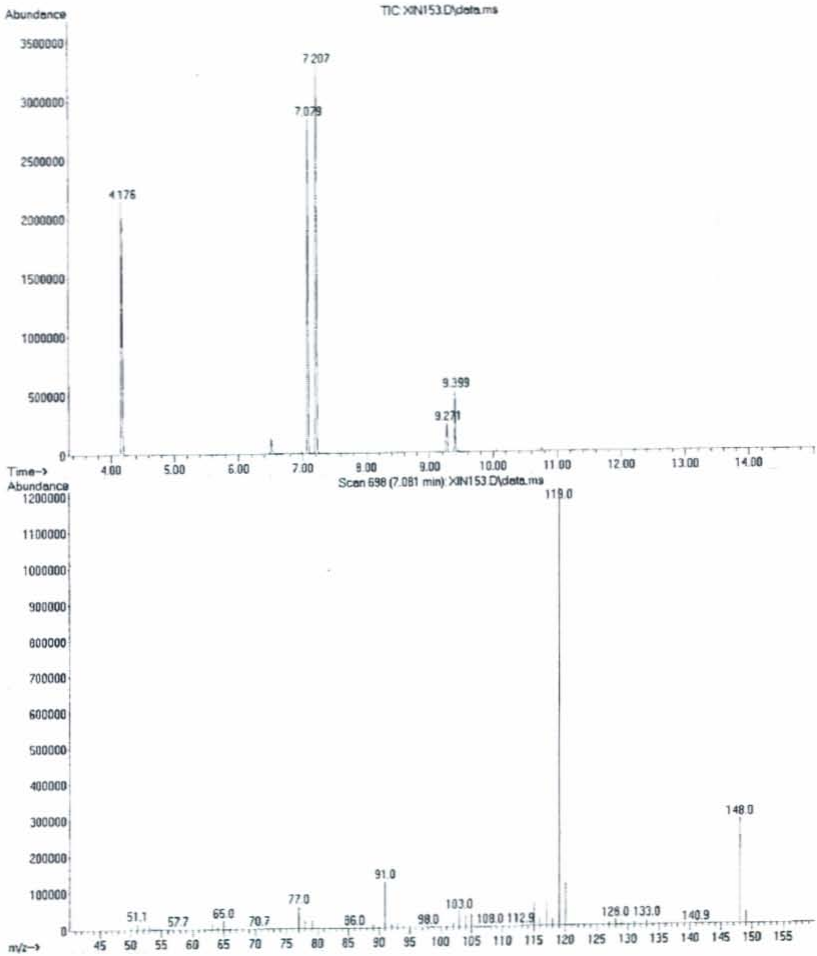

Table 3.4, Entry 2: Dodecane internal standard R_t = 7.203 min. 1-*sec*-butyl-4-methoxybenzene, R_t = 7.733 min.

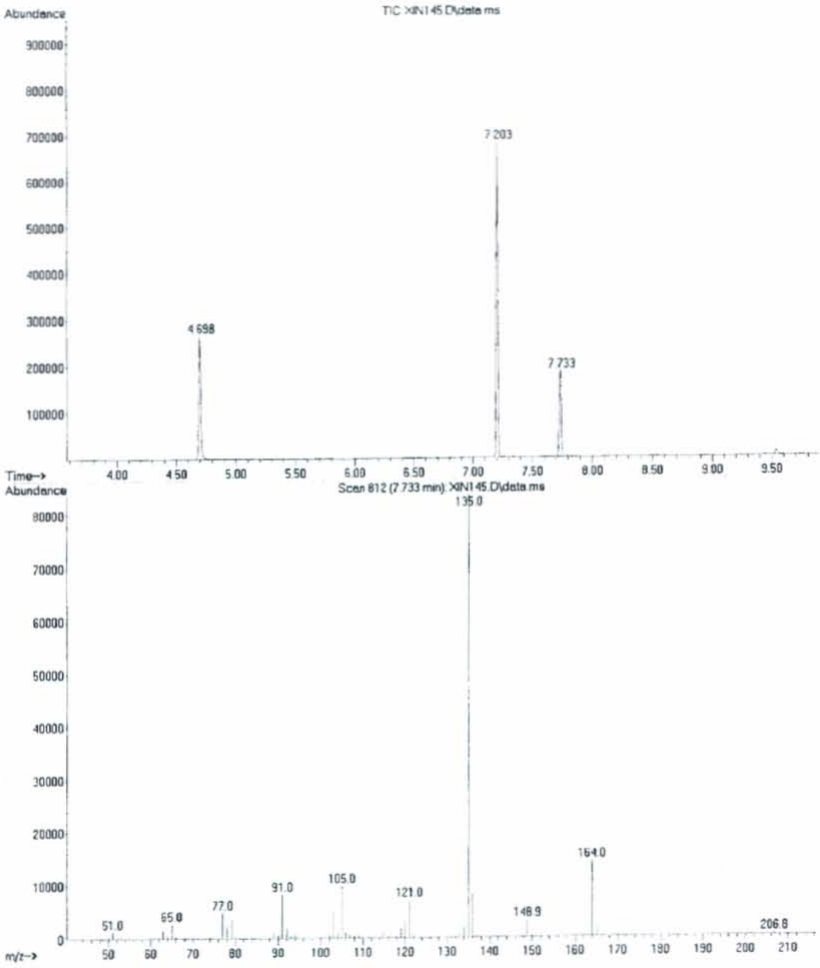

Table 3.4, Entry 2 (MW method): Dodecane internal standard R_t = 7.205 min. 1-*sec*-butyl-4-methoxybenzene, R_t = 7.734 min.

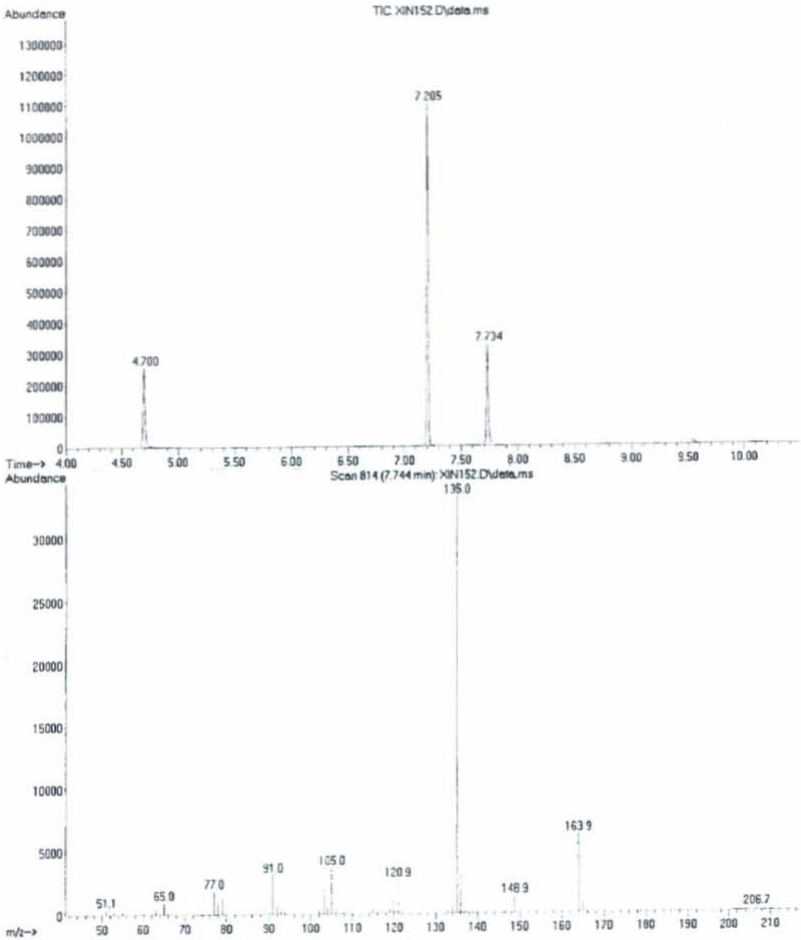

Table 3.4, Entry 3: Dodecane internal standard R_t = 7.205 min. 1-*sec*-butyl-2-methylbenzene, R_t = 6.605 min. By-product: 2,2'-dimethylbiphenyl, R_t = 8.907 min.

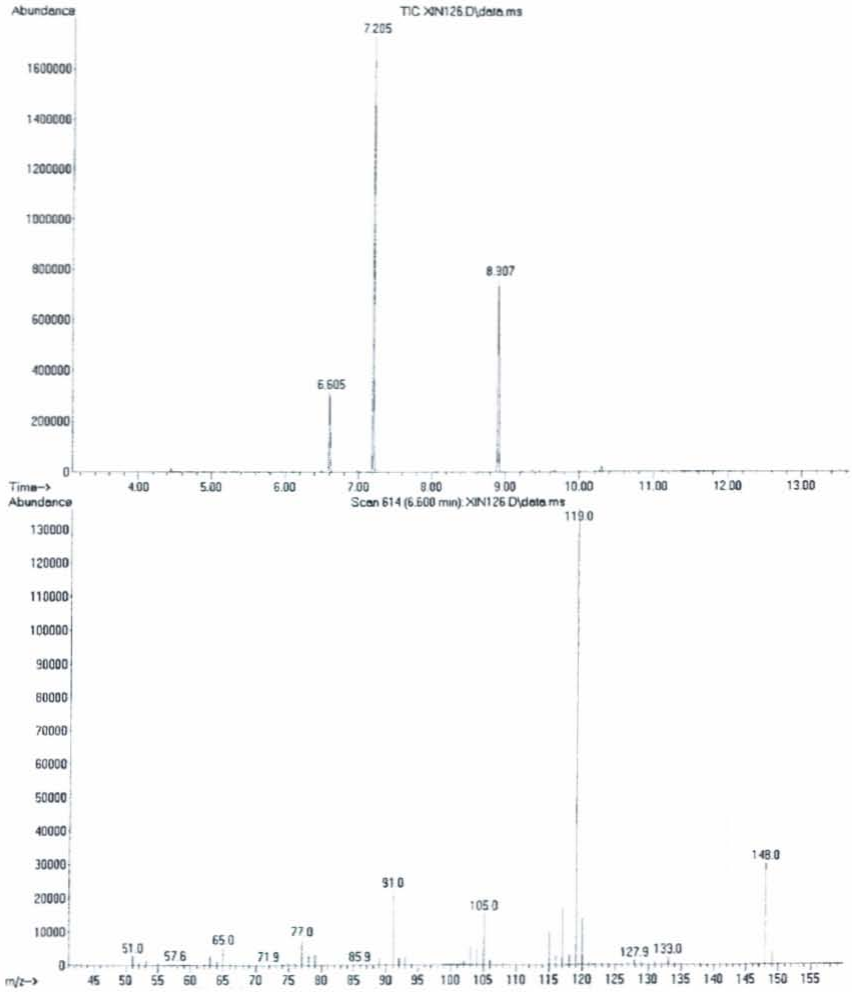

Table 3.4, Entry 3 (MW method at 100 °C): Dodecane internal standard R_t = 7.202 min. 1-*sec*-butyl-2-methylbenzene, R_t = 6.602 min. By-product: 2,2'-dimethylbiphenyl, R_t = 8.905 min.

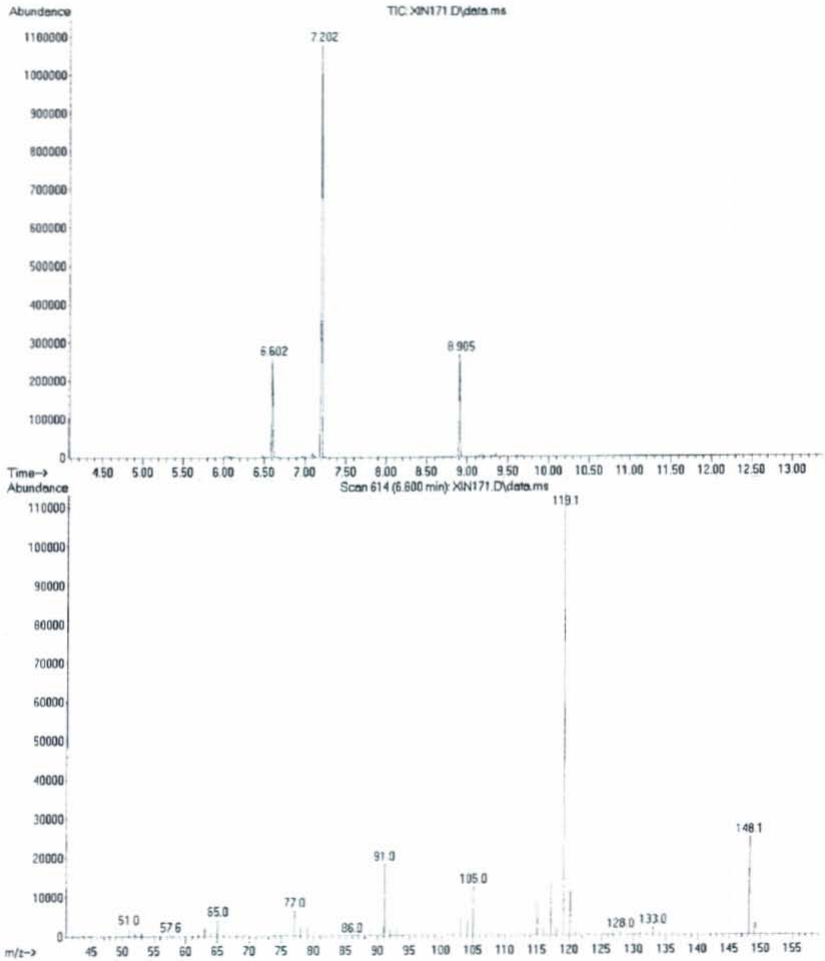

Table 3.4, Entry 3 (MW method at 180 °C): Dodecane internal standard R_t = 7.205 min. 1-*sec*-butyl-2-methylbenzene, R_t = 6.605 min. By-product: 2,2'-dimethylbiphenyl, R_t = 8.908 min.

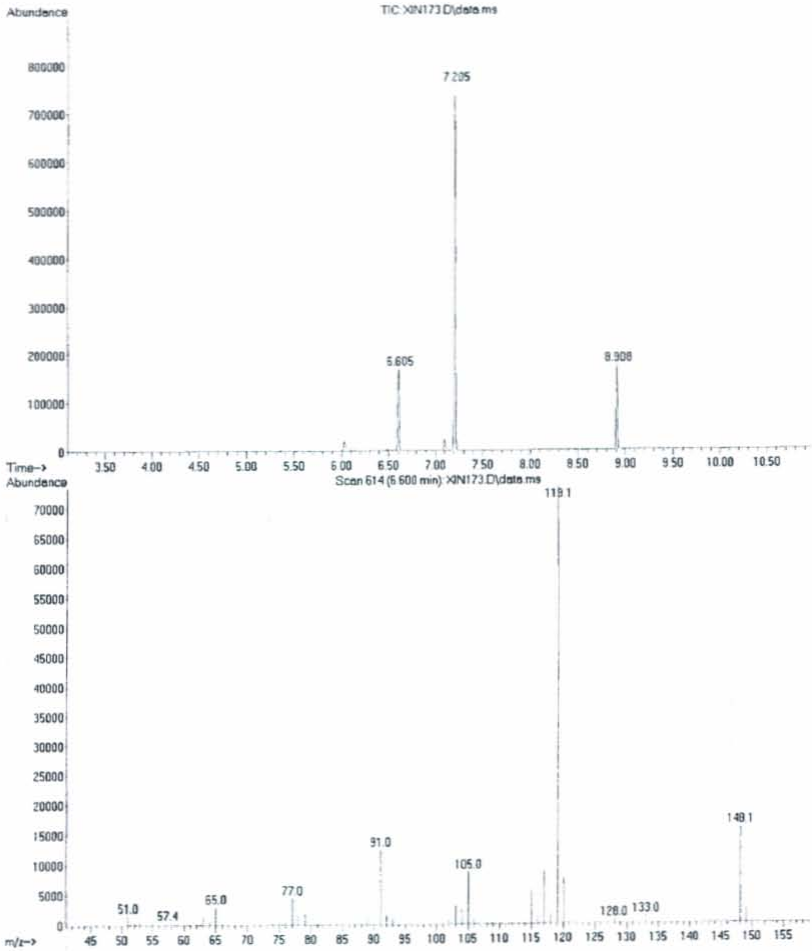

Table 3.4, Entry 4: Dodecane internal standard R_t = 7.204 min. *sec*-butylbenzene, R_t = 5.649 min. By-product: biphenyl, R_t = 8.623 min.

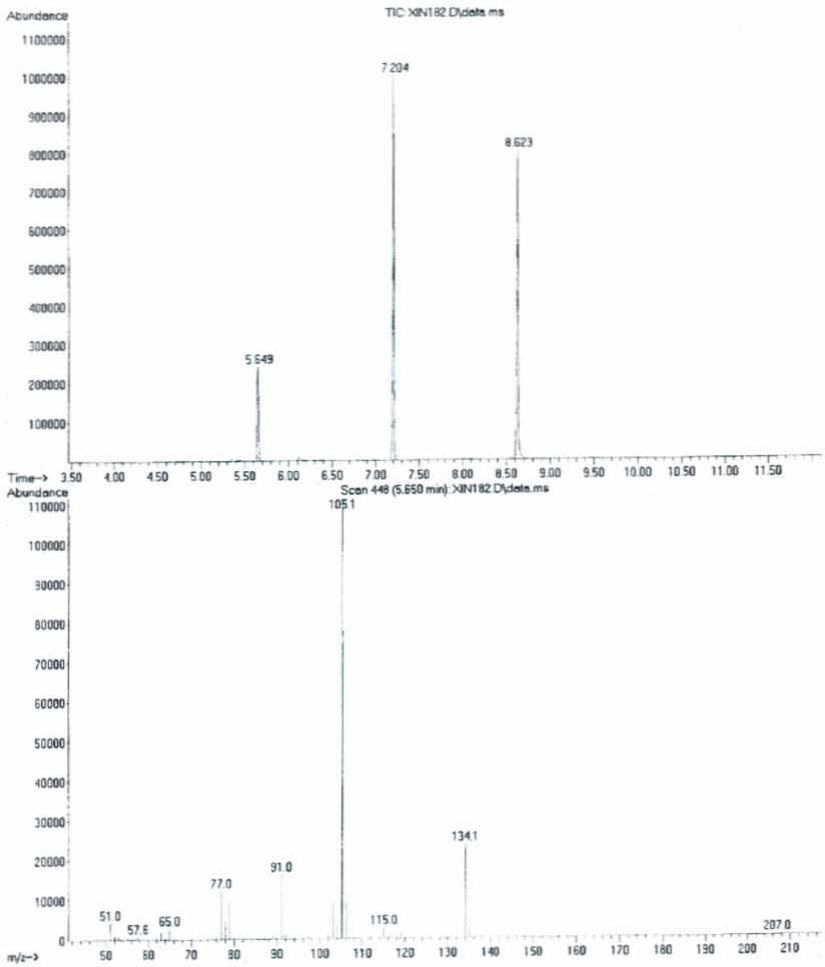

Table 3.4, Entry 4 (MW method): Dodecane internal standard R_t = 7.220 min. *sec*-butylbenzene, R_t = 5.650 min. By-product: biphenyl, R_t = 8.631 min.

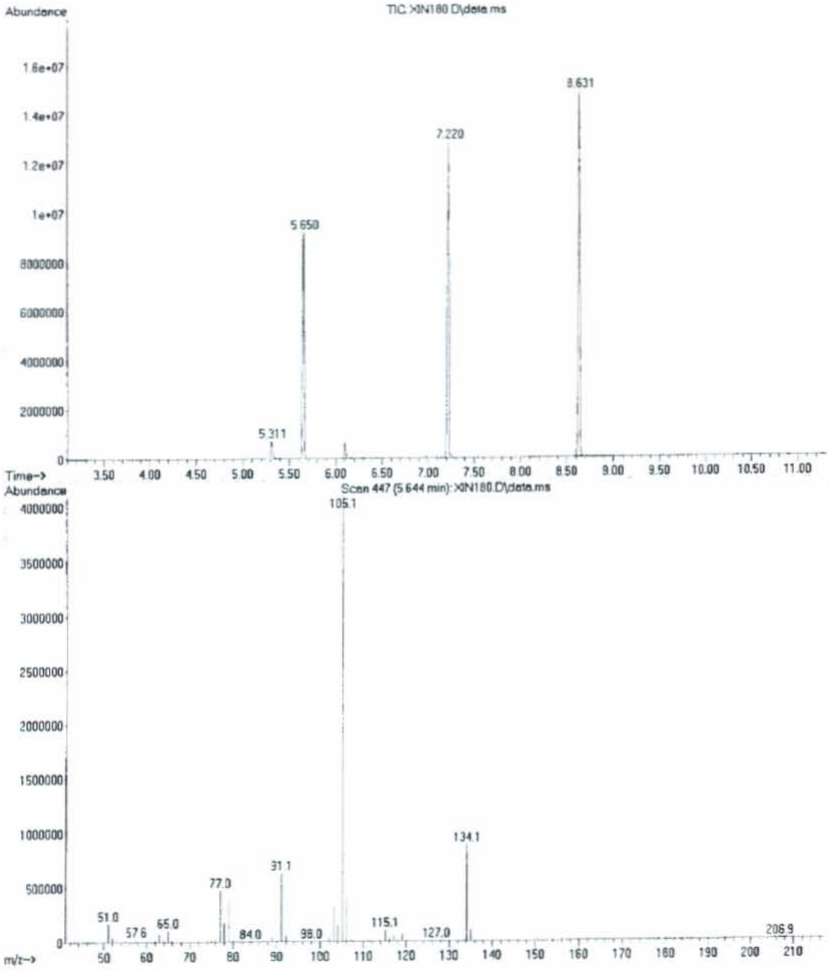

Table 3.4, Entry 5: Dodecane internal standard R_t = 7.204 min. 1-*sec*-butyl-2-methylbenzene, R_t = 6.538 min. By-product: 4,4'-dimethylbiphenyl, R_t = 10.124 min.

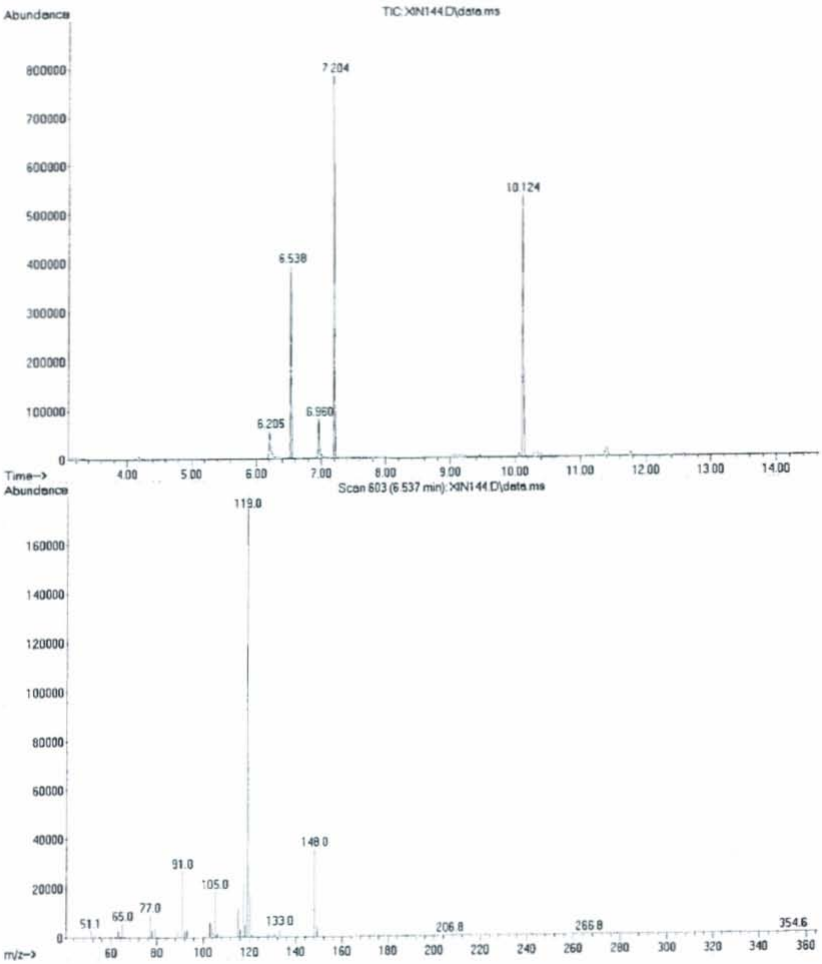

Table 3.5, Entry 1: Dodecane internal standard R_t = 7.206 min. 2-(2-methylphenethyl)-1,3-dioxane, R_t = 10.264 min. By-product: 2,2'-dimethylbiphenyl, R_t = 8.908 min.

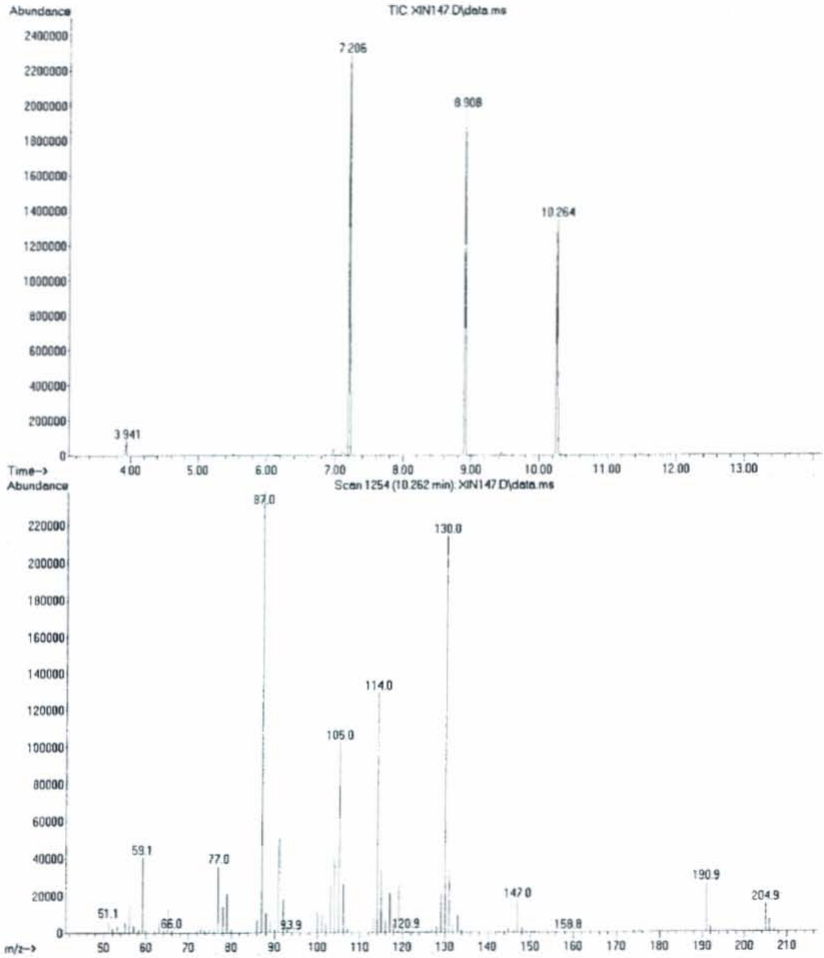

Table 3.5, Entry 3: Dodecane internal standard R_t = 7.209 min. Ethyl-6-*o*-tolylhexanoate, R_t = 11.398 min. By-product: 2,2'-dimethylbiphenyl, R_t = 8.908 min. Other small peaks are impurities from the starting material, ethyl-6-bromohexanoate.

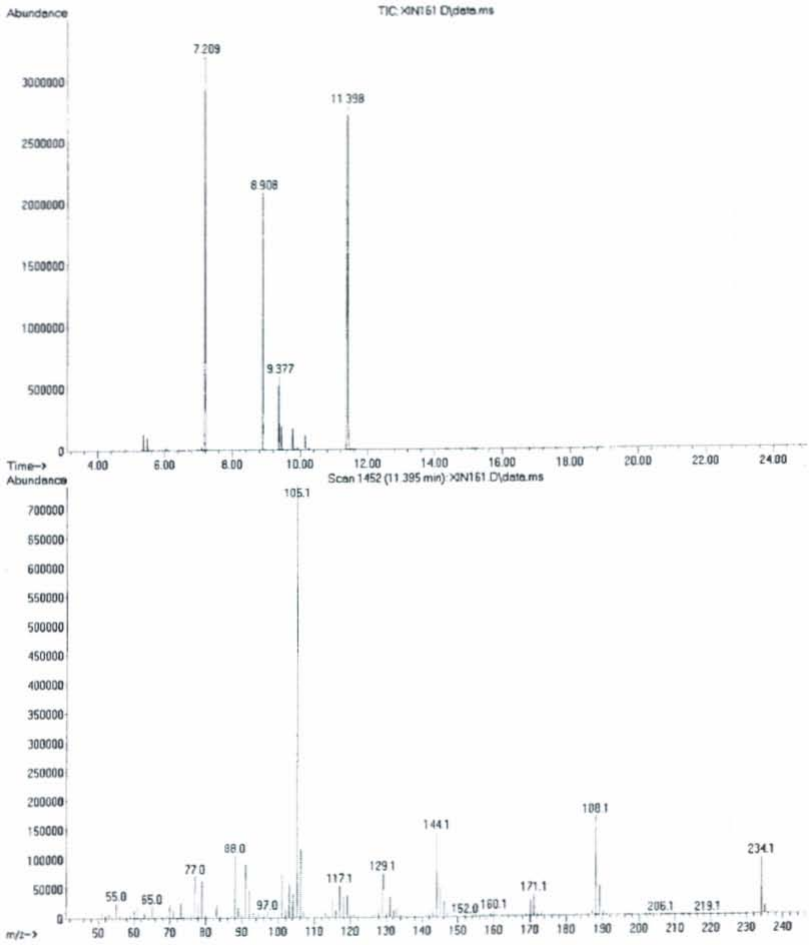

Table 3.5, Entry 4: Dodecane internal standard R_t = 7.206 min. Ethyl 6-(4-fluorophenyl)hexanoate, R_t = 10.497 min. By-product: 4,4'-difluorobiphenyl, R_t = 8.593 min.

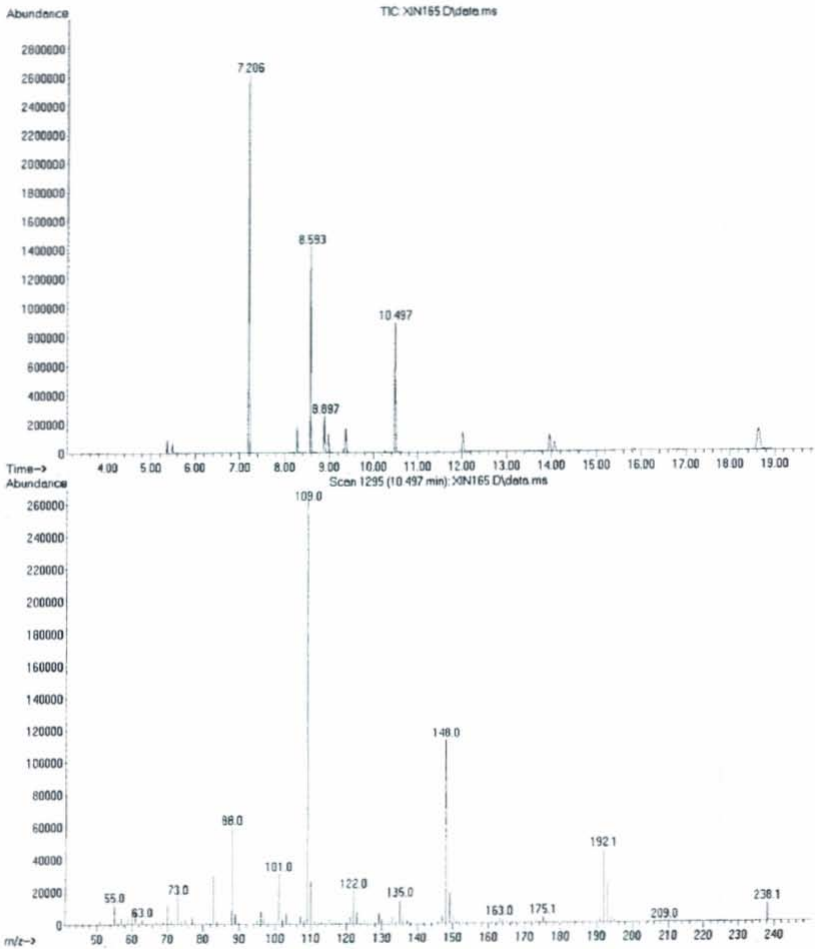

Table 3.5, Entry 4 (MW method): Dodecane internal standard R_t = 7.203 min): Ethyl 6-(4-fluorophenyl)- hexanoate, R_t = 10.495 min. By-product: 4,4'-difluorobiphenyl, R_t = 8.592 min.

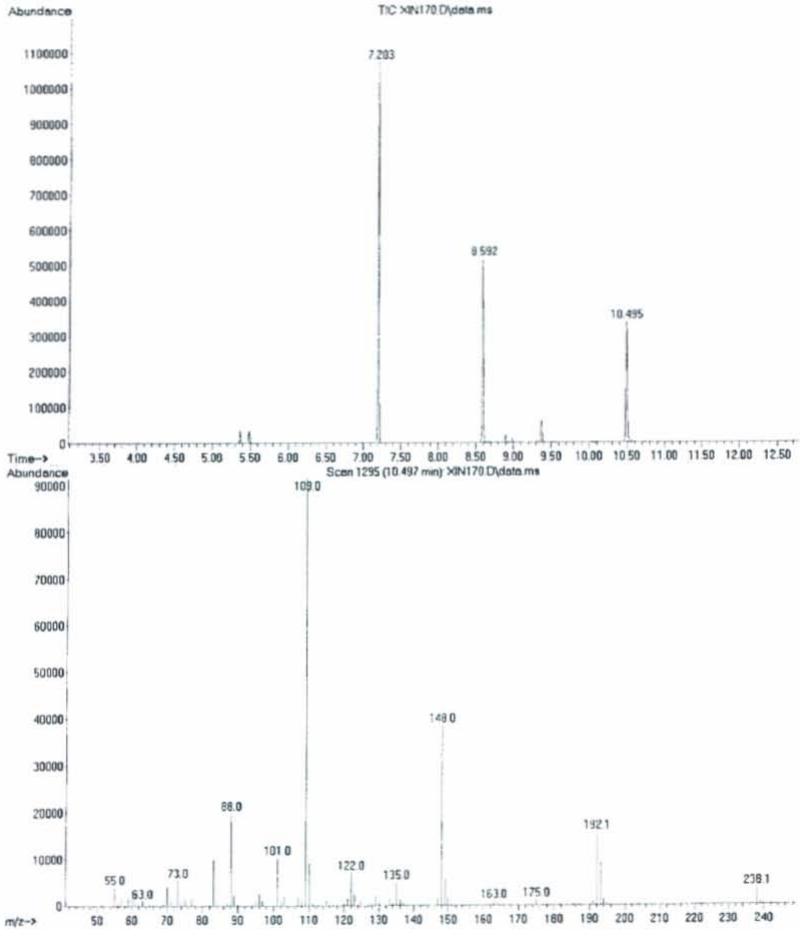

Table 3.5, Entry 7: Dodecane internal standard R_t = 7.206 min. (1S,2S,4R)-2-phenylbicyclo[2.2.1]heptane, R_t = 8.964 min. By-product: biphenyl, R_t = 8.621 min.

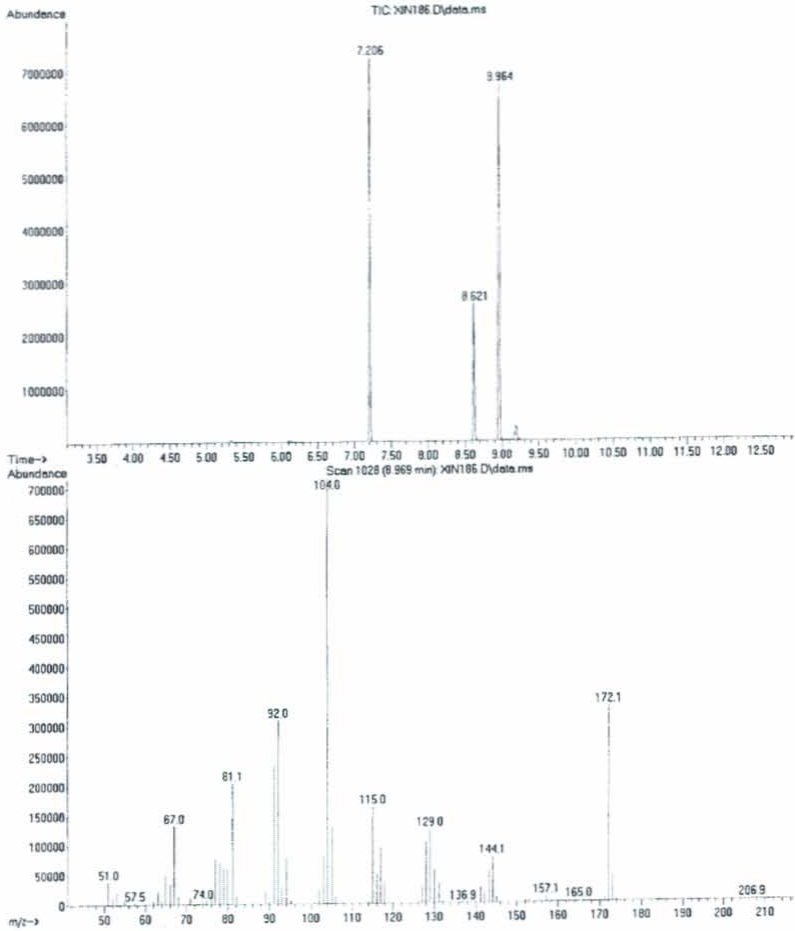

Table 3.5, Entry 7 (MW method): Dodecane internal standard R_t = 7.209 min. (1S,2S,4R)-2-phenylbicyclo[2.2.1] heptane, R_t = 8.968 min. By-product: biphenyl, R_t = 8.624 min.

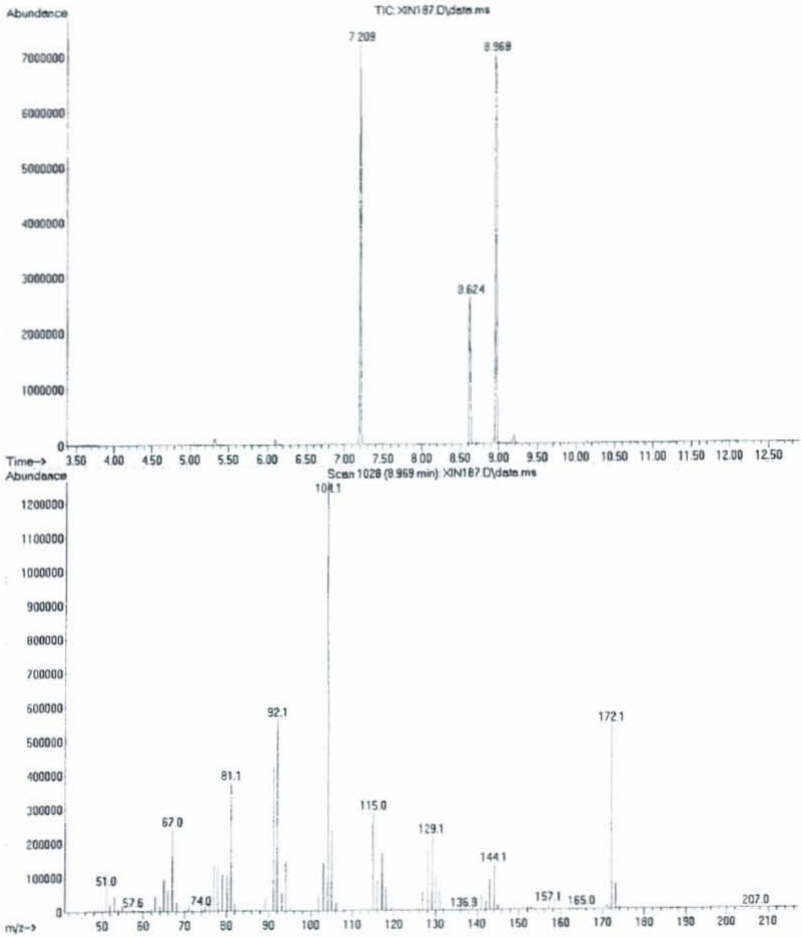

GC traces of radical clock experiments

Dodecane internal standard R_t = 5.83 min. 1-(but-3-enyl)-2-methylbenzene, R_t = 5.34 min. 1-(cyclopropylmethyl)-2-methylbenzene, R_t = 6.24 min. 2,2'-dimethylbiphenyl, R_t = 8.06 min.

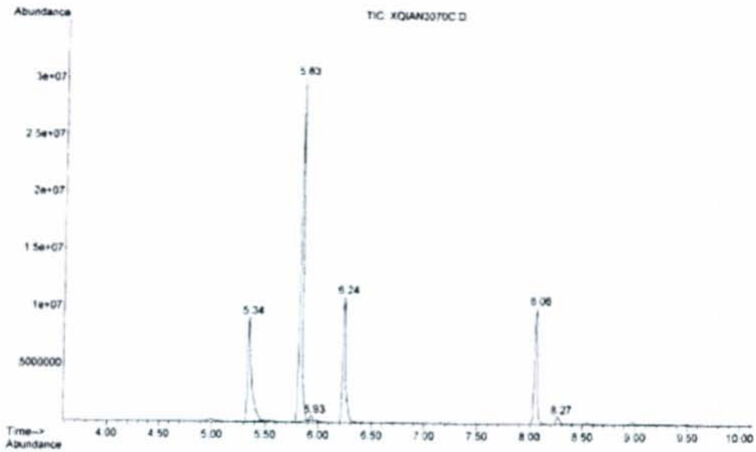

Dodecane internal standard R_t = 5.83 min. 1-(hex-5-enyl)-2-methylbenzene, R_t = 7.39 min. 1-(cyclopentylmethyl)-2-methylbenzene, R_t = 7.98 min. 2,2'-dimethylbiphenyl, R_t = 8.05 min.

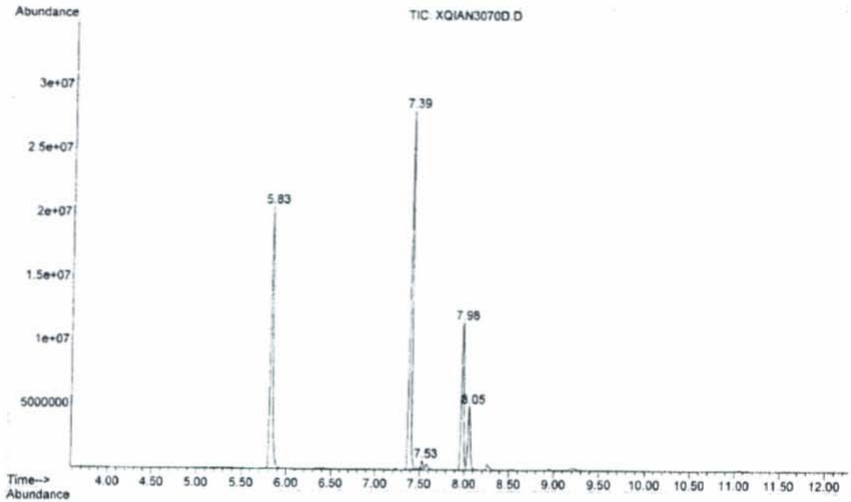

^{1}H NMR data of cross-coupled products (for Chapter 4)

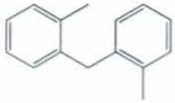

Di-*o*-tolylmethane (500 MHz, $CDCl_3$, δ): 3.84(s, CH_2, 2H,); 2.19 (s, CH_3, 6H,).

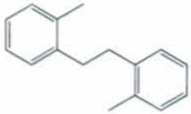

1,2-di-*o*-tolylethane (500 MHz, $CDCl_3$, δ): 2.78(s, CH_2, 4H,); 2.24(s, CH_3, 6H,).

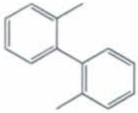

2,2'-dimethylbiphenyl (500 MHz, $CDCl_3$, δ): 1.98(s, CH_3, 6H,).

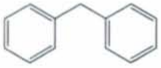

Diphenylmethane (500 MHz, $CDCl_3$, δ): 3.87(s, CH_2, 2H,).

1,2-diphenylethane (500 MHz, $CDCl_3$, δ): 2.82(s, CH_2, 4H,).

GC traces of cross-coupling products: *o*-tolyl Grignard Reagent with Dichloromethane

Table 4.1, Entry 1: Dodecane internal standard R_t = 6.728 min, di-*o*-tolylmethane, R_t = 9.768 min, 1,2-di-*o*-tolylethane, R_t = 10.340 min, 2,2'-dimethylbiphenyl, R_t = 8.450 min.